STUDIES
ON
THE ELECTRONIC STRUCTURES AND INTERACTIONS
OF
MOLECULAR SYSTEMS AND AGGREGATES

KAZUYOSHI TANAKA

DEPARTMENT OF HYDROCARBON CHEMISTRY

FACULTY OF ENGINEERING

KYOTO UNIVERSITY

1978

STUDIES
ON
THE ELECTRONIC STRUCTURES AND INTERACTIONS
OF
MOLECULAR SYSTEMS AND AGGREGATES

KAZUYOSHI TANAKA

Preface

It was when Heitler and London applied quantum mechanical theory to hydrogen molecule in 1927 that quantum chemistry came into the world. Since then quantum chemistry has been proved not only to provide an effective strategy for the interpretations of a lot of chemical phenomena that had been explained unsatisfactorily by the classical theories in chemistry, but also to afford non-empirical nature to chemistry, thanks to ceaseless efforts of chemists and physicists. This should be regarded, however, as a reasonable consequence since the chemical behaviours of atoms and molecules are ruled to a greater extent by the motions of electrons that are subject to what is described by quantum mechanics, on which quantum chemistry is grounded.

The field of intermolecular interactions, which plays important roles in a great deal of chemical and physical phenomena, is one of the most significant branches in quantum chemistry. There are two main methods that have been established in the course of the study of these interactions by means of the quantum chemical approach. One is the perturbation theory based on the separate molecules in order to treat long-range intermolecular interactions. This theory is also applicable to the systems interacting with external field. The other is variational methods based on the Hartree-Fock approximation

dealing with the intermediate- and short-range interactions, where the interacting species should be regarded as a molecule.

Particularly, the applications of the molecular orbital (MO) theory to the latter interactions have been of routine work and yielded a great deal of results in the calculations of electronic structures of molecules and the interpretations of various chemical reactions. Varieties of fruitful theories of chemical reactivities have been also proposed on the basis of MO concepts and the important role of the particular orbitals in the orientation and stereoselection of many chemical reactions has been pointed out.

However, recent developments of experimental techniques for determining weak interaction energies have caused an inevitable re-examination of theoretical treatment for long-range interactions. Furthermore, the studies on the electronic structures of molecules in the excited state and the intermolecular interactions in molecular aggregates are highly needed at present according to the recent explosive expansion of experimental works in photochemistry and low-dimensional cooperative phenomena in condensed phases.

The main theme of this thesis is to study the elecronic structures and interactions in molecular systems and aggregates. It is composed of the studies on (i) long-range to short-range interactions in the ground state, (ii) deformations in molecu-

lar geometries and reactions caused by the intramolecular interactions in the excited state, (iii) treatment of local perturbations such as local defects or impurities in molecular aggregates, and (iv) electronic structures and interactions in polymeric sulfur nitride, $(SN)_x$, and its precursors, which are of particular interest because of anomalous low-dimensional metallic conductivity of $(SN)_x$ polymer. The present studies on the interactions in molecular aggregates would be regarded to involve a challenge by quantum chemistry to the field of solid state science.

Acknowledgement

The present thesis is the summary of the author's studies from 1973 to 1977 at the Department of Hydrocarbon Chemistry, Faculty of Engineering, Kyoto University.

The author wishes to express his cordial gratitude to Professor Kenichi Fukui for his kind guidance, valuable suggestions, stimulating discussions and continuing encouragement throughout these studies. He also wishes to thank Dr. Tokio Yamabe, Professor Hiroshi Kato, and Professor Akira Imamura for their instructive discussions, suggestions and encouragement. Acknowledgement is also made to Dr. Shingo Ishimaru, Dr. Hideyuki Konishi, Dr. Shigeki Kato, and Mr. Tsutomu Minato for their useful discussions and generous permission to use various programs for molecular orbital calculations, and to other members of Quantum Chemistry Group for their active and valuable discussions. Thanks are also due to Mr. Hiroshi Ueno for his joint effort and Mr. Akinori Noda for his valuable informations on sulfur nitride chemistry. The author is grateful to Professor Alan G. MacDiarmid for his communicating original results of synthesis and properties of polymeric sulfur nitride and so on.

Numerical calculations were carried out with FACOM 230-60,, 230-75, and M190 Computers of the Data Processing Center of Kyoto University, of which staffs he would wish to thank.

Finally, it is also a pleasure of the author to thank his families for their understanding and encouragement.

Contents

Introduction		1
Chapter 1	Theoretical Ground for the Study of Long-range Interactions	4
I	Introduction	4
II	Formulation	6
III	Results and Discussion	14
IV	Appendix (A)	20
V	Appendix (B)	23
Chapter 2	Long-range Interaction between a Hydrogen Atom and a Hydride Ion	26
I	Introduction	26
II	Method of Calculation	28
III	Results and Discussion	35
IV	Appendix	47
Chapter 3	Interactions in Ion-Molecule Complexes	57
I	Introduction	57
II	Method of Calculation	59
III	Results and Discussion	62
Chapter 4	Stereoselection in Cross-bicyclization	84
I	Introduction	84
II	Formulation	89
III	Stereoselective Modes of Cross-bicyclization and Cycloaddition	93

IV	Application	101
V	Conclusion	109
Chapter 5	Interactions in Biradicals	113
I	Introduction	113
II	Stabilization of Singlet Biradical by a Correlated Motion of Electrons	113
III	Bonding Character between Two Radical Sites	117
IV	Polar Character of Two Radical Sites	120
V	Biradical Character of Singlet Biradicals	121
VI	Nonbonding Biradicals	123
VII	Biradical with Cyclic Orbitals	125
VIII	General Characterization of Biradicals	130
IX	Bonding Deformation of Singlet Biradicals	132
X	Unpaired-Electron Isolating Deformation or Bonding in Triplet Biradicals	140
Chapter 6	Electronic Structures of an Infinite Polyene under Local Perturbations	154
I	Introduction	154
II	Formulation	155
III	Application to Infinite Polyene	158

Chapter 7	Orbital Interaction in the Dimerization of S_2N_2 into S_4N_4	169
Chapter 8	The Initial Stage of Polymerization from $(SN)_2$ Molecules to $(SN)_x$ Polymer	177
I	Introduction	177
II	Electronic Structure of S_2N_2	179
III	Electronic Structures of "Deformed" $(SN)_2$	181
IV	Electronic Structures of $(SN)_4$ and $(SN)_6$	193
V	Conclusion	196
Chapter 9	Electronic Structures of $(SN)_x$ and $(SCH)_x$ Polymers	201
I	Introduction	201
II	Method of Calculation	202
III	Results and Discussion	205
Chapter 10	Interchain Interaction in $(SN)_x$ Polymer	217
Conclusion		234

Introduction

A series of studies on several current problems in the field of intra- and intermolecular interactions is performed in this thesis. Nowadays, it admits of no doubt that one ought to analyze the wavefunctions of the concerned chemical systems on the basis of quantum chemistry in order to obtain theoretical interpretations for various chemical phenomena. An opportune utilization of quantum chemical methodology will permit us to obtain useful informations on these interactions.

In Chapter 1 (published in Bull. Chem. Soc. Jpn., 47, 1578(1974)), a formulation of the upper and lower bounds of the exact second-order perturbation energy affording a theoretical ground for the study of the long-range interactions is presented. This formulation is applied to the polarizability of a hydrogen atom and the long-range force in H-H system.

In Chapter 2 (published in Bull. Chem. Soc. Jpn., 48, 3500(1975)), the long-range interaction in the anionic system is studied by means of the second-order perturbation theory, and the nature of the interaction operating in the system is discussed.

In Chapter 3 (published in Bull. Chem. Soc. Jpn., 48, 1740(1975)), intramolecular interactions and optimum configurations of several ion-molecule complexes (NH_4^+-CH_4, H_3O^+-CH_4, and NH_4^+-H_2 systems) are examined. The contributions from

the charge transfer configurations to the total wavefunctions of the systems are also estimated by the configuration analysis.

In Chapter 4 (submitted for publication), a concept of the cross-bicyclization complementary to that of the cycloaddition is defined concerning simultaneous bicyclization in a linear conjugated polyene. The stereoselective modes in thermal and, especially, photo-induced reactions are discussed.

In Chapter 5 (published in Bull. Chem. Soc. Jpn., 50, 1391(1977)), an interpretation is given on the characteristics of singlet biradicals. Systematization of the reactivities of singlet and triplet biradicals caused by the intramolecular interactions is investigated as well.

In Chapter 6 (published in Chem. Phys. Lett., 48, 141(1977)), a theoretical method is developed in order to deal with non-periodical molecular aggregates such as having local defects or impurities. An infinite polyene is employed there as a model system.

In Chapter 7 (submitted for publication; partly reported in Ann. New York Acad. Sci., (1977) in press), the process of the dimerization of disulfur dinitride, S_2N_2, into tetrasulfur tetranitride, S_4N_4, is investigated from the viewpoint of the frontier orbital interaction.

In Chapter 8 (published in J. Phys. Chem., 81, 727(1977)

), the initial stage of polymerization from S_2N_2 molecules to $(SN)_x$ polymer is examined with the use of the MO theory. The mechanism of polymerization at this stage is discussed based on the interactions in deformed S_2N_2 molecules.

In Chapter 9 (published in Bull. Chem. Soc. Jpn., 50, 798(1977)), one-dimensional $(SN)_x$ and its isoelectronic system $(SCH)_x$ polymers are studied on the basis of the SCF-tight-binding MO theory. The band structures and the electronic structures of them, and the possibility of electrical conductivity in $(SCH)_x$ polymer are discussed.

In Chapter 10 (Chem. Phys. Lett., in press), the interchain interactions in $(SN)_x$ polymer are studied on the basis of the method similar to what is used in the previous Chapter. The crystallographic plane in which the significant interchain interactions operate is pointed out and the main reason of the interactions is discussed.

Chapter 1

Theoretical Ground for the Study of Long-range Interactions

I. Introduction

The second-order perturbation energy, E_2, is given by:

$$E_2 = - \sum_{i>0}^{\infty} |H_{1i}|^2/\varepsilon_i \ , \qquad (1)$$

where $H_{1i}=\langle\psi_0^{(i)}|H_1|\psi_0^{(0)}\rangle$ and $\varepsilon_i=E_0^{(i)}-E_0^{(0)}$, in which H_1 is the perturbation, and $\psi_0^{(i)}$ and $E_0^{(i)}$ are the i-th eigenfunction and eigenvalue of the unperturbed Hamiltonian H_0, respectively. In the following, $\psi_0^{(0)}$ and $E_0^{(0)}$ are denoted to be ψ_0 and E_0, respectively, since only the ground state is treated in this Chapter.

Generally it is difficult to calculate the summation of Eq.(1); therefore, many approximate methods have been devised. Among them, the most useful method is Hylleraas's variation condition for the second-order perturbation energy:[1)]

$$\langle\tilde{\psi}_1|H_0-E_0|\tilde{\psi}_1\rangle + \langle\tilde{\psi}_1|H_1-E_1|\psi_0\rangle + \langle\psi_0|H_1-E_1|\tilde{\psi}_1\rangle$$

$$\geqq E_2, \qquad (2)$$

in which $\tilde{\psi}_1$ is an arbitrary function corresponding to the first-order perturbation function. One of the effective forms which have been applied for $\tilde{\psi}_1$ is that of Goodisman,[2] who, using Eq.(2), obtained the upper bound of the second-order energy for the case in which first n excited states of unperturbed system are known. On the other hand, neglecting energies of a higher order than the second-order, Prager and Hirschfelder[3] found the lower bound of the second-order energy based on the Temple principle:[4]

$$\langle (H-E^{(0)})\tilde{\psi} | (H-E^{(1)})\tilde{\psi} \rangle \geq 0 , \qquad (3)$$

where $E^{(i)}$ is the i-th eigenvalue associated with i-th eigenfunction, $\psi^{(i)}$, of the total Hamiltonian, $H=H_0+H_1$, and where $\tilde{\psi}$ is a variational function for $\psi^{(0)}$, which may be divided into $\psi_0+\tilde{\psi}_1$.

Other theories estimating the upper and lower bounds were developed by Lindner and Löwdin[5] and subsequently by Miller.[6] They utilized operator techniques in the direction of using a finite arbitrary basis set for $\tilde{\psi}_1$. Especially Miller extended the theory of Lindner and Löwdin, who treated only the second-order energy in the ground state, to a theory which can be adopted to the second-order energy in the arbitrary excited state.

It seems, however, that the form of Ψ_1 used by Goodisman is rather tractable for performing the calculation. Therefore,, in this Chapter, we will try to improve both the upper bound of Goodisman and the lower bound of Prager and Hirschfelder by the use of a form of Ψ_1 similar to that of Goodisman.

II. Formulation

(i) Derivation of the Upper Bound

Let us consider the following first-order variational function:

$$\Psi_1(n,\lambda,\{\mu_i|i\geqq n+1\}) = -\sum_{i>0}^{n} H_{1i}\psi_0^{(i)}/\varepsilon_i + \lambda\sum_{i=n+1}^{\infty}\mu_i H_{1i}\psi_0^{(i)}, \qquad (4)$$

where λ and each μ_i are arbitrary real parameters. Substituting this function into Hylleraas's condition in Eq.(2), one obtains:

$$E_2^{up}(n,\lambda,\{\mu_i|i\geqq n+1\}) = (\sum_{i=n+1}^{\infty}\mu_i^2|H_{1i}|^2\varepsilon_i)\lambda^2$$

$$+ 2\left(\sum_{i=n+1}^{\infty} \mu_i |H_{1i}|^2\right)\lambda + A_n, \qquad (5)$$

where:

$$A_n = -\sum_{i>0}^{n} |H_{1i}|^2/\varepsilon_i \ . \qquad (6)$$

$E_2^{up}(n,\lambda,\{\mu_i | i\geq n+1\})$ in Eq.(5) is a quadratic formula with regard to λ and takes the minimum value:

$$E_2^{up}(n,\{\mu_i | i\geq n+1\}) = A_n - \left(\sum_{i=n+1}^{\infty} \mu_i |H_{1i}|^2\right)^2 / \left(\sum_{i=n+1}^{\infty} \mu_i^2 |H_{1i}|^2 \varepsilon_i\right) \qquad (7)$$

when λ is:

$$\lambda = -\left(\sum_{i=n+1}^{\infty} \mu_i |H_{1i}|^2\right) / \left(\sum_{i=n+1}^{\infty} \mu_i^2 |H_{1i}|^2 \varepsilon_i\right). \qquad (8)$$

After modifying μ_i into some more convenient form, as will be shown below, one can further optimize $E_2^{up}(n,\{\mu_i | i\geq n+1\})$ with respect to $\{\mu_i\}$ for each n to get the desired upper bound, $E_2^{up}(n)$. If the simplest form of μ_i is chosen, *i.e.*, $\mu_i=1$ for any i, the result is just that obtained by Goodisman.

It can easily be proved that the upper bound thus obtained really satisfies the relation that $E_2^{up}(n-1)\geq E_2^{up}(n)$. In order

to prove this, let us calculate the following subtraction between $E_2^{up}(n,\{\mu_i|i\geqq n+1\})$ and $E_2^{up}(n-1,\{\mu_i|i\geqq n\})$ of Eq.(7), keeping $\{\mu_i\}$ in common for both:

$$E_2^{up}(n,\{\mu_i|i\geqq n+1\}) - E_2^{up}(n-1,\{\mu_i|i\geqq n\})$$

$$= -|H_{1n}|^2/\varepsilon_n - (\sum_{i=n+1}^{\infty}\mu_i|H_{1i}|^2)^2/(\sum_{i=n+1}^{\infty}\mu_i^2|H_{1i}|^2\varepsilon_i)$$

$$+ (\sum_{i=n}^{\infty}\mu_i|H_{1i}|^2)^2/(\sum_{i=n}^{\infty}\mu_i^2|H_{1i}|^2\varepsilon_i). \qquad (9)$$

The right-hand side in Eq.(9) becomes:

$$-|H_{1n}|^2\{\sum_{i=n+1}^{\infty}\mu_i|H_{1i}|^2(\mu_i\varepsilon_i-\mu_n\varepsilon_n)\}^2$$

$$\div\{(\sum_{i=n}^{\infty}\mu_i^2|H_{1i}|^2\varepsilon_i)(\sum_{i=n+1}^{\infty}\mu_i^2|H_{1i}|^2\varepsilon_i)\varepsilon_n\} \leqq 0,$$

and is always nonpositive, since all of ε_i values are non-negative. Consequently, when n becomes infinite, $E_2^{up}(n,\{\mu_i|i\geqq n+1\})$; hence, $E_2^{up}(n)$ also approaches to E_2 in Eq.(1) from the upper side.

Next, we set the modified form of μ_i as $\mu_i=1+\mu E_0^{(i)}/E_0$ to get the optimal value, $E_2^{up}(n)$.[7] Substituting this μ_i into Eq.(7) and optimizing with respect to μ, one gets:

$$E_2^{up}(n) = A_n - \{\langle\psi_0|H_1^2|\psi_0\rangle + (\mu_{opt}/E_0)\langle\psi_0|H_1H_0H_1|\psi_0\rangle$$

$$- \sum_{i>0}^{n} (1+\mu_{opt}E_0^{(i)}/E_0)|H_{1i}|^2\}^2/\{\langle\psi_0|H_1(H_0-E_0)H_1|\psi_0\rangle$$

$$+ (2\mu_{opt}/E_0)\langle\psi_0|H_1H_0(H_0-E_0)H_1|\psi_0\rangle$$

$$+ (\mu_{opt}^2/E_0^2)\langle\psi_0|H_1H_0(H_0-E_0)H_0H_1|\psi_0\rangle$$

$$- \sum_{i>0}^{n} (1+\mu_{opt}E_0^{(i)}/E_0)^2|H_{1i}|^2\varepsilon_i\}, \qquad (10)$$

where:

$$\mu_{opt} = [-(a^2e-b^2c) - \{(a^2e-b^2c)^2 - (a^2d-2abc)(2abe-b^2d)$$

$$\}^{1/2}]/(a^2d-2abc) = (bd-2ae)/(ad-2bc), \qquad (11)$$

and where:

$$a = \langle\psi_0|H_1H_0H_1|\psi_0\rangle/E_0 - \sum_{i=0}^{n} (E_0^{(i)}/E_0)|H_{1i}|^2,$$

$$b = \langle\psi_0|H_1^2|\psi_0\rangle - \sum_{i=0}^{n} |H_{1i}|^2,$$

$$c = \langle\psi_0|H_1H_0(H_0-E_0)H_0H_1|\psi_0\rangle/E_0^2 - \sum_{i>0}^{n} (E_0^{(i)}/E_0)^2|H_{1i}|^2\varepsilon_i,$$

$$d = 2\{\langle\psi_0|H_1H_0(H_0-E_0)H_1|\psi_0\rangle/E_0 - \sum_{i>0}^{n}(E_0^{(i)}/E_0)|H_{1i}|^2\varepsilon_i\}\ ,$$

and:

$$e = \langle\psi_0|H_1(H_0-E_0)H_1|\psi_0\rangle - \sum_{i>0}^{n}|H_{1i}|^2\varepsilon_i. \qquad (11')$$

(ii) Derivation of the Lower Bound

If the variational function $\tilde{\Psi}$, which is divided into $\psi_0+\tilde{\psi}_1$, as has previously been mentioned, is orthogonal to the first several excited eigenfunctions of the total Hamiltonian, *i.e.*:

$$\langle\tilde{\Psi}\ |\Psi^{(k)}\rangle = 0\ (k=1,2,\cdots,n)\ , \qquad (12)$$

the following Temple-type inequality:

$$\langle(H-E^{(0)})\tilde{\Psi}\ |(H-E^{(n+1)})\tilde{\Psi}\rangle \geqq 0\ , \qquad (13)$$

is easily established and can be utilized as the base to get the lower bound. Employing the same form as in Eq.(4) for $\tilde{\psi}_1$, $\tilde{\Psi}$ becomes:

$$\tilde{\Psi} = \psi_0 + \tilde{\psi}_1 = \psi_0 - \sum_{i>0}^{n}H_{1i}\psi_0^{(i)}/\varepsilon_i + \lambda\sum_{i=n+1}^{\infty}\mu_iH_{1i}\psi_0^{(i)}, \qquad (14)$$

which satisfies Eq.(12) as far as the second-order energy is considered.[8] Substituting this $\tilde{\Psi}$ into Eq.(13) and neglecting the energies of a higher order than the second-order one, a lower bound for the second-order energy is obtained as follows:

$$\begin{aligned} E_2 \geq & \{ \sum_{i=n+1}^{\infty} \mu_i^2 |H_{1i}|^2 \varepsilon_i (1-\varepsilon_i/\varepsilon_{n+1}) \} \lambda^2 \\ & + 2\{ \sum_{i=n+1}^{\infty} \mu_i |H_{1i}|^2 (1-\varepsilon_i/\varepsilon_{n+1}) \} \lambda \\ & + \{ A_n - \sum_{i=n+1}^{\infty} |H_{1i}|^2/\varepsilon_{n+1} \} \\ \equiv & E_2^{\mathrm{low}}(n, \lambda, \{\mu_i | i \geq n+1\}), \end{aligned} \tag{15}$$

which takes the maximum value:

$$\begin{aligned} E_2^{\mathrm{low}}(n, \{\mu_i | i \geq n+1\}) = & -\{ \sum_{i=n+1}^{\infty} \mu_i |H_{1i}|^2 (1-\varepsilon_i/\varepsilon_{n+1}) \}^2 / \\ & \{ \sum_{i=n+1}^{\infty} \mu_i^2 |H_{1i}|^2 \varepsilon_i (1-\varepsilon_i/\varepsilon_{n+1}) \} \\ & + \{ A_n - \sum_{i=n+1}^{\infty} |H_{1i}|^2/\varepsilon_{n+1} \}, \end{aligned} \tag{16}$$

when:

$$\lambda = -\{\sum_{i=n+1}^{\infty} \mu_i |H_{1i}|^2 (1-\varepsilon_i/\varepsilon_{n+1})\}/$$

$$\{\sum_{i=n+1}^{\infty} \mu_i^2 |H_{1i}|^2 \varepsilon_i (1-\varepsilon_i/\varepsilon_{n+1})\}. \qquad (17)$$

$E_2^{low}(n,\{\mu_i | i\geqq n+1\})$ can be further optimized with regard to $\{\mu_i\}$ to obtain $E_2^{low}(n)$. If n=0 and μ_i=1, the result coincides with that obtained by Prager and Hirschfelder.

Furthermore, the relation that $E_2^{low}(n)\geqq E_2^{low}(n-1)$ can be proved by calculating the following subtraction with the use of Eq.(15), keeping λ and $\{\mu_i\}$ in common for both $E_2^{low}(n,\lambda,\{\mu_i | i\geqq n+1\})$ and $E_2^{low}(n-1,\lambda,\{\mu_i | i\geqq n\})$:

$$E_2^{low}(n,\lambda,\{\mu_i | i\geqq n+1\}) - E_2^{low}(n-1,\lambda,\{\mu_i | i\geqq n\})$$

$$= \{(\varepsilon_{n+1}-\varepsilon_n) \sum_{i=n+1}^{\infty} \mu_i^2 |H_{1i}|^2 \varepsilon_i^2/\varepsilon_n\varepsilon_{n+1}\}\lambda^2$$

$$+ 2\{(\varepsilon_{n+1}-\varepsilon_n) \sum_{i=n+1}^{\infty} \mu_i |H_{1i}|^2 \varepsilon_i/\varepsilon_n\varepsilon_{n+1}\}\lambda$$

$$+ \{(\varepsilon_{n+1}-\varepsilon_n) \sum_{i=n+1}^{\infty} |H_{1i}|^2/\varepsilon_n\varepsilon_{n+1}\}. \qquad (18)$$

Eq.(18) is a quadratic formula of λ and is always positive, since the coefficient of λ^2 is positive and since the discriminant of Eq.(18):

$$D = (\varepsilon_{n+1}-\varepsilon_n)^2\{(\sum_{i=n+1}^{\infty}\mu_i|H_{1i}|^2\varepsilon_i)^2$$

$$-(\sum_{i=n+1}^{\infty}\mu_i^2|H_{1i}|^2\varepsilon_i^2)(\sum_{i=n+1}^{\infty}|H_{1i}|^2)\}/(\varepsilon_{n+1}^2\varepsilon_n^2),$$

is always negative, which is ensured by the Schwartz inequality. Therefore, when n becomes infinite, $E_2^{low}(n,\lambda,\{\mu_i|i\geq n+1\})$; hence, $E_2^{low}(n)$ also approaches to the true E_2 value from the lower side.

As a special case, by substituting $\mu_i=1$[7] into Eq.(16) one gets the lower bound, $E_2^{low}(n)$:

$$E_2^{low}(n) = -\{\sum_{i=n+1}^{\infty}|H_{1i}|^2(1-\varepsilon_i/\varepsilon_{n+1})\}^2/$$

$$\{\sum_{i=n+1}^{\infty}|H_{1i}|^2\varepsilon_i(1-\varepsilon_i/\varepsilon_{n+1})\}$$

$$+\{A_n - \sum_{i=n+1}^{\infty}|H_{1i}|^2/\varepsilon_{n+1}\}\ , \qquad (19)$$

which can then be rewritten by using the a, b, d, and e defined in Eq.(11'):

$$E_2^{low}(n) = -[b-(a-b)E_0/\varepsilon_{n+1}]^2/[(a-b)E_0-(d/2-2e+aE_0-bE_0)E_0/$$

$$\varepsilon_{n+1}] + (A_n-b/\varepsilon_{n+1})\ . \qquad (20)$$

III. Results and Discussion

(i) Polarizability of a Hydrogen Atom in the Ground State

The value of the polarizability, α, is twice the absolute value of E_2 caused by the perturbation, H_1, which, in this case, is z (in a.u.), the coordinate of the direction of the electric field (throughout this Chapter the atomic unit is used). Then,

$$\alpha = -2E_2 = 2 \sum_{i>0}^{\infty} |\langle \psi_0^{(i)} | z | \psi_0 \rangle|^2 / (E_0^{(i)} - E_0) \quad . \tag{21}$$

In order to examine the usefulness of the present theory for the upper and lower bounds, we have to calculate Eqs.(10), (11), and (20). In the calculation, the following values of integrals are required:

$$\langle \psi_0 | z | \psi_0 \rangle = 0,$$

$$\langle \psi_0 | z^2 | \psi_0 \rangle = 1,$$

$$\langle \psi_0 | z H_0 z | \psi_0 \rangle = 0,$$

$$\langle \psi_0 | z H_0^2 z | \psi_0 \rangle = 1/12,$$

and

$$\langle\psi_0|zH_0^3z|\psi_0\rangle = 5/12, \tag{22}$$

in which ψ_0 is the 1s-function of a hydrogen atom and in which E_0 is -1/2.

In Table 1, the results for n=0, 1, 2, 3, and 4 are shown. The values of λ and μ are also shown, since they are the parameters corresponding to $1/E_0$ and $E_0/(E_0-E_0^{(i)})$, respectively [7] Compared with the results of the lower bounds of α reported by Goodisman (μ_i=1), the present lower bounds are fairly well improved because of the existence of the μ_i parameter; the upper bounds are also better than that reported by Prager and Hirschfelder. For both the upper and lower bounds, the improvement from n=0 to n=1 is meaningful, but for $n\geq 2$ the improvement does not seem to be substantial.

(ii) The Dispersion Force between Two Hydrogen Atoms

When the internuclear distance, R, between two hydrogen atoms in the ground state is large enough, the overlap and, hence, the exchange are insignificant; one can take $\psi_0=\psi_A(1)\psi_B(2)$ as the unperturbed wavefunction for this system, where $\psi_A(1)$ and $\psi_B(2)$ are the isolated atomic wavefunctions of the two hydrogen atoms. Besides, the perturbation, H_1, in usual notations:[10]

Table 1. The Upper and Lower Bounds for Polarizability of a Hydrogen Atom in the Ground State (Exact=4.5[a])

n	$\alpha^{low}(n)$ [b] $=-2E_2^{up}(n)$	λ	μ	$\alpha^{low}(n)$ [c] $(\mu_i=1)$	$\alpha^{up}(n)$ [b] $=-2E_2^{low}(n)$	λ	$\{\alpha^{low}(n)+\alpha^{up}(n)\}/2$
0	4.125	-2.063	0.09091	4.0000	4.762*	-0.8571	4.444
1	4.363	-1.611	0.07286	4.3162	4.646	-0.7495	4.505
2	4.391	-1.499	0.06644	4.3636	4.623	-0.7156	4.507
3	4.415	-1.457	0.06638	4.3800	4.612	-0.7007	4.514
4	4.420	-1.435	0.06525	-	4.607	-0.6929	4.514

a) Ref. 9.

b) Present results (*; Ref. 3).

c) Ref. 2.

$$H_1 = -1/r_{B1} - 1/r_{A2} + 1/R + 1/r_{12} \ , \qquad (23)$$

can be expanded in an inverse power series of R, and the second-order energy is generally represented by:

$$-E_2 = C_6/R^6 + C_8/R^8 + \cdots\cdots \ , \qquad (24)$$

where:

$$C_6 = \sum_{i>0}^{\infty} |\langle\psi_0^{(i)}|H_{dd}|\psi_0\rangle|^2/(E_0^{(i)}-E_0) \ ,$$

$$H_{dd} = x_1x_2 + y_1y_2 - 2z_1z_2 \ , \qquad (25)$$

and

$$C_8 = \sum_{i>0}^{\infty} |\langle\psi_0^{(i)}|H_{qd}|\psi_0\rangle|^2/(E_0^{(i)}-E_0) \ ,$$

$$H_{qd} = (3/2)\{r_1^2z_2 - r_2^2z_1 + (2x_1x_2 + 2y_1y_2 - 3z_1z_2)$$

$$(z_1 - z_2)\}. \qquad (26)$$

In the calculation of the bounds for C_6, one needs various kinds of integrals, which are evaluated as follows:

$$\langle\psi_0|H_{dd}|\psi_0\rangle = 0,$$

$$\langle\psi_0|H_{dd}^2|\psi_0\rangle = 6,$$

$$\langle\psi_0|H_{dd}H_0H_{dd}|\psi_0\rangle = 0,$$

$$\langle\psi_0|H_{dd}H_0^2H_{dd}|\psi_0\rangle = 1,$$

and

$$\langle\psi_0|H_{dd}H_0^3H_{dd}|\psi_0\rangle = 5 \ . \tag{27}$$

In Table 2, the results for C_6 using n=0, 1, 2, 3, 4, 5, 6, and 7 are shown. As in the case of polarizability, the improvement from n=0 to n=1 is remarkable, but for $n \geq 2$ the effect is not so large.

When calculating the bounds for C_8, the following integrals are required:

$$\langle\psi_0|H_{qd}|\psi_0\rangle = 0 \ ,$$

$$\langle\psi_0|H_{qd}^2|\psi_0\rangle = 135 \ ,$$

$$\langle\psi_0|H_{qd}H_0H_{qd}|\psi_0\rangle = 45/2 \ ,$$

Table 2. The Upper and Lower Bounds for Dispersion Force Constant C_6 between Two Hydrogen Atoms in the Ground State (Reliable Value $=6.4990267$[a])

n	$C_6^{low}(n)$ [b] $= -E_2^{up}(n)$	λ	μ	$C_6^{low}(n)$ [c] $(\mu_i=1)$	$C_6^{up}(n)$ [b] $= -E_2^{low}(n)$	λ	$\{C_6^{low}(n)+C_6^{up}(n)\}/2$
0	6.171	-1.029	0.1667	6.000	6.800	-0.6000	6.486
1	6.302	-0.9393	0.1445	6.201	6.709	-0.5560	6.506
2	6.339	-0.9049	0.1365	6.256	6.684	-0.5412	6.512
3	6.345	-0.8917	0.1335	6.269	6.674	-0.5345	6.510
4	6.357	-0.8853	0.1321	6.284	6.668	-0.5310	6.513
5	6.360	-0.8817	0.1313	6.289	6.665	-0.5288	6.513
6	6.362	-0.8794	0.1308	-	6.663	-0.5274	6.513
7	6.364	-0.8779	0.1304	-	6.662	-0.5264	6.513

a) Ref. 5.

b) Present results.

c) Ref. 2. The values are recalculated in the present work.

$$\langle\psi_0|H_{qd}H_0^2H_{qd}|\psi_0\rangle = 207/8 \ ,$$

and

$$\langle\psi_0|H_{qd}H_0^3H_{qd}|\psi_0\rangle = 12501/160 \ . \qquad (28)$$

In Table 3, the results for C_8 are presented in the case of n=0 and 1. It can also be seen that the improvement of the lower bound is remarkable when variable parameters, μ_i, are used in comparison with that obtained by using a constant μ_i=1 (μ=0); moreover, the improvement for both bounds from n=0 to n =1 is appreciable. The present result for the upper bound for C_8 is the best so far calculated in a non-empirical way.

From the above numerical results, it is clear that the present treatment is very tractable because of the convenient form of the variational function used. Although the numerical results are rather inferior to those in Refs. 5 and 11, the average of the both bounds for each n give good approximations to the exact or reliable values as may be seen in Tables 1, 2, and 3. Hence the present treatment may be expected to be effective for larger molecular systems.

IV. Appendix (A)

Table 3. The Upper and Lower Bounds for Dispersion Force Constant C_8 between Two Hydrogen Atoms in the Ground State (Reliable Value $=124.3991^{a)}$)

n	$C_8^{low}(n)$ b) $= -E_2^{up}(n)$	λ	μ	$C_8^{low}(n)$ c) $(\mu_i=1)$	$C_8^{up}(n)$ b) $= -E_2^{low}(n)$	λ	$\{C_8^{low}(n)+C_8^{up}(n)\}/2$
0	119.749	-0.9225	0.2306	115.714	129.837	-0.6103	124.793
1	120.035	-0.9136	0.2262	-	127.368	-0.5552	123.702

a) Ref. 11.

b) Present results.

c) The value obtained in the present work.

In deriving the upper bounds, the following form of $\tilde{\psi}_1$ was considered:

$$\tilde{\psi}_1(n,\lambda,\mu) = -\sum_{i>0}^{n}(H_{1i}/\varepsilon_i)\psi_0^{(i)} + \lambda\sum_{i=n+1}^{\infty}(1+\mu E_0^{(i)}/E_0)H_{1i}\psi_0^{(i)} \quad . \qquad \text{(A-1)}$$

Now, let us refer to the first-order function derived by Lennard-Jones in order to compare it with the $\tilde{\psi}_1$ of Eq.(A-1). The function derived by Lennard-Jones is:[12]

$$\psi_1 = (H_1-E_1)\psi_0/E_0 + \sum_{i>0}^{\infty}E_0^{(i)}H_{1i}\psi_0^{(i)}/\{E_0(E_0-E_0^{(i)})\}, \qquad \text{(A-2)}$$

which is reduced to:

$$\psi_1 = -\sum_{i>0}^{n}(H_{1i}/\varepsilon_i)\psi_0^{(i)} + (1/E_0)\sum_{i=n+1}^{\infty}\{1+E_0^{(i)}/(E_0-E_0^{(i)})\}H_{1i}\psi_0^{(i)} \quad . \qquad \text{(A-3)}$$

Comparing Eq.(A-1) with Eq.(A-3), it may be seen that λ and μ are taken to correspond to $1/E_0$ and the average of $E_0/(E_0-E_0^{(i)})$, respectively. If one also chooses $\mu_i=1+\mu E_0^{(i)}/E_0$ for the derivation of lower bounds, there appears an integral such as $\langle\psi_0|zH_0^4z|\psi_0\rangle$ which diverges. Hence, the simplest form, μ_i

=1, is adopted for any i.

V. Appendix (B)

The inequality in Eq.(13) can be established not for a completely arbitrary function, but for a restricted one, under the conditions of Eq.(12). Since the present variational function satisfies Eq.(12) only approximately, there remains the necessity of estimating the resulting error.

Using an arbitrary $\tilde{\Phi}$ function, Θ, which strictly satisfies the next relation:

$$< \Theta | \Psi^{(k)} > = 0 \quad (k=1, 2, \cdots\cdots, n) \ , \tag{B-1}$$

may be rewritten as follows:

$$\Theta = \tilde{\Phi} - \sum_{i>0}^{n} <\Psi^{(i)} | \tilde{\Phi}> \Psi^{(i)} \ . \tag{B-2}$$

Then, instead of Eq.(13), the inequality;

$$< (H-E^{(0)}) \tilde{\Phi} \ | (H-E^{(n+1)}) \tilde{\Phi} >$$

$$\geq \sum_{i>0}^{n} | <\Psi^{(i)} | \tilde{\Phi}> |^2 (E^{(i)}-E^{(0)}) (E^{(i)}-E^{(n+1)}) \ , \tag{B-3}$$

may easily be obtained. Setting the exact $\Psi^{(i)}$ as:

$$\Psi^{(i)} = \psi_0^{(i)} + \psi_1^{(i)} + \cdots\cdots$$

$$= \psi_0^{(i)} + \sum_{j\neq i}^{\infty} \{\langle\psi_0^{(j)}|H_1|\psi_0^{(i)}\rangle/(E_0^{(i)}-E_0^{(j)})\}\psi_0^{(j)} + \cdots\cdots, \quad \text{(B-4)}$$

and setting Φ as Ψ in Eq.(14), one obtains:

$$\langle\Phi|\Psi^{(k)}\rangle = \langle\Psi|\Psi^{(k)}\rangle = \langle\psi_0|\psi_0^{(k)}\rangle + \langle\psi_0|\psi_1^{(k)}\rangle$$

$$+ \langle\Psi_1|\psi_0^{(k)}\rangle + \langle\Psi_1|\psi_1^{(k)}\rangle + \cdots\cdots \quad (k=1, 2, \ldots,n). \quad \text{(B-5)}$$

It can be easily seen that the first term on the right-hand side of Eq.(B-5) vanishes, and that the second and the third terms cancel each other out using the form of Ψ_1 in Eq.(14) and that of $\psi_1^{(i)}$ in Eq.(B-4). As a result, the first non-vanishing term in Eq.(B-5) is of the second-order of the perturbation. Therefore, the value of the right-hand side of Eq.(B-3) is of the fourth-order of the perturbation and can be neglected as long as one considers the second-order energy.

References and Notes

1) E. A. Hylleraas, Z. Phys., 65, 209(1930).

2) J. Goodisman, J. Chem. Phys., 47, 2707(1967).

3) S. Prager and J. O. Hirschfelder, J. Chem. Phys., 39, 3289(1963).

4) G. Temple, Proc. Roy. Soc.(London), A119, 276(1928).

5) P. Lindner and P. O. Löwdin, Intern. J. Quant. Chem., IIs, 161(1968).

6) W. H. Miller, J. Chem. Phys., 50, 2758(1969).

7) See Appendix A.

8) See Appendix B.

9) For example, see L. D. Landau and E. M. Lifshitz, "Quantum Mechanics," translated by J. B. Sykes and J. S. Bell, Pergamon Press, London (1965), p.269.

10) L. Pauling and E. B. Wilson, Jr., "Introduction to Quantum Mechanics with Application to Chemistry," McGraw Hill Book Co., Inc., New York (1935), p.384.

11) W. Kołos, Intern. J. Quant. Chem., 1, 169(1967).

12) J. E. Lennard-Jones, Proc. Roy. Soc.(London), A129, 598 (1930).

Chapter 2

Long-range Interaction between a Hydrogen Atom and a Hydride Ion

I. Introduction

Generally, long-range forces among atoms and molecules are conveniently classified into two categories: the induction force and the dispersion force. The former is due to the long-range interaction energy between a neutral system and a cationic one, and the latter, to that between two neutral systems. Numerous theoretical studies have been devoted to these forces, particularly the systems composed of combinations of H^+, H, and He; the perturbation theory or equivalent variational methods have been used.[1] As a matter of course, the long-range interaction between a cation and an anion is Coulombic. Now, then, what kind of interaction operates between a neutral system and an anionic one ? In order to clarify the nature of the interaction energy between such systems, the long-range force between H and H^- is investigated in this Chapter as the simplest system.

The long-range force between H and H^- actually has an important role in the dissociation process of the H_2^- molecule

ion into H and H^- in the solar corona[2] and is referred to as considerably strong in spite of its anionic nature.[3] Theoretical investigations of the $H-H^-$ long-range force have been done only by Dalgarno and Kingston[4] and by Davison[5] using the usual multipole expansion of the second-order perturbation energy. The latter has evaluated the coefficients of the R^{-4}, R^{-6}, and R^{-8} terms in the series expansion of the inverse powers of the internuclear distance, R, between H and H^- (hereafter the above quantities are briefly represented as C_4, C_6, and C_8 *etc.* and the atomic unit is used for energies and distances throughout this Chapter). The results, however, were too poor to get the interaction energy by means of the multipole expansion, since the convergency of the series was bad, even in the asymptotic sense:

$$\bar{E}_2(\text{Davison}) = -\left(\frac{2.25}{R^4} + \frac{93}{R^6} + \frac{7\cdot 10^3}{R^8}\right) . \qquad (1)$$

For instance, the values of these terms are comparable at R=10; hence, one needs to estimate the higher-order terms at least in the region of *ca.* R=10.

In view of this inherent defect in the series expansion, an analytical form is desirable instead. The analytical formulae for the second-order perturbation energies with respect to the $H-H^+$, H-H, and He-He systems, neglecting exchange in the

framework of the Unsöld approximation, have been already investigated in the present author's laboratory.[6a-6d] In this Chapter, we will try to obtain a closed form of the second-order perturbation energy of the interaction between H and H^-, both in their ground states and, afterwards, to show an expansion form again derived from the closed one in order to discuss the nature of the force operating in this system.

II. Method of Calculation

As is well known, in the framework of the Unsöld approximation,[7] neglecting the exchange for a larger R, the second-order perturbation energy caused by a perturbation, H_1, can be represented by:

$$\bar{E}_2(\text{Unsöld}) = -\frac{\langle H_1^2 \rangle_{00} - \langle H_1 \rangle_{00}^2}{\langle \Delta E \rangle_{AV}} , \qquad (2)$$

where 0 means the eigenfunction, Φ_0, in the ground state with respect to the unperturbed Hamiltonian, H_0; $\langle \Delta E \rangle_{AV}$ is called an 'average excitation energy,' after Unsöld. In the cases of the H-H^- system, neglecting the exchange, Φ_0 appears as

follows:

$$\Phi_0 = \Psi_a(1)\Psi_b(2,3) \ , \qquad (3)$$

where $\Psi_a(1)$ is the 1s-function of a hydrogen atom, a, and where $\Psi_b(2,3)$ is a wavefunction of a hydride ion, b. In order to get an analytical form of $\bar{E}_2$(Unsöld), one needs a wavefunction, $\Psi_b(2,3)$, simple enough to be used for Φ_0, but also accurate enough to show the stability of H^-. The simplest form is one for the $1s^2\ {}^1S$ state, but it gives no stabilization of H^-.[8] The form employed here is a linear combination of the product of the 1s-like functions with different orbital exponents, z and z', for different spins:

$$\Psi_b(2,3) = \frac{1}{\sqrt{2(1+s^2)}} \left[\Psi_b(2)\Psi_b'(3) + \Psi_b(3)\Psi_b'(2) \right], \qquad (4)$$

where:

$$\Psi_b(i) = \frac{z^{3/2}}{\sqrt{\pi}} \exp[-zr_i] \ , \qquad (5\text{-a})$$

and

$$\Psi_b'(j) = \frac{z'^{3/2}}{\sqrt{\pi}} \exp[-z'r_j] \ , \qquad (5\text{-b})$$

and where:

$$s = \left(\frac{2\sqrt{zz'}}{z+z'} \right)^3 \ . \qquad (6)$$

The notations in the H-H^- system are shown in Figure 1. This wavefunction, which was first obtained by Chandrasekhar[9] and was thereafter used by Dalgarno *et al.*[3] and Fischer-Hjalmars[10] for the calculation of the energy of H_2^-, predicts the stability of H^- when $z' \sim z/3$; hence, it is assumed here that this wavefunction is the correct one for H^-. Using this $\Psi_b(2,3)$, an unperturbed wavefunction is constructed as follows:

$$\Phi_0 = \left(\frac{zz'}{\pi} \right)^{3/2} \frac{1}{\sqrt{2(1+s^2)}} \Big[\exp[-r_1] \cdot \{ \exp[-zr_2] \exp[-z'r_3] + \exp[-zr_3] \exp[-z'r_2] \} \Big] \ . \qquad (7)$$

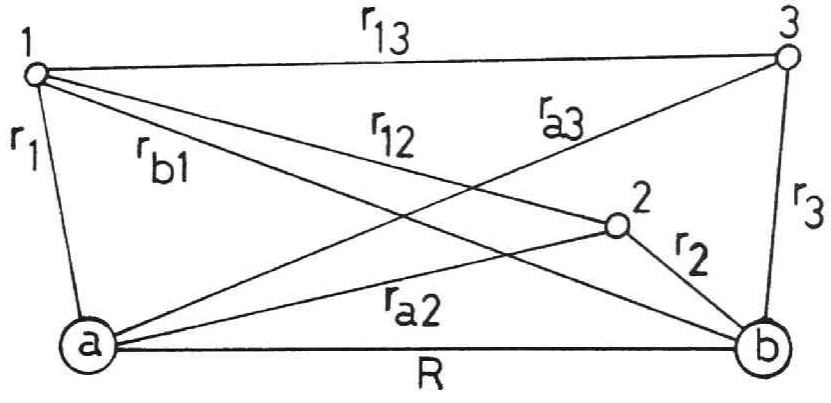

Figure 1. Notation for distances among electrons 1, 2, and 3, and nuclei a and b in the $H\text{-}H^-$ system.

The perturbation, H_1, between H and H^- at an internuclear distance, R, is written by:

$$H_1 = \frac{1}{R} - \frac{1}{r_{a2}} - \frac{1}{r_{a3}} - \frac{1}{r_{b1}} + \frac{1}{r_{12}} + \frac{1}{r_{13}} \quad , \tag{8}$$

which is then rearranged into three parts:

$$H_1 = [\frac{1}{r_{12}} + \frac{1}{R} - \frac{1}{r_{b1}} - \frac{1}{r_{a2}}] + [\frac{1}{r_{13}} + \frac{1}{R} - \frac{1}{r_{b1}} - \frac{1}{r_{a3}}]$$

$$- [\frac{1}{R} - \frac{1}{r_{b1}}] \equiv H_1(1,2) + H_1(1,3) - H_1(1) \quad . \tag{9}$$

It can easily be seen that the first two terms and the last term furthest to the right correspond to the interactions between H-H and that between $H-H^+$, respectively. Using the wavefunction in Eq.(7), $\langle H_1 \rangle_{00}$ and $\langle H_1^2 \rangle_{00}$ may be rewritten as:

$$\langle H_1 \rangle_{00} = \langle H_1(1,2) \rangle_{00} + \langle H_1(1,3) \rangle_{00} - \langle H_1(1) \rangle_{00}$$

$$= 2\langle H_1(1,2) \rangle_{00} - \langle H_1(1) \rangle_{00} \quad , \tag{10}$$

and:

$$\langle H_1^2 \rangle_{00} = \langle H_1^2(1,2) \rangle_{00} + \langle H_1^2(1,3) \rangle_{00} + \langle H_1^2(1) \rangle_{00}$$

$$+ 2\langle H_1(1,2)H_1(1,3)\rangle_{00} - 2\langle H_1(1,2)H_1(1)\rangle_{00}$$

$$- 2\langle H_1(1,3)H_1(1)\rangle_{00}$$

$$= 2\langle H_1^2(1,2)\rangle_{00} + \langle H_1^2(1)\rangle_{00} + 2\langle H_1(1,2)H_1(1,3)\rangle_{00}$$

$$- 4\langle H_1(1,2)H_1(1)\rangle_{00} \cdot \qquad (11)$$

It should be noticed that only the first two terms furthest to the right in Eq.(11) contain non-exponentially decreasing terms and therefore contribute to the origin of the long-range interaction. That is, the first term, $\langle H_1^2(1,2)\rangle_{00}$, corresponds to the second-order interaction energy of H-H with the well-known R^{-6} decay, while the second term, $\langle H_1^2(1)\rangle_{00}$, corresponds to that of $H\text{-}H^+$ giving the first leading term of R^{-4} in the Unsöld approximation except for the factors of the 'average excitation energy.'

Using Eqs.(10) and (11), Eq.(2) can be rewritten as:

$$\bar{E}_2(\text{Unsöld}) = -\frac{1}{\langle\Delta E\rangle_{AV}}\left[-\frac{2}{R^2} + \frac{4}{R}\langle H_1(2)\rangle_{00} - \langle H_1^2(1)\rangle_{00}\right.$$

$$\left. - 2\langle H_1^2(2)\rangle_{00} + 4\left\langle\frac{1}{r_{a2}}W(2,1)\right\rangle_{00} + 2\left\langle\frac{1}{r_{12}^2}\right\rangle_{00}\right.$$

$$+ 2\langle H_1(2)H_1(3)\rangle_{00} - 2\langle H_1(2)W(1,3)\rangle_{00}$$

$$- 2\langle H_1(3)W(1,2)\rangle_{00} + 2\langle W(1,2)W(1,3)\rangle_{00}$$

$$- 4\langle H_1(1,2)\rangle_{00}^2 - \langle H_1(1)\rangle_{00}^2$$

$$+ 4\langle H_1(1,2)\rangle_{00}\langle H_1(1)\rangle_{00} \quad], \qquad (12)$$

where:

$$W(1,i) = \frac{1}{r_{b1}} - \frac{1}{r_{1i}} \qquad (i=2,\ 3),$$

$$W(i,1) = \frac{1}{r_{ai}} - \frac{1}{r_{1i}} \qquad (i=2,\ 3)\ . \qquad (13)$$

In order to avoid complexity arising from the presence of many terms, some further notations are introduced. For any hermitian operator, F, the expectation value, $\langle F\rangle_{00}$, in which 0 stands for the function defined as in Eq.(7), is decomposed into three parts:

$$\langle F\rangle_{00} = \frac{1}{2(1+s^2)}[\{F|R,z,z'\} + \{F|R,z',z\} + 2s^2\{F|R,z'',z''\}$$

$$] \ , \qquad (14)$$

where s is defined as in Eq.(6), where z"=(z+z')/2, and where:

$$\{F|R,z,z'\} = \langle \Psi_a^*(1)\Psi_b^*(2)\Psi_b'^*(3)|F|\Psi_a(1)\Psi_b(2)\Psi_b'(3)\rangle \ ,$$

$$\{F|R,z',z\} = \langle \Psi_a^*(1)\Psi_b'^*(2)\Psi_b^*(3)|F|\Psi_a(1)\Psi_b'(2)\Psi_b(3)\rangle \ ,$$

and

$$\{F|R,z",z"\} = \langle \Psi_a^*(1)\Psi_b"^*(2)\Psi_b"^*(3)|F|\Psi_a(1)\Psi_b"(2)\Psi_b"(3)\rangle . \qquad (15)$$

In Eq.(15), the asterisk indicates the hermitian conjugate, $\Psi_b(i)$ and $\Psi_b'(j)$ are defined by Eqs.(5-a) and (5-b), and

$$\Psi_b"(k) = \frac{z"^{3/2}}{\sqrt{\pi}} \exp[-z"r_k] \ . \qquad (5\text{-c})$$

All the integrals used in Eq.(12) are shown in the Appendix. Thus, Eq.(12) may be evaluated exactly without resorting to a series expansion and can be given in a closed analytical form applicable to an arbitrary internuclear distance, R, and orbital exponents, z and z'.

III. Results and Discussion

In the calculation of $\bar{E}_2$(Unsöld), the values of the orbital exponents used by Fischer-Hjalmars[10] are adopted, that is, z=1.00, z'=0.30, and hence z"=(z+z')=0.65. As to $\langle\Delta E\rangle_{AV}$, three kinds of values can be considered: 1) the sum of the first ionization potentials of H and H^-, 0.52775[11], which is reasonable and is usually adopted, 2) the sum of the first excitation energies, 0.40275, which gives an approximate lower bound of $\bar{E}_2$(Unsöld), and 3) the sum of the ground state energies of H and H^-, -1.02775, which gives an approximate upper bound.[6c,6d] By substituting these values into Eq.(12), three kinds of $\bar{E}_2$(Unsöld) values for various R values are obtained as is shown in Table 1. The first-order perturbation energy, E_1, is equal to the expectation value, $\langle H_1\rangle_{00}$; it is also shown in Table 1 for each R.

On the other hand, Taylor and Harris have previously obtained a potential curve for the $^2\Sigma_u^+$ state of the H_2^- system using a CI method until R=7.0;[12] this seems to be the most reliable value at present. In Figure 2, three kinds of total interaction energy curves, (A), (B), and (C) taken as far as the second-order between the H and H^- obtained by means of the above criterion, are compared with the results of the variational calculation done by Taylor and Harris and also with the version modified here using the exact sum of the ground state energies of H and H^-, -1.02775, as the standard of the

Table 1. Long-range Interaction Energy ΔW between H and H^- in 10^{-3}a.u.

R (a.u.)	$-E_1$	$-\bar{E}_2$(Unsöld)[a]			$\Delta W=-E_1-\bar{E}_2$(Unsöld)[a]			CI[b]	Modified CI[c]
		(A)	(B)	(C)	(A)	(B)	(C)	(D)	(E)
4.0	5.8912	17.749	34.565	45.293	23.640	40.456	51.184	13.3	6.25
5.0	2.6218	8.4450	16.446	21.550	11.067	19.068	24.172	11.3	4.25
6.0	1.2900	4.3092	8.3919	10.996	5.5992	9.6819	12.286	9.3	2.25
7.0	0.67434	2.3220	4.5219	5.9253	2.9963	5.1962	6.5996	8.3	1.25
8.0	0.36306	1.2996	2.5309	3.3164	1.6627	2.8940	3.6795	-	-
9.0	0.19804	0.74726	1.4552	1.9069	0.94530	1.6532	2.1049	-	-
10.0	0.10863	0.43891	0.85473	1.1200	0.54754	0.96336	1.2287	-	-
11.0	0.059717	0.26288	0.51195	0.67084	0.32260	0.57167	0.73056	-	-
12.0	0.032853	0.16068	0.31292	0.41004	0.19353	0.34577	0.44289	-	-

a) $\langle\Delta E\rangle_{AV}$=1.02775, 0.52775, and 0.402775 in the cases (A), (B), and (C), respectively.

b) Ref. 12.

c) At R=∞, E=-1.02775.

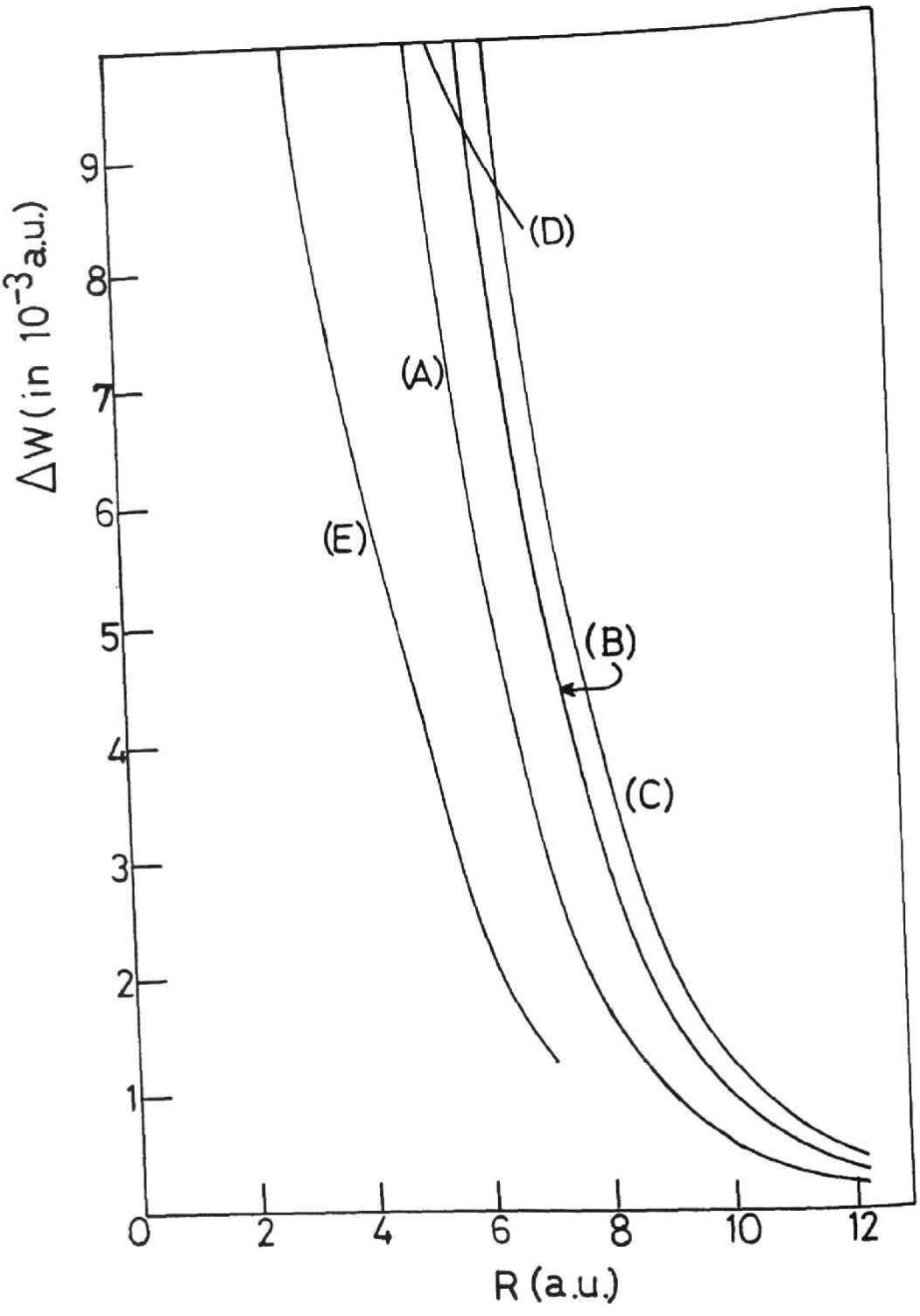

Figure 2. Long-range interaction energy ΔW between H and H^-. The notations (A), (B), (C), (D), and (E) are the same with those indicated in Table 1.

separated system. This modified version can afford a strict lower bound of the total interaction energy.[13] The potential curve (A) represents almost the lower bound of the interaction energy taken up to the second-order term, and (C), almost the upper bound. The exact one would lie in the zone between (A) and (C). The result of the original variational calculation, (D), lies above the zone obtained here. However, the modified version, (E), lies below.

Now, discarding the terms attenuating exponentially with an increase in R in Eq.(12), a reduced formula is obtained:

$$\bar{E}_2(\text{Unsöld}) \simeq -\frac{1}{\langle \Delta E \rangle_{AV}} \frac{1}{2(1+s^2)} [V(r,z) + V(R,z') + 2s^2 V(R,z'')] \quad (16)$$

where:

$$V(R,z) = \exp[-2R]\tilde{E}_i[2R] \{-1 + \frac{2z^4}{(1-z^2)^2} + (-\frac{1}{2} + \frac{z^4(5-z^2)}{(1-z^2)^3}) \frac{1}{R}\}$$

$$+ \exp[2R]Ei[-2R] \{-1 + \frac{2z^4}{(1-z^2)^2} + (\frac{1}{2} -$$

$$\frac{z^4(5-z^2)}{(1-z^2)^3}\Big)\frac{1}{R}\Big\}$$

$$+\exp[-2zR]\hat{\mathrm{Ei}}[2zR]\left\{-2z^2+\frac{2z^2}{(1-z^2)^2}+\Big(-z+\right.$$

$$\left.\frac{z(1-5z^2)}{(1-z^2)^3}\Big)\frac{1}{R}\right\}$$

$$+\exp[2zR]\mathrm{Ei}[-2zR]\left\{-2z^2+\frac{2z^2}{(1-z^2)^2}+\Big(z-\right.$$

$$\left.\frac{z(1-5z^2)}{(1-z^2)^3}\Big)\frac{1}{R}\right\}. \qquad (17)$$

In Eq.(17), $\hat{\mathrm{Ei}}[x]$ is the usual exponential integral, defined as:

$$\hat{\mathrm{Ei}}[x] = -\int_{-x}^{\infty}\frac{\exp[-t]}{t}\,dt, \text{ and, } \mathrm{Ei}[-x] = -\int_{x}^{\infty}\frac{\exp[-t]}{t}dt\,.$$

Using the well-known asymptotic expansion,

$$\exp[-x]\hat{\mathrm{Ei}}[x] \sim \sum_{n=1}^{\infty}\frac{(n-1)!}{x^n}, \text{ and } \exp[x]\mathrm{Ei}[-x] \sim$$

$$\sum_{n=1}^{\infty} \frac{(-1)^n (n-1)!}{x^n} \quad ,$$

the next formula is obtained:

$$V(R,z) = \frac{1}{R^4} + \frac{3(8+3z^2)}{2z^2}\frac{1}{R^6} + \frac{45(3+3z^2+z^4)}{z^4}\frac{1}{R^8}$$

$$+ \frac{315(16+18z^2+16z^4+5z^6)}{2z^6}\frac{1}{R^{10}}$$

$$+ \frac{14175(3z^8+10z^6+12z^4+12z^2+10)}{2z^8}\frac{1}{R^{12}} + \cdots \quad . \tag{18}$$

Using Eqs.(16) and (18), and substituting z=1.00, z'=0.30, and z"=0.65, a form of series expansion is obtained with respect to the inverse powers of R, which can be compared with Davison's result using Eq.(1), as follows:

$$\bar{E}_2(\text{Unsöld}) = -\frac{1}{\langle \Delta E \rangle_{AV}} \left(\frac{1}{R^4} + \frac{65.497}{R^6} + \frac{7116.8}{R^8} + \right.$$

$$\left. \frac{1.4302 \cdot 10^6}{R^{10}} + \frac{4.4604 \cdot 10^8}{R^{12}} + \cdots \right) . \tag{19}$$

In this series, at R=18, 14, and 10, the R^{-12} term is comparable with the R^{-10} term, the R^{-10} term with the R^{-8} term, and the R^{-8} term with the R^{-6} term. Adopting $\langle \Delta E \rangle_{AV}=0.52775$, which gives the potential (B) in Figure 2, $\bar{E}_2$(Unsöld) becomes:

$$\bar{E}_2(\text{Unsöld}) = -\left(\frac{1.8948}{R^4} + \frac{1.2411\cdot 10^2}{R^6} + \frac{1.3485\cdot 10^4}{R^8} + \frac{2.7100\cdot 10^6}{R^{10}} + \frac{8.4517\cdot 10^8}{R^{12}} + \cdots\cdot\right). \tag{20}$$

The results definitely show the divergent nature of the sequence C_{2n} (n=2, 3, 4, 5, 6, and so on). On the contrary, the use of the closed form obtained in this Chapter easily affords the value of $\bar{E}_2$(Unsöld) at any given R. It can easily be seen that the R^{-4} term comes from the first term of the induction force in the $H\text{-}H^+$ system:[14]

$$\bar{E}_2 = -\left(\frac{2.25}{R^4} + \frac{7.50}{R^6} + \frac{65.625}{R^8} + \frac{1063.125}{R^{10}} + \frac{27286.875}{R^{12}} + \cdots\cdots\right). \tag{21}$$

The other terms in Eq.(21) contribute little to Eq.(20). In

order to clarify this, we have calculated another series expansion with regard to the perturbation H_1:

$$H_1 = H_1(1,2) + H_1(1,3), \tag{22}$$

which involves no $H\text{-}H^+$ interaction, in contrast with Eq.(9). The results of expansion are as follows:

$$\bar{E}_2(\text{Unsöld}) = -\frac{1}{\langle \Delta E \rangle_{AV}} \left(\frac{60.998}{R^6} + \frac{7071.8}{R^8} + \frac{1.4294 \cdot 10^6}{R^{10}} + \frac{4.4601 \cdot 10^8}{R^{12}} + \cdots\cdots \right). \tag{23}$$

In this case, V(R,z) as defined in Eq.(16) becomes:

$$V(R,z) = \frac{12}{z^2} \cdot \frac{1}{R^6} + \frac{135(1+z^2)}{z^4} \cdot \frac{1}{R^8} + \frac{2520(1+z^4)+2835z^2}{z^6} \cdot \frac{1}{R^{10}} + \frac{70875(1+z^6)+85050(z^4+z^2)}{z^8} \cdot \frac{1}{R^{12}} + \cdots\cdots . \tag{24}$$

If one substitutes unity into z, this V(R,z) is clearly reduced to twice the value of the well-known H-H long-range interac-

tion previously obtained by Dalgarno and Lewis.[15] Comparing Eq.(19) with Eq.(23), the terms of higher-order than R^{-4}, therefore, prove to be mainly due to the dispersion force.

In Figure 3, some $\bar{E}_2$(Unsöld) curves obtained by the partial summation of the series in Eq.(20) are shown along with the result by Davison's series expansion in Eq.(1). It should be noticed that his expansion may be rather near to the present closed form at R values less than 6.0, while at larger R values there appears an underestimating tendency. On the other hand, the series expansion until the R^{-10} or R^{-12} term leads to an overestimation of the interaction energy at R values less than *ca.* 9.0.

In conclusion, it turns out that the closed form obtained above is effective for describing the long-range interaction for the $H\text{-}H^-$ system. Although the values of the second-order interaction energy predicted here have some ambiguousness because of the arbitrariness of the 'average excitation energy,' the upper and lower bounds obtained are reliable to a considerable extent. The series expansion described here shows that the dispersion force contributes to the nature of the interaction: when R is much larger, the R^{-4} term comes to be dominant, and hence the induction force begins to prevail over the dispersion. The former extraordinay large magnitude of the dispersion force mainly comes from the quantity of z' in Eq.

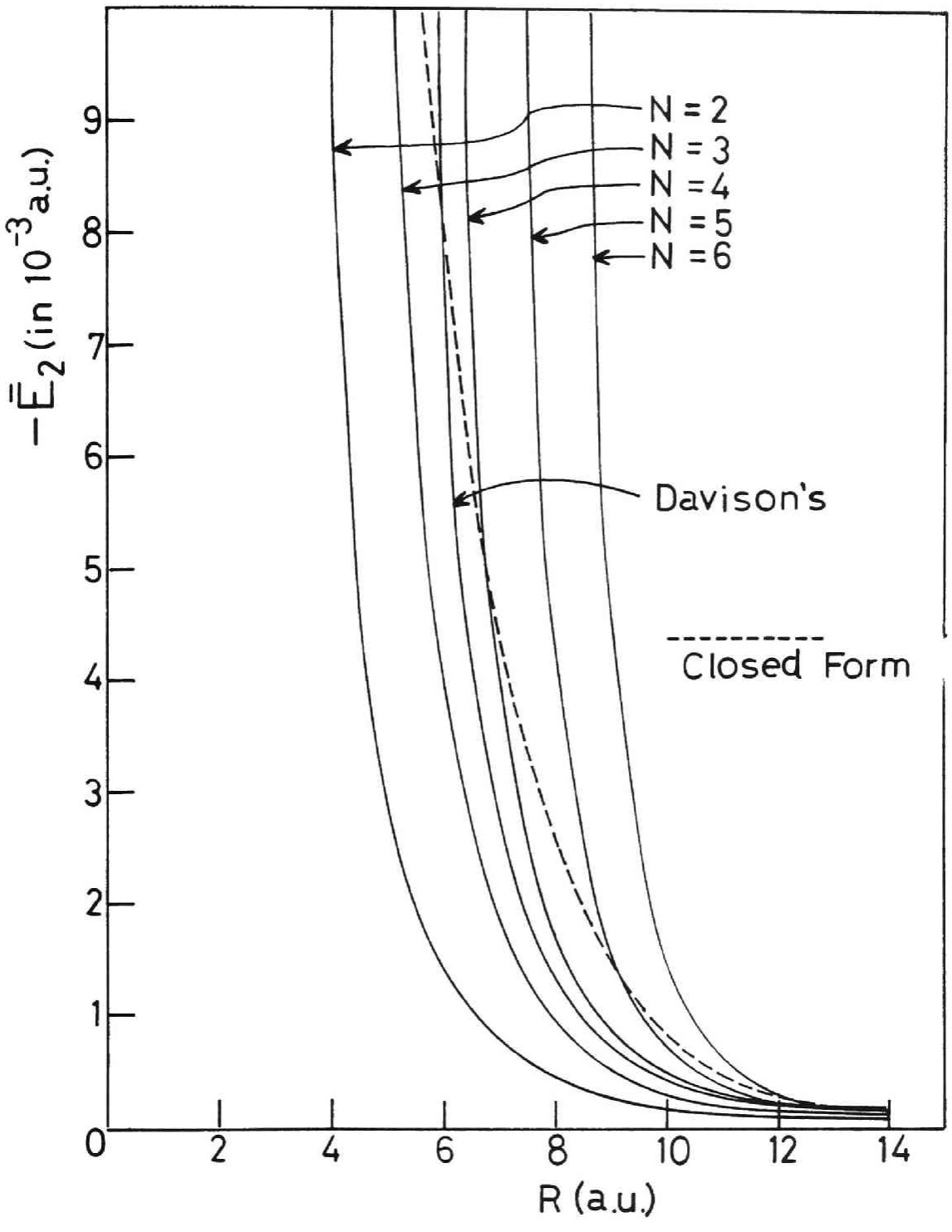

Figure 3. Various curves of the second-order perturbation energy in the $H\text{-}H^-$ system obtained by partial summations,

(to be continued on the next page)

$-\bar{E}_2$(Unsöld) = $\sum_{n=2}^{N} \frac{C_{2n}}{R^{2n}}$ in Eq.(20). The closed form curve corresponds to (B) in Table 1 and Davison's curve is based on the result in Ref. 5.

(7) -namely, the orbital exponent of the outer orbital in H^-. In other words, the weakly bound electron plays an important role in the origin of the large dispersion force in the system. Generally speaking, a weakly bound electron, which exists also in such anions as F^- or Cl^-, or the electron in frontier orbital with a similar physical nature, will maintain its importance when the system interacts with other distant species.

IV. Appendix

The miscellaneous integrals used in Eq.(12) are shown in the form of $\{F|R,z,z'\}$ in Eq.(15).

$$\{H_1(1)|R,z,z'\} = \int_{-\infty}^{\infty} \frac{1}{\pi} \exp[-2r_1]\left(\frac{1}{R} - \frac{1}{r_{b1}}\right) d\tau(1)$$

$$= \left(1 + \frac{1}{R}\right)\exp[-2R] \quad . \tag{A-1}$$

$$\{H_1(2)|R,z,z'\} = \int_{-\infty}^{\infty} \frac{z^3}{\pi} \exp[-2zr_2]\left(\frac{1}{R} - \frac{1}{r_{a2}}\right) d\tau(2)$$

$$= \left(z + \frac{1}{R}\right)\exp[-2zR]. \tag{A-2}$$

$$\{H_1(1,2)|R,z,z'\} = \int_{-\infty}^{\infty} \frac{z^3}{\pi^2} \exp[-2(r_1+zr_2)]\left(\frac{1}{R} + \frac{1}{r_{12}} - \frac{1}{r_{b1}} - \frac{1}{r_{a2}}\right)d\tau(1)d\tau(2)$$

$$= \frac{1}{(1-z^2)^3} \exp[-2R]\left\{(2z^4-3z^2+1) + \frac{1}{R}(-3z^2+1)\right\}$$

$$+ \frac{z^3}{(1-z^2)^3} \exp[-2zR]\left\{(-z^4+3z^2-2) + \frac{z}{R}(-z^2+3)\right\}, \quad (z\neq 1) \tag{A-3}$$

if $z=1$,

$$\{H_1(1,2)|R,1,z'\} = \exp[-2R]\left(\frac{1}{R} + \frac{5}{8} - \frac{3R}{4} - \frac{R^2}{6}\right). \tag{A-3'}$$

$$\{H_1^2(1)|R,z,z'\} = \int_{-\infty}^{\infty} \frac{1}{\pi} \exp[-2r_1]\left(\frac{1}{R^2} - \frac{2}{r_{b1}R} + \frac{1}{r_{b1}^2}\right)d\tau(1)$$

$$= -\frac{1}{R^2} + \frac{2}{R}\left(1 + \frac{1}{R}\right)\exp[-2R] + \left(1 + \frac{1}{2R}\right)\exp[-2R]\hat{E}i[2R]$$

$$+ \left(1 - \frac{1}{2R}\right)\exp[2R]Ei[-2R]. \tag{A-4}$$

$$\{H_1^2(2)|R,z,z'\} = \int_{-\infty}^{\infty} \frac{z^3}{\pi} \exp[-2zr_2]\left(\frac{1}{R^2} - \frac{2}{r_{a2}R} + \frac{1}{r_{a2}^2}\right)$$

$$d\tau(2) = -\frac{1}{R^2} + \frac{2}{R}(z + \frac{1}{R})\exp[-2zR]$$

$$+ (z^2 + \frac{z}{2R})\exp[-2zR]\hat{E}i[2zR] +$$

$$+ (z^2 - \frac{z}{2R})\exp[2zR]Ei[-2zR]. \qquad (A-5)$$

$$\{\frac{1}{r_{a2}}W(2,1)\,|\,R,z,z'\} = \int_{-\infty}^{\infty} \frac{z^3}{\pi^2}\exp[-2(r_1+zr_2)](\frac{1}{r_{a2}^2}$$

$$- \frac{1}{r_{a2}r_{12}})d\tau(1)d\tau(2)$$

$$= \exp[-2zR]\left[-z^2\log\left|\frac{z-1}{z+1}\right| + \frac{z^3}{1-z^2} + \frac{1}{R}(\frac{-z^2}{(1-z^2)^2}\right.$$

$$\left. - \frac{z}{2}\log\left|\frac{z-1}{z+1}\right|)\right] + \frac{z^2}{(1-z^2)^2R}\exp[-2R]$$

$$+ (z^2 + \frac{z}{2R})\exp[-2zR]Ei[-2(1-z)R]$$

$$+ (z^2 - \frac{z}{2R})\exp[2zR]Ei[-2(1+z)R], \quad (z\neq 1)$$

(A-6)

if z=1,

$$\{\frac{1}{r_{a2}} W(2,1)\,|R,1,z'\} = \exp[-2R]\left[-\frac{3}{4}+\frac{R}{2}+\left(1+\frac{1}{2R}\right)(\gamma + \log 4R)\right] + \exp[2R]\,Ei[-4R]\left(1-\frac{1}{2R}\right), \qquad \text{(A-6')}$$

where γ is Euler's constant, 0.5772156649····.

$$\{\frac{1}{r_{12}^2}\,|R,z,z'\} = \int_{-\infty}^{\infty} \frac{z^3}{\pi^2} \exp[-2(r_1+zr_2)]\,\frac{1}{r_{12}^2}\,d\tau(1)d\tau(2)$$

$$= \left[\frac{z^4}{(1-z^2)^2} + \frac{z^4(5-z^2)}{2(1-z^2)^3 R}\right]\exp[-2R]\,\tilde{Ei}[2R]$$

$$+\left[\frac{z^4}{(1-z^2)^2} - \frac{z^4(5-z^2)}{2(1-z^2)^3 R}\right]\exp[2R]\,Ei[-2R]$$

$$+\left[\frac{z^2}{(1-z^2)^2} + \frac{z(1-5z^2)}{2(1-z^2)^3 R}\right]\exp[-2zR]\,\tilde{Ei}[2zR]$$

$$+\left[\frac{z^2}{(1-z^2)^2} - \frac{z(1-5z^2)}{2(1-z^2)^3 R}\right]\exp[2zR]\,Ei[-2zR], \quad (z\neq 1) \qquad \text{(A-7)}$$

if z=1,

$$\{\frac{1}{r_{12}^2}|R,1,z'\} = -\frac{7}{12} + (\frac{5}{16R}+\frac{5}{8}+\frac{R}{2}+\frac{R^2}{6})\exp[-2R]\tilde{E}i[2R]$$

$$+ (-\frac{5}{16R}+\frac{5}{8}-\frac{R}{2}+\frac{R^2}{6})\exp[2R]Ei[-2R]. \quad (A-7')$$

$$\{H_1(2)H_1(3)|R,z,z'\} = \int_{-\infty}^{\infty} \frac{z^3 z'^3}{\pi^2} \exp[-2(zr_2+z'r_3)]$$

$$(\frac{1}{R^2} - \frac{1}{r_{a2}R} - \frac{1}{r_{a3}R} + \frac{1}{r_{a2}r_{a3}})d\tau(2)d\tau(3)$$

$$= (\frac{1}{R^2} + \frac{z}{R} + \frac{z'}{R} + zz')\exp[-2(z+z')R].$$

(A-8)

$$\{H_1(2)W(1,3)|R,z,z'\} = \{H_1(2)|R,z,z'\}\{W(1,3)|R,z,z'\}$$

$$= \frac{1}{(1-z'^2)^2}(z+\frac{1}{R})\left[\frac{1}{R}(-1+3z'^2)+(-1+2z'^2)\right]$$

$$\exp[-2(1+z)R] + \frac{1}{(1-z'^2)^2}(z+\frac{1}{R})\left[z' + \frac{1-3z'^2}{(1-z'^2)R}\right]$$

$$\exp[-2(z+z')R], \qquad (z'\neq 1) \qquad (A-9)$$

if $z'=1$,

$$\{H_1(2)W(1,3)|R,z,1\} = \exp[-2(1+z)R](z+\frac{1}{R})(\frac{R^2}{6}+\frac{3R}{4}+\frac{3}{8}).$$

(A-9')

$$\{H_1(3)W(1,2)|R,z,z'\} = \{H_1(3)|R,z,z'\}\{W(1,2)|R,z,z'\}$$

$$= \frac{1}{(1-z^2)^2}(z'+\frac{1}{R})\left[\frac{1}{R}(-1+3z^2)+(-1+2z^2)\right]$$

$$\exp[-2(1+z')R]$$

$$+\frac{1}{(1-z^2)^2}(z'+\frac{1}{R})\left[z+\frac{1-3z^2}{(1-z^2)R}\right]\exp[-2(z+z')R], \quad (z\neq 1)$$

(A-10)

if $z=1$,

$$\{H_1(3)W(1,2)|R,1,z'\} = \exp[-2(1+z')R](z'+\frac{1}{R})(\frac{R^2}{6}+\frac{3R}{4}$$

$$+\frac{3}{8}). \qquad \text{(A-10')}$$

$$\{W(1,2)W(1,3)|R,z,z'\} = \int_{-\infty}^{\infty}\frac{z^3z'^3}{\pi^3}\exp[-2(r_1+zr_2+z'r_3)]$$

$$\left(\frac{1}{r_{b1}}-\frac{1}{r_{12}}\right)\left(\frac{1}{r_{b1}}-\frac{1}{r_{13}}\right)d\tau(1)d\tau(2)d\tau(3)$$

$$= \exp[-2R]\left[\left[-\log\left|\frac{z+z'-1}{z+z'+1}\right| + \frac{(z+z')\{(z+z')^2+zz'-1\}}{\{1-(z+z')^2\}^2}\right.\right.$$

$$+\frac{1}{R}\left[-\frac{1}{2}\log\left|\frac{z+z'-1}{z+z'+1}\right|\right.$$

$$\left.\left.\left. + \frac{(z+z')\{(z+z')^4-(z+z')^2+zz'(z+z')^2+zz'\}}{\{1-(z+z')^2\}^3}\right]\right]\right.$$

$$+ \exp[-2(z+z')R]\left[\left[\frac{-zz'}{\{1-(z+z')^2\}^2} - \frac{z+z'}{\{1-(z+z')^2\}^3 R}\right.\right.\{$$

$$\left.\left.(z+z')^3-(z+z')^2-2(z+z')-2zz'+1\}\right]\right]$$

$$+ \exp[2R]\mathrm{Ei}[-2(z+z'+1)R]\left(1-\frac{1}{2R}\right)$$

$$+ \exp[-2R]\mathrm{Ei}[-2(z+z'-1)R]\left(1+\frac{1}{2R}\right). \qquad (|z+z'|\neq 1)$$

(A-11)

References and Notes

1) For example, see (a)"Intermolecular Force," in 'Advances in Chemical Physics,' ed. by J. O. Hirschfelder, Vol.12, Interscience Publishers, New York (1967); (b) P. R. Certain and L. W. Bruch, "Intermolecular Forces," in 'MTP International Review of Science, Theoretical Chemistry,' ed. by W. B. Brown, Vol.1, Univ. of Park Press, Baltimore (1972).

2) (a) Y. Öhman, Arkiv. Astron., 2, 1(1955); (b) H. A. Bethe and E. E. Salpeter, "Quantum Mechanics of One- and Two-Electron Atoms," Academic Press Inc., New York (1957), p.240.

3) A. Dalgarno and M. R. C. McDowell, Proc. Phys. Soc.(London), A69, 615(1956).

4) A. Dalgarno and K. E. Kingston, Proc. Phys. Soc.(London), A73, 455(1959).

5) W. D. Davison, Proc. Phys. Soc.(London), A87, 133(1966).

6) (a) K. Fukui and T. Yamabe, Intern. J. Quant. Chem., 2, 359(1968); 5, 478(1971); (b) T. Yamabe, S. Ishimaru, and K. Fukui, Bull. Chem. Soc. Jpn., 43, 2012(1970); (c) T. Yamabe, S. Ishimaru, and K. Fukui, Bull. Chem. Soc. Jpn., 45, 1384(1972); (d) T. Yamabe, S. Ishimaru, and K. Fukui, Bull. Chem. Soc. Jpn., 46, 2361(1973).

7) A. Unsöld, Z. Phys., 43, 374(1927).

8) H. Eyring, J. O. Hirschfelder, and H. S. Taylor, J. Chem. Phys., 4, 479(1936).

9) S. Chandrasekhar, Astrophys. J., 100, 176(1944).

10) I. Fischer-Hjalmars, Ark. Fys., 16, 33(1959).

11) Pekeris has obtained, by concentrated numerical efforts, the ground state energy of H^- as -0.52775 (Phys. Rev., 126, 1470(1962)). He has also thought that H^- has no more than one bound state; that is, the first ionization potential of H^- is 0.02775 to make the $H+e^-$ system. Power and Somorjai have tried to prove the above fact (Phys. Rev., A5, 2401(1972)), but in vain (Phys. Rev., A6, 1996(1972)). It is very likely, however, that H^- has no more than one bound state (Ref. 2(b)); hence, it is assumed here that the first ionization potential is 0.02775.

12) H. S. Taylor and F. E. Harris, J. Chem. Phys., 39, 1012 (1963).

13) It should be noticed that the lower and the upper bound alternate in the case of the interaction energy, since it is defined as a positive quantity.

14) A. Dalgarno and N. Lynn, Proc. Phys. Soc.(London), A70, 223(1957).

15) A. Dalgarno and J. T. Lewis, Proc. Phys. Soc.(London), A86,

239(1965).

Chapter 3

Interactions in Ion-Molecule Complexes

I. Introduction

In the field of intermolecular forces, there has been recent progress in the theoretical development of weak interactions, such as hydrogen bonds or ion-molecule bonds, based on *ab initio* calculations or fairly reliable semi-empirical calculations.[1,2)]

Of these, ion-molecule bonds consist of interaction between ions and neutral molecules in the singlet ground state. Such bonds have usually been investigated in order to comprehend the solvation process of ions in polar solvents, such as H_2O and NH_3.[1a,1b)] In contrast with the extensive studies of these ion-polar molecule complexes, there have been only a few studies of ion-non polar molecule complexes.

Recently it has become possible to obtain direct thermodynamical data on some ion-non polar molecule complexes in the gaseous state through the mass spectrometry of ion beams at low temperatures. Bennett, Field, and Beggs have obtained the equilibrium constants and thereby evaluated the ΔG_{300}, ΔH^0, and ΔS^0 values of the following reactions:[3-5)]

$$CH_5^+ + CH_4 \rightleftharpoons CH_5^+\text{-}CH_4 \qquad \Delta H^0 = -4.14\text{kcal/mol}$$

$$NH_4^+ + CH_4 \rightleftharpoons NH_4^+\text{-}CH_4 \qquad \Delta H^0 = -3.59\pm0.11\text{kcal/mol}$$

$$CF_3^+ + CH_4 \rightleftharpoons CF_3^+\text{-}CH_4 \qquad \Delta H^0 = -4.55\pm0.05\text{kcal/mol}$$

$$H_3O^+ + CH_4 \rightleftharpoons H_3O^+\text{-}CH_4 \qquad \Delta H^0 = -8.0\text{kcal/mol}$$

The $-\Delta H^0$ means the interaction energy needed to stabilize such an ion-molecule complex. They have also calculated the classical electrostatic interaction energy in order to discuss the stable configurations of these complexes.

Geometries suggested by the popular semi-classical electrostatic model[6] are often consistent with the experimental results or those calculated by MO method[7] for small ion-non polar molecule complexes, such as H_5^+ and HeH_3^+. It is, however, questionable whether this method yields reliable results for larger complexes such as the NH_4^+-CH_4 system, since it quite neglects the effect of charge transfer, which seems to play an important role in stabilizing these complexes. Indeed, the models proposed by the experimentalists are far from those conjectured from the reliable geometries of the H_3O^+-H_2O and NH_3-NH_3 systems.[1a,1b]

It may, therefore, be worthwhile to discuss the geometries of some typical ion-non polar molecule systems. In this Chapter, we will calculate the interaction energies in order to predict the stable configurations of the NH_4^+-CH_4, H_3O^+

$-CH_4$, and, additionally, $NH_4^+-H_2$ systems by means of the CNDO/2 method.[8] This method has yielded considerably reliable results on the interaction energies and stable configurations for neutral molecule systems and for cationic systems as well.[9] Furthermore, we will carry out the configuration analysis by expanding the MO of the optimized configuration in order to show the contributing factors which stabilize each complex.

II. Method of Calculation

The bond distances and angles in the isolated cations and molecules are optimized individually by the CNDO/2 calculation; they are shown in Table 1. For the $NH_4^+-CH_4$ system, in which both NH_4^+ and CH_4 have the C_2 axis and the C_3 axis, ten different kinds of configurations within the probable symmetries have been selected. The optimized configuration is determined for each interacting system by changing the intermolecular distance between NH_4^+ and CH_4; subsequently, several prominent parameters are optimized in the order of their magnitudes for the interaction energy.

For the $H_3O^+-CH_4$ system and the $NH_4^+-H_2$ system, details will be described later.

The method of configuration analysis[10] is applied to the most optimized configuration of each complex. A CI wavefunc-

Table 1. Bond Distances and Angles Used for Isolated Systems

Species	Bond	Distance (Å)	Angle	Size. deg
CH_4	C-H	1.115	H-C-H	109°28'
H_2	H-H	0.741[a)]	-	-
NH_4^+	N-H	1.077	H-N-H	109°28'
H_3O^+ [b)]	O-H	1.045	H-O-H	114°45'

a) Assumed.

b) Pyramidal form.

tion is briefly outlined here:

$$\Psi = C_0\Psi_0 + \sum_{i}^{occ}\sum_{l}^{uno} C_{i\to l}\Psi_{i\to l} + \sum_{k}^{occ}\sum_{j}^{uno} C_{k\to j}\Psi_{k\to j}$$

$$+ \sum_{i}^{occ}\sum_{j}^{uno} C_{i\to j}\Psi_{i\to j} + \sum_{k}^{occ}\sum_{l}^{uno} C_{k\to l}\Psi_{k\to l} + \cdots , \qquad (1)$$

where i, j, k, and l represent the i-th occupied MO of an isolated system, A, the j-th unoccupied of A, the k-th occupied of B, and the l-th unoccupied of B, respectively, and where the sign i→l indicates the one-electron shift from MO i to MO l and so on. One can thus make the CI wavefunction of the complexes if the coefficients are known. In order to see the contributing factors to the stabilization of the complexes, we construct a wavefunction:

$$\Psi = C_0\Psi_0 + \Big[\sum_{i}^{occ}\sum_{l}^{uno} (C_{i\to l})^2\Big]^{1/2}\Psi(A^+\cdot B^-)$$

$$+ \Big[\sum_{k}^{occ}\sum_{j}^{uno} (C_{k\to j})^2\Big]^{1/2}\Psi(A^-\cdot B^+) + \Big[\sum_{i}^{occ}\sum_{j}^{uno} (C_{i\to j})^2\Big]^{1/2}$$

$$\cdot\Psi(A^*\cdot B) + \Big[\sum_{k}^{occ}\sum_{l}^{uno} (C_{k\to l})^2\Big]^{1/2}\Psi(A\cdot B^*) + \cdots , \qquad (2)$$

where, for instance, $\Psi(A^+\cdot B^-)$ and $\Psi(A^*\cdot B)$ represent all of the

one-electron transferred configurations from A to B, and all of the one-electron excited configurations in A, respectively.

III. Results and Discussion

(i) The NH_4^+-CH_4 System

The selected configurations are shown in Figure 1, while the changes in the interaction energies with varying the distance between NH_4^+ and CH_4 are drawn in Figure 2. The optimized configuration turns out to be (A). The starred hydrogen atom in (A), (B), and (C) seems to play an important role in binding the systems. The values of the net charge of the hydrogen atoms are as follows: (A)+0.300, (B)+0.296, and (C) +0.289. It can easily be seen that the (A) configuration is the most advantageous for bonding, since the positively charged hydrogen contributes to bind the system as a bridging centre through Coulomb interaction with the carbon atom in CH_4. Henceforth, it may be said that the optimized configuration for the ion-molecule complex is mainly guaranteed by the existence of a positively charged hydrogen atom in the cation situated on the bonding axis of the complex as a bridging centre. Furthermore, the neutral molecule retains its highest symmetry and avoids the form in which a hydrogen atom in the molecule confronts the positively charged hydrogen atom in the cation.

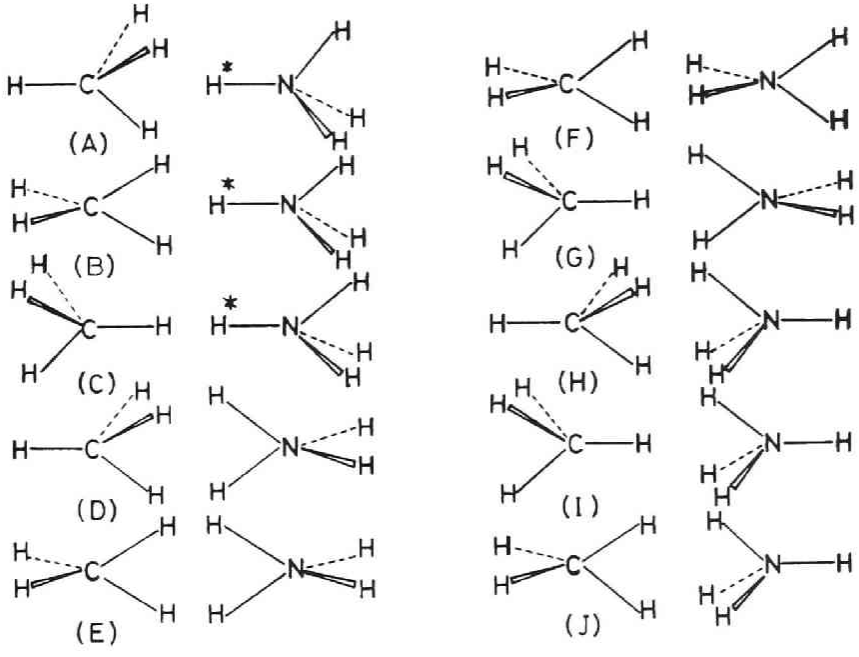

Figure 1. The selected configurations for the NH_4^+-CH_4 system.

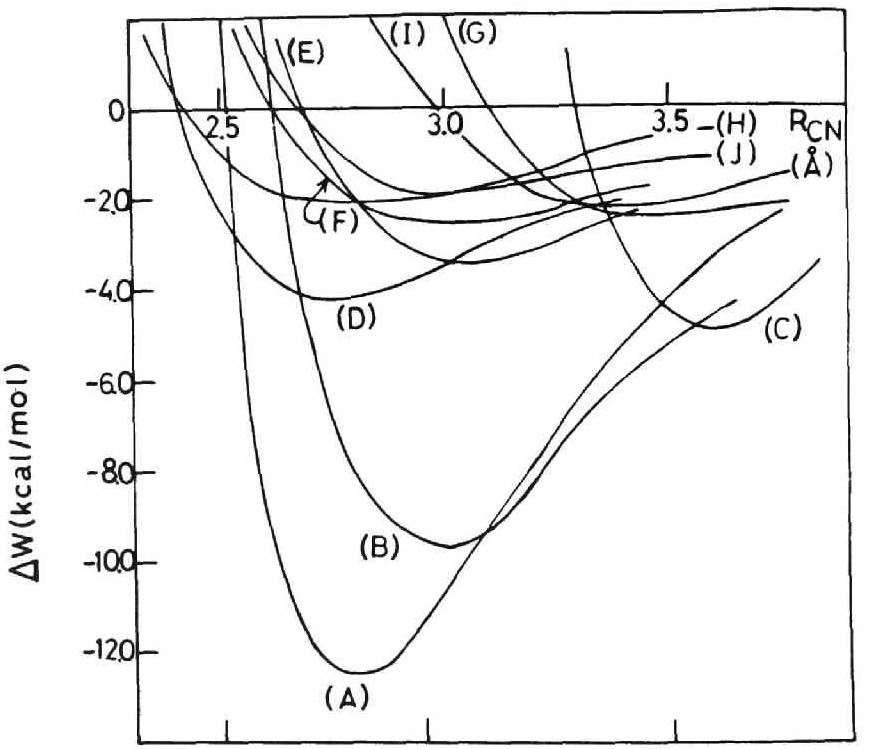

Figure 2. Potential curves of the selected configurations for the NH_4^+-CH_4 system. The 90° rotation of either fragment along the C-N axis in (B), (D), (G), or (j) or 180° rotation in (A) yields no energy change within an error.

Such a tendency coincides with the previous calculation results as to, for instance, the H_3O^+-H_2O and the H_2O-H_3O^+-H_2O systems. 1a)

The (A) configuration is next treated so as to be optimized with other parameters. The optimized (A) configuration in Figure 3 shows that R_{6N7H} stretches toward 1C as far as 1.117Å and that ∠3H1C4H *etc.* open a little to be 112°. Thus, the optimized energy of this system is 14.49kcal/mol (experimental: 3.59kcal/mol). One needs not further optimize the (B) configuration and those following in Figure 1, since they would not exceed the optimized (A) in Figure 3 in interaction energy. Interestingly, the configuration in Figure 4 proposed by Bennett and Field[5] is converse in the direction of the CH_4 and NH_4^+ from the optimized configuration predicted here. The E_{AB} analysis in the CNDO/2 method shows that the E_{1C7H} and E_{6N7H}-attractive energies have the largest effect in stabilizing the complex among the other attractive and repulsive energies. In fact, the eclipsed form yields the same $-\Delta W$ as that of the staggered form in Figure 3. Therefore, in this configuration, CH_4 and NH_4^+ seem to rotate along their bonding axis. The values of atomic net charge are also given in Figure 3; the quantity of the transferred charge from CH_4 to NH_4^+ is estimated to be -0.071.

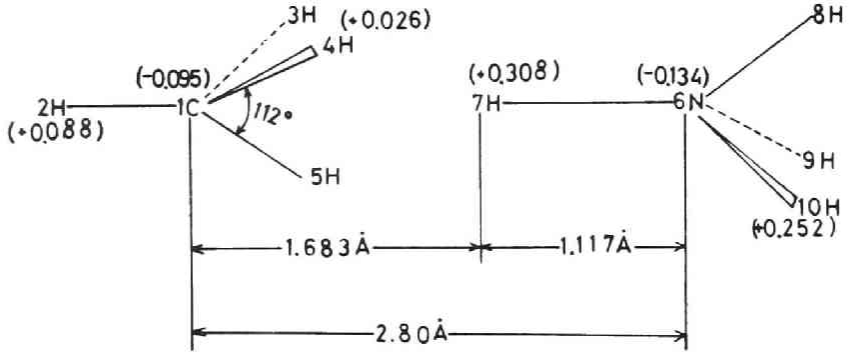

Figure 3. The optimized configuration of the NH_4^+-CH_4 system. R_{4H7H}=1.729Å and other bond distances remain unchanged.

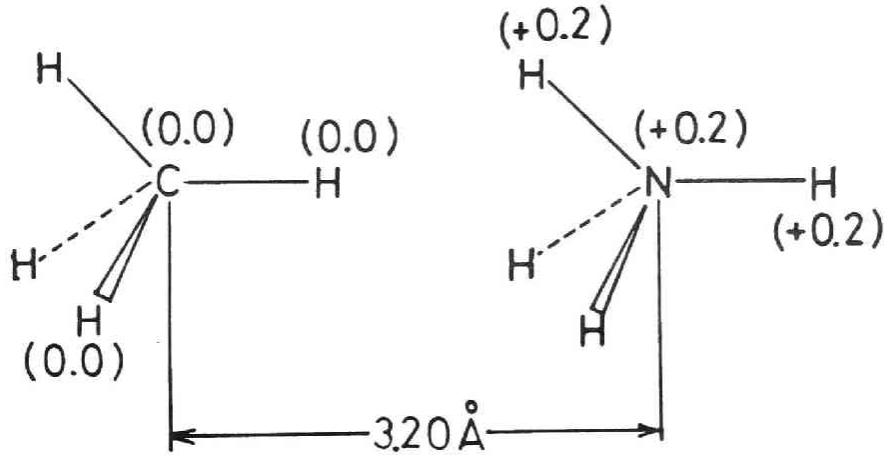

Figure 4. Bennett and Field's model for the NH_4^+-CH_4 system.

(ii) The H_3O^+-CH_4 System

For this system, five kinds of configurations are treated. The (A) configuration in Figure 5 is selected by the criterion noted above, and others that have C_{3v} geometries in both fragments are compared with (A). In Figure 6 the optimized configuration is shown to be (A), as was expected. The other configurations are far less stable than (A) in spite of their symmetries. A further optimized form of (A) is shown in Figure 7, where R_{6O7H} stretches toward 1C to be 1.115Å and where ∠3H1C4H *etc.* in CH_4 open until 114°. This is also quite the same pattern as in the NH_4^+-CH_4 system in Figure 3. The calculated interaction energy gives 31.56kcal/mol (experimental: 8.0kcal/mol). The configurations in Figure 8, previously proposed by Bennett and Field,[4] are quite different from the most optimized one predicted here.

As to the E_{AB} values, E_{1C7H} and E_{6O7H} are the dominant attractive energies, and the 90° **or** 180° rotation of either fragment along the C-H-O axis **yields** no energy change as in the NH_4^+-CH_4 system. Therefore, this system should also rotate freely along the C-H-O axis. The quantity of the transferred charge from CH_4 to H_3O^+ is -0.166, which is considerably larger than that in the NH_4^+-CH_4 system.

(iii) The NH_4^+-H_2 System

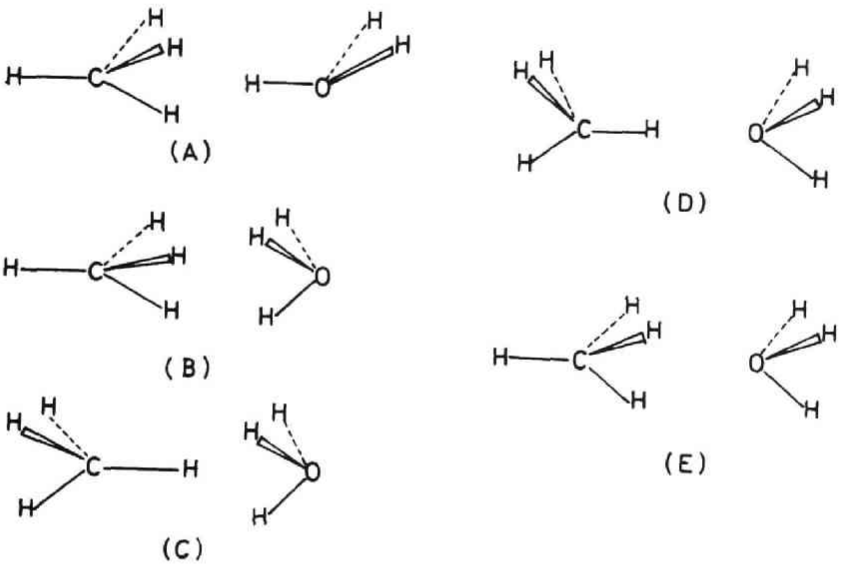

Figure 5. The selected configurations for the H_3O^+-CH_4 system.

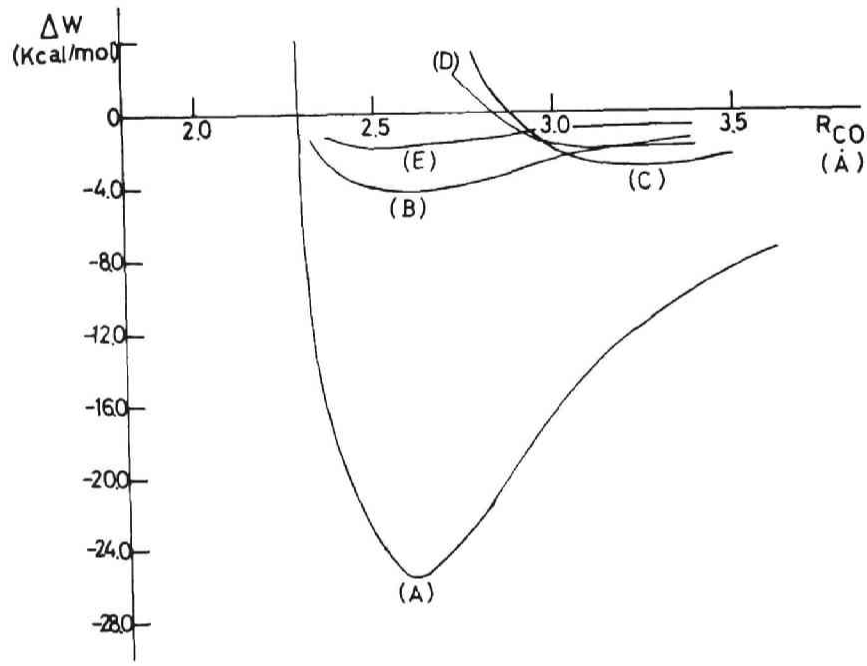

Figure 6. Potential curves of the selected configurations for the H_3O^+-CH_4 system. The 90° **or** 180° rotation of either fragment along the C-O axis in (A) yields no energy change within an error.

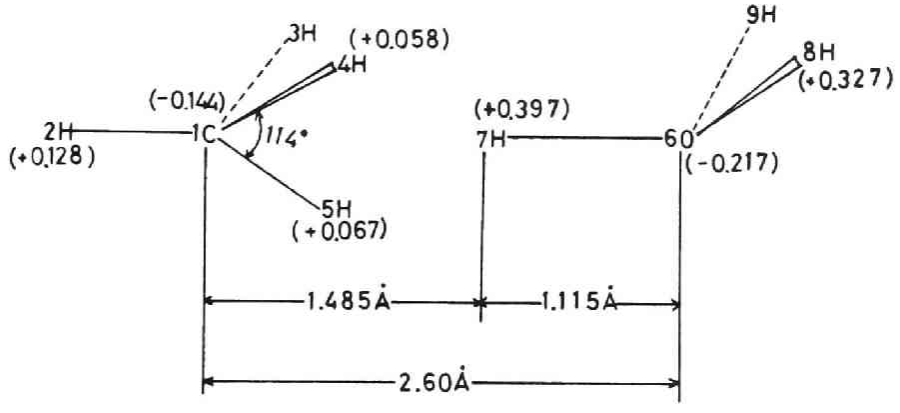

Figure 7. The optimized configuration for the H_3O^+-CH_4 system. R_{4H7H}=1.619Å and other bond distances remain unchanged.

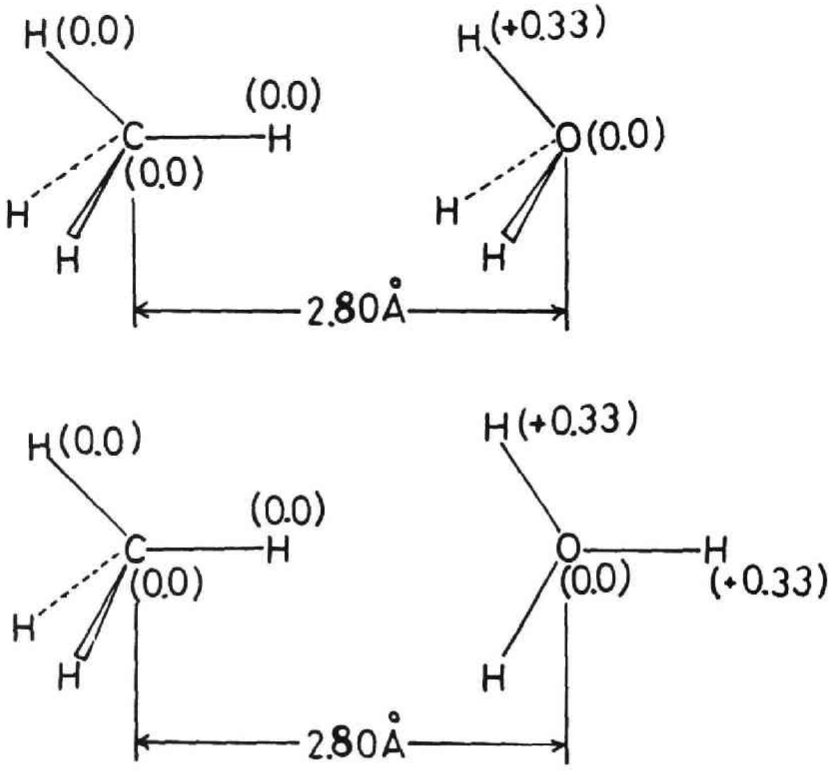

Figure 8. Bennett and Field's model for the H_3O^+-CH_4 system.

This system is considered to be a simple model of the ion-molecule complexes, although there are no previous experimental data available. Therefore, it seems that it would be interesting to predict the interaction energy and the optimized configuration for this system by MO theoretical treatment. In order to do so, four kinds of configurations were selected and their maximum interaction energies were calculated. The selected configurations and the potential curves are shown in Figure 9 and Figure 10, respectively. The interaction energy, $-\Delta W$, of the optimized (A) configuration is 3.07kcal/mol, while that of the secondary optimized (B) configuration is 2.13kcal/mol. Since these values are very close, both (A) and (B) should be further optimized. The results, presented in Table 2, show that the $-\Delta W$ in (A) remains unchanged, while that in (B) becomes 2.26kcal/mol. Therefore, the (A) configuration is still most stable. In Figure 11 the detailed form of the (A) configuration is presented. The quantity of the **transferred** charge from H_2 to NH_4^+ is -0.013, much less than those of the NH_4^+-CH_4 and the H_3O^+-CH_4 systems, and it produces less stabilization energy. The result that the difference in $-\Delta W$ values between (A) and (B) is only 0.81kcal/mol, which is the same order as kT at room temperature, implies that H_2 rotates in the space near NH_4^+. Furthermore, the experimental data of $-\Delta H^0$ of this system, if any, would be about 0.5∿0.75

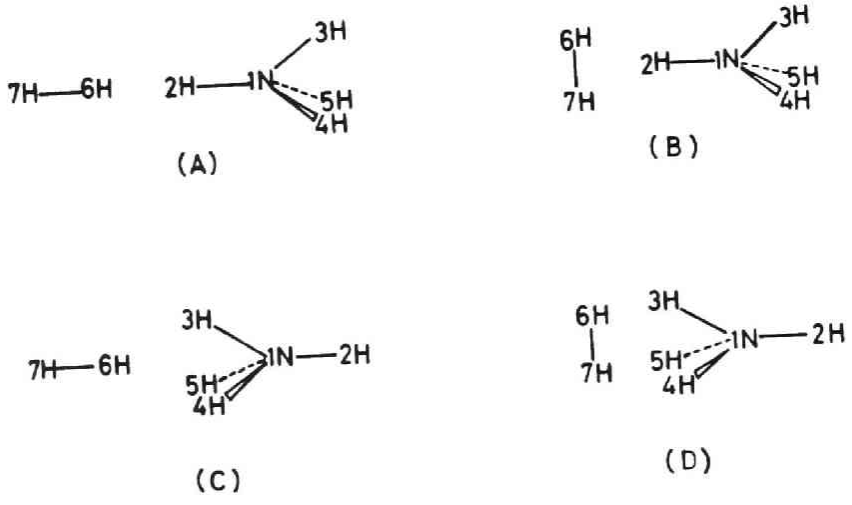

Figure 9. The selected configurations for the NH_4^+-H_2 system. .

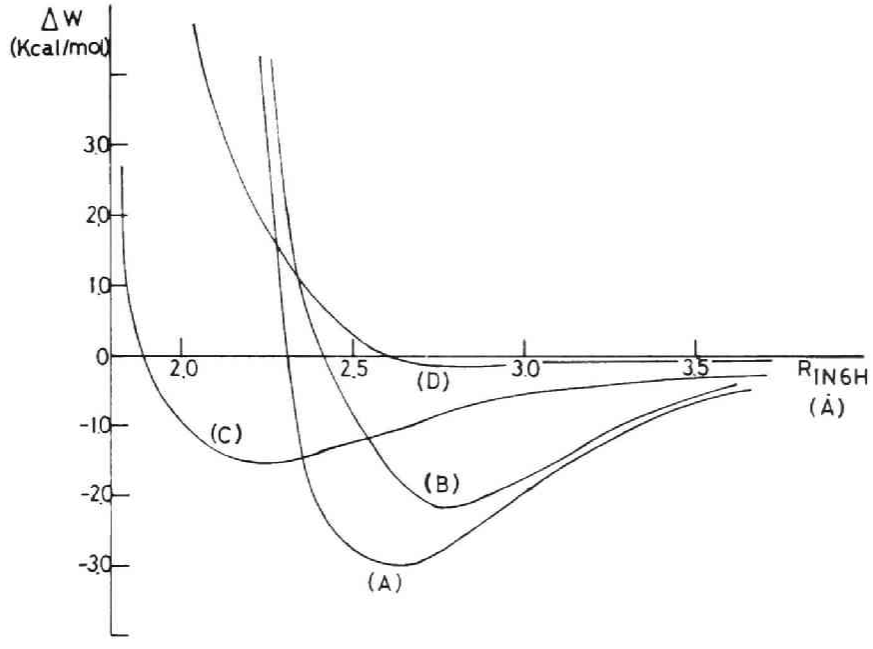

Figure 10. Potential curves of the selected configurations for the NH_4^+-H_2 system.

Table 2. The Interaction Energy of the NH_4^+-H_2 System

Configuration	Parameters	Interaction energy(kcal/mol)
(A)	R_{6H7H}[a)]=0.641Å	-7.45(Repulsive)
	0.741Å	3.07
	0.841Å	2.45
	R_{1N2H}=0.977Å	-9.98(Repulsive)
	1.077Å	3.07
	1.117Å	-3.70(Repulsive)
(B)	R_{6H7H}=0.721Å	1.57
	0.741Å	2.13
	0.761Å	2.13
	0.781Å	1.51
	R_{1N2H}=1.067Å	1.88
	1.077Å	2.13
	1.087Å	2.26
	1.097Å	2.20

a) 7H is fixed.

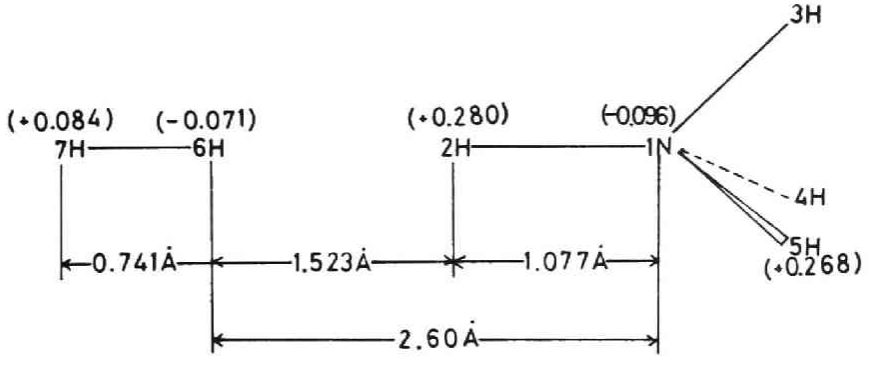

Figure 11. The optimized configuration for the NH_4^+-H_2 system.

kcal/mol, referring that the calculated -ΔW values for both the NH_4^+-CH_4 and the H_3O^+-CH_4 systems are four times the respective experimental values. If so, the -ΔW values for the (A), (B), (C), and (D) configurations will become closer, and (A) may change into (B), (C), or (D) in rapid succession, at least in the range of room temperature.

Thus, the NH_4^+-H_2 system is far from being a rigid complex. The two fragments, NH_4^+ and H_2, retain most of their individual integrity in the cluster. H_2 should be considered as distributed on a sphere about NH_4^+, with only a slight maximum probability at the calculated equilibrium configuration.

(iv)Configuration Analysis

Table 3 shows the results of the configuration analysis for the optimized configurations of the above systems. The values represent the weights (*i.e.*, the square of the coefficients in Eq.(2)) of the wavefunctions of various configurations. It can easily be seen that the more the weights of the charge transfer terms increase and that of the ground state decreases, the larger the stabilization energy appears, namely, the NH_4^+-H_2, the NH_4^+-CH_4, and the H_3O^+-CH_4 system, in order. The **percentage** contribution of the charge transfer term from the neutral molecule to the cation is particularly remarkable-that is, 1.47%, 7.22%, and 15.44% in the NH_4^+-H_2,

Table 3. The Weights of Various Configurations for Each System

Configurations	NH_4^+-CH_4	H_3O^+-CH_4	NH_4^+-H_2
Ground State	0.9130	0.8048	0.9797
Neutral→Cation Charge transfer	0.0722	0.1544 (0.0074)[a]	0.0147
Cation→Neutral Charge Transfer	0.0049	0.0058	0.0022
Polarization of Neutral Molecule	0.0031	0.0089	0.0030
Polarization of Cation	0.0044	0.0140	0.0002
Sum of the above Values	0.9977	0.9964[b]	0.9999

a) Two-electron transfer configuration.

b) All contributions from two-electron transfer are added.

NH_4^+-CH_4, and H_3O^+-CH_4 systems, respectively, compared with the contributions from the other configurations. The weight of the polarization term of the cation is larger than that of the neutral molecule in the NH_4^+-CH_4, and H_3O^+-CH_4 systems, while for the NH_4^+-H_2 system the weight in H_2 is 0.0030, surpassing that of NH_4^+.

In conclusion, it turns out that the previous results for these complexes obtained by the classical electrostatic method are deficient, since that method apparently neglects the charge transfer, which has a significant effect in stabilizing the complexes. On the contrary, the MO treatment allows us to predict the optimized configurations and display the essential factors which stabilize the complexes, as has been mentioned above. Lastly, it is interesting that the ion-molecule complexes investigated here are held by a kind of hydrogen bond, X··H-Y, in which X represents a carbon atom, and Y, a nitrogen or an oxygen atom. Since the H bears most of the positive charge in the cation, this X··H-Y bond is strong enough to hold the complex, and it yields a larger interaction energy than those of the ordinary hydrogen bond systems. Either fragment of the systems treated here is able to rotate freely along the axis of the X··H-Y because of the dominance of the E_{XH} and E_{HY}-attractive energies, which are isotropic with regard to this type of rotation. Furthermore, in the

NH_4^+-H_2 system H_2 would rotate three-dimensionally near NH_4^+, according to the CNDO/2 calculation. In the present calculation the convenient semi-empirical MO method has been used. An *ab initio* MO treatment for these complexes would be further expected.

References and Notes

1) (a) M. D. Newton and S. Ehrenson, J. Am. Chem. Soc., 93, 4971(1971); (b) P. A. Kollman and L. C. Allen, J. Am. Chem. Soc., 93, 4991(1971); (c) G. Alagona, R. Cimiraglia, and U. Lamanna, Theoret. Chim. Acta(Berl.), 29, 93(1973).

2) M. Losonczy, J. W. Moskowitz, and F. H. Stillinger, J. Chem. Phys., 59, 3264(1973).

3) F. H. Field and D. P. Beggs, J. Am. Chem. Soc., 93, 1585(1971).

4) S. L. Bennett and F. H. Field, J. Am. Chem. Soc., 94, 5188(1972).

5) S. L. Bennett and F. H. Field, J. Am. Chem. Soc., 94, 6305(1972).

6) K. G. Spears, J. Chem. Phys., 57, 1850(1972).

7) (a) R. D. Poshusta and V. P. Agrawal, J. Chem. Phys., 59, 2477(1973); (b) W. I. Salmon and R. D. Poshusta, J. Chem. Phys., 59, 4867(1973).

8) As to CF_3^+-CH_4 and CH_5^+-CH_4 systems, it is doubtful whether the CNDO/2 method is suitable to treat CF_3^+ and CH_5^+ isolated systems. Thus the reliable MO calculation results of these systems are of further indices.

9) For example, see O. Sinanoğlu and K. B. Wiberg, "Sigma Molecular Orbital Theory," Yale Univ. Press (1970).

10) (a) H. Baba, S. Suzuki, and T. Takemura, J. Chem. Phys., 50, 2078(1969); (b) H. Fujimoto, S. Kato, S. Yamabe, and K. Fukui, J. Chem. Phys., 60, 572(1974); (c) S. Kato, H. Fujimoto, S. Yamabe, and K. Fukui, J. Am. Chem. Soc., 96, 2024(1974).

Chapter 4

Stereoselection in Cross-bicyclization

I. Introduction

The stereoselective rules from the concept of the concerted cycloaddition reactions by Woodward and Hoffmann[1] or those from the orbital interaction approach, particularly among the highest occupied (HO) MO, the lowest unoccupied (LU) MO, and the singly occupied (SO) MO, by Fukui[2] have clearly interpreted steric control modes of both thermal and photo-induced (2+2) or (4+2) cycloadditions and so on. These rules have also been applied to most of the intramolecular cases without hesitation. Some of the recent experimental informations, however, have shown discrepancies with the predictions issued from the above rules with regard to the stereoselections in photo-induced (2+2) and (4+2) cycloadditions in the conjugated dienes and trienes, respectively. For instance, Padwa *et al.* have essentially provided (4_s+2_a) photoisomerizations of (1) and (2) in accordance with the rules of cycloadditions,[3]

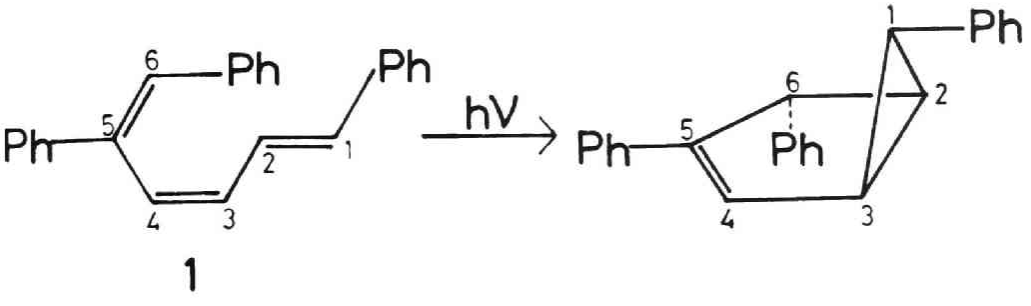

1

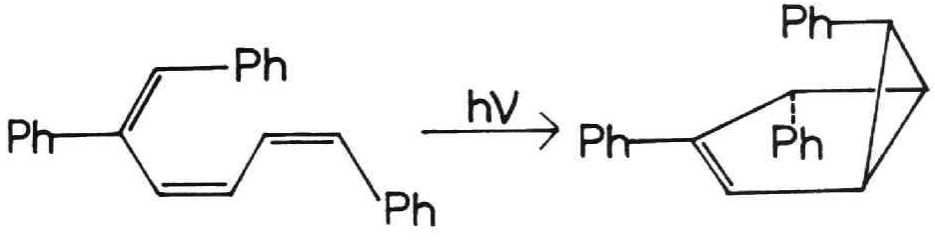

2

while, on the contrary, Courtot *et al.* have unambiguously observed disfavoured (4_a+2_a) modes in those of (3), (4), and (5) with monitoring by NMR.[4)]

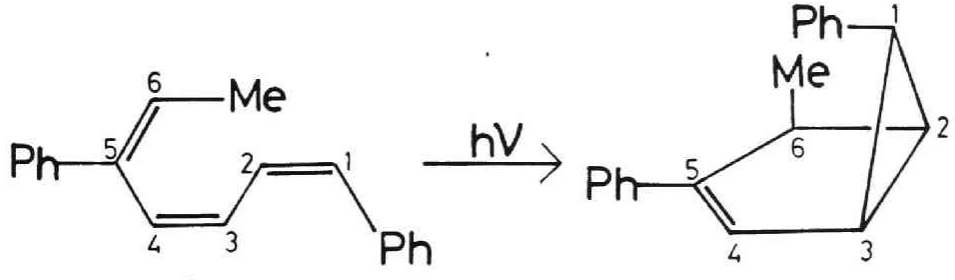

3

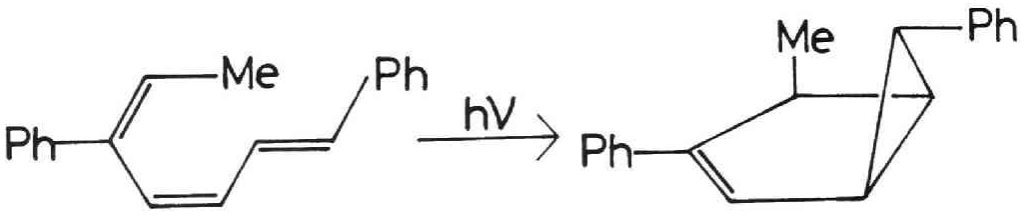

4

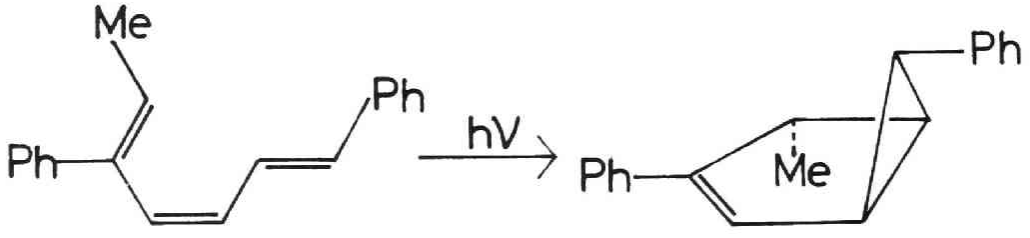

5

Other examples of disfavoured modes in photoisomerizations of dienes or trienes have also been found out[5-8] as will be shown later. Almost all of these "troublesome" reactions within the category of the usual cycloadditions have been excluded out from the concerted reactions. But why concerted in (1) and (2), and non-concerted in (3), (4), and (5) ? Can we not interpret the concertedness and the stereoselective modes of these bicyclizations in conjugated polyenes ? The

answer is yes. At first it should be pointed out that the stereoselective rules of the cycloaddition mentioned above are suitable for merely cyclic additions between two separate conjugated polyene parts whichever they are in different molecules or in a molecule. Therefore, from the theoretical point of view, one had better distinguish the nature of the bicyclizations in a conjugated polyene from the usual cyclic additions. In this Chapter, we will present a new theoretical interpretation, which is complementary to the concept of the concerted cycloaddition reactions, so that one might comprehend the concertedness and the stereoselective rules of the above reactions with "disfavoured" mode.

We define a simultaneous bicyclization between the r-th and the s-th and between the t-th and the u-th carbons ((6)→(7)) in a linear conjugated polyene containing 2n π electrons as a $[r,s/t,u]$ *cross-bicyclization* under the condition that r and s are odd and t and u are even or *vice versa*, where the numbering of carbons is counted from the end of conjugated carbon chain and $r<t<s<u$ holds. In the cross-bicyclization thus defined, the conjugation between the s-th and the t-th carbons generally exists throughout the process of reaction. This is the point of essential importance. If this conjugation does not exist, the reaction would turn out as a usual cycloaddition. In what follows, we try to es-

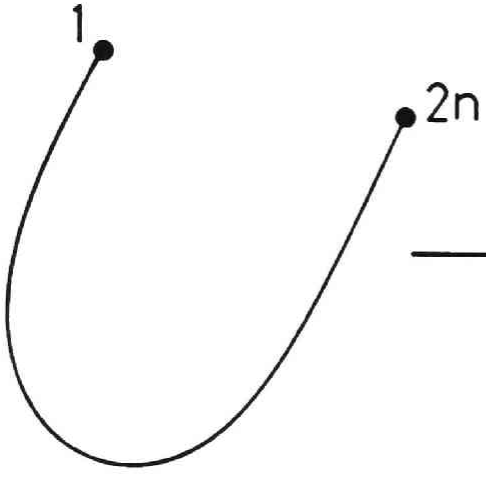

6

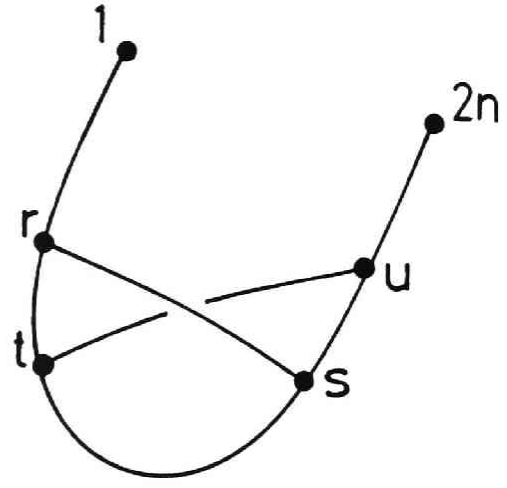

7

tablish a simple but reasonable method in such reactions employing the perturbation theory in the scheme of the Hückel MO approach.[9] Similar method has been used successfully to treat the stereospecific ring-closure of conjugated polyenes.[10] Then the predicted stereoselective rules will be applied to interpret the latest several experimental results.

II. Formulation

Consider two simultaneous conjugations, $k\beta$ and $l\beta$, appearing as a perturbation as indicated in (6').

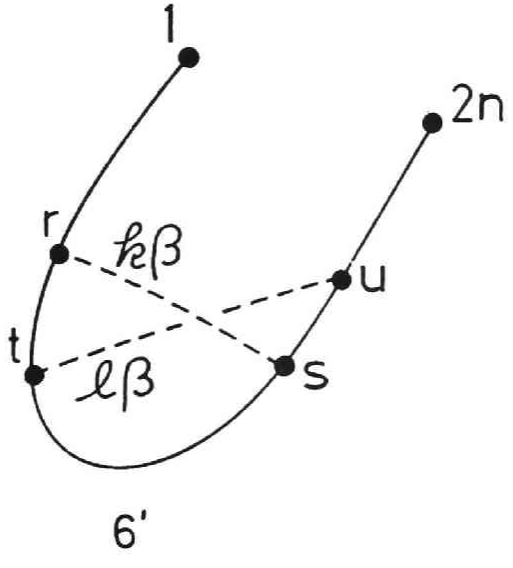

The quantity β is the resonance integral between two adjacent 2pπ atomic orbitals (AO's). Hence, $k\beta$, for instance, is adopted to be the resonance integral between ϕ_r and ϕ_s when σ-like overlapping of these two AO's in the distorted π electron system occurs, where ϕ_r denotes 2pπ AO of the r-th carbon. The sign of $k\beta$ and $l\beta$ concerns the mode of overlap stabilization as indicated below.

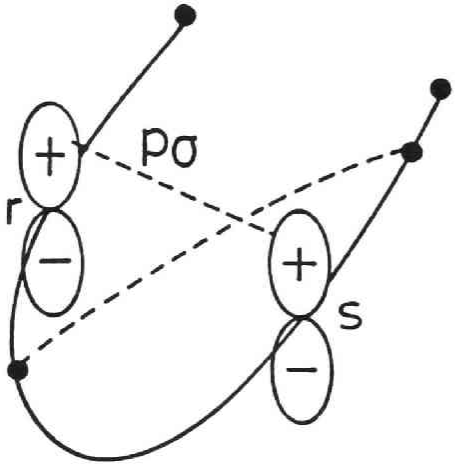

$k\beta<0$ ($k>0$); Disrotatory

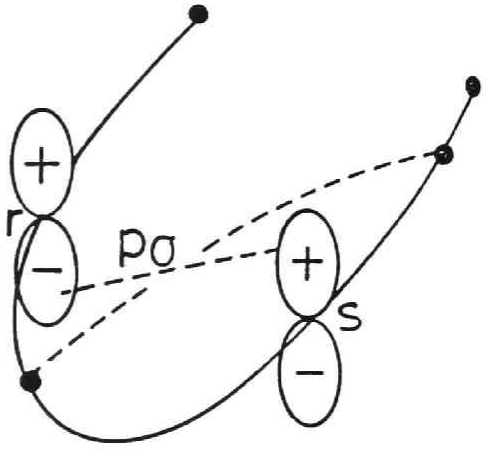

$k\beta>0$ ($k<0$); Conrotatory

Letting α be the Coulomb integral of 2pπ AO, the perturbed secular determinant in the present case becomes as follows.

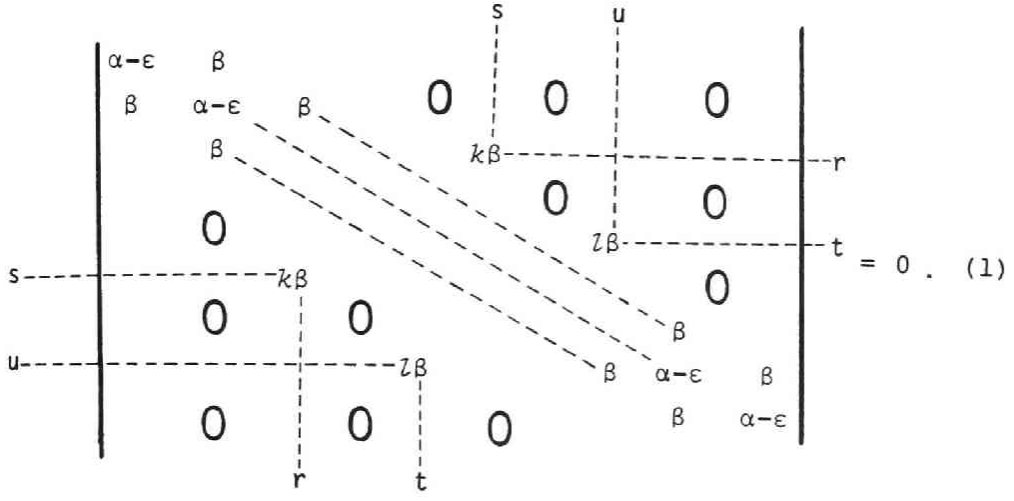

$$= 0 . \quad (1)$$

According to the procedure previously reported ("method of perturbed secular determinant"),[11] we get the following formula within the second-order perturbation treatment.

$$\frac{\Delta E}{\beta} = 2kP_{rs} + 2lP_{tu} + k^2\Pi_{rs,rs} + 2kl\Pi_{rs,tu} + l^2\Pi_{tu,tu} . \quad (2)$$

Here ΔE represents the change in the π-electronic energy, and P_{rs} and $\Pi_{rs,tu}$ are the same quantities as the usual bond-order and bond-bond-polarizability, respectively, defined as

$$P_{rs} = \sum_{i}^{all} n_i C_r{}^i C_s{}^i \ , \qquad (3)$$

$$\Pi_{rs,tu} = \frac{1}{2} \sum_{i}^{all} \sum_{j(\neq i)}^{all} n_i (2 - n_j)$$

$$\cdot \frac{(C_r{}^i C_s{}^j + C_r{}^j C_s{}^i)(C_t{}^i C_u{}^j + C_t{}^j C_u{}^i)}{x_i - x_j} \ , \qquad (4)$$

$$\left(x_i = \frac{\varepsilon_i - \alpha}{\beta}\right)$$

where n_i, ε_i, and $C_r{}^i$ represent the occupation number, the orbital energy, and the coefficient of ϕ_r, respectively, of the i-th MO of the unperturbed system (6). Since the sign of β is negative, the overlap stabilization is brought about in the system when the sign of right hand side in Eq.(2) becomes positive. We have only to judge the sign of the next formula, because the required values of P_{rs} and P_{tu} vanish in the case of the present 2n conjugated polyene.

$$\frac{\Delta E}{\beta} = k^2 \Pi_{rs,rs} + 2kl\Pi_{rs,tu} + l^2 \Pi_{tu,tu} \ . \qquad (2')$$

It is easily shown that this quadratic form is positive by the Cauchy-Schwartz' inequality. According to the sign of the $\Pi_{rs,tu}$ value, the mode of cross-bicyclization may be classified into the following four types of rotation in the direction of increasing value of $\Delta E/\beta$.

$\Pi_{rs,tu}$	k	l	Rotating Mode
positive	positive	positive	A(disrotatory-disrotatory)
	negative	negative	B(conrotatory-conrotatory)
negative	positive	negative	C(disrotatory-conrotatory)
	negative	positive	D(conrotatory-disrotatory)

No distinction can be made of mode A from B, nor of mode C from D within the present second-order perturbation treatment. However, in some favourable cases, consideration of steric circumstances, which is important in such cases as the cross-bicyclization, may assist in predicting the more probable mode.

III. Stereoselective Modes of Cross-bicyclization and Cycloaddition

For the cases of diene, triene, and tetraene, we show all kinds of rotating modes in thermal and photo-induced cross-bicyclizations in Table 1 along with the numerical values of $\Pi_{rs,tu}$. In photo-induced cases, $\Pi_{rs,tu}$ is calculated in regard to the first excited configuration. It is clearly seen that the predicted modes make no difference in both thermal and photo-induced reactions in each cross-bicyclization. These predictions are remarkably different from those issued from the concept of the cycloaddition by Woodward and Hoffmann or from the frontier orbital interaction approach. It should be also emphasized that mode A and B are favoured when (s-r)+(u-t) is equal to 4m+2, while mode C and D are favoured when it is 4m in the polyenes. The cases of longer polyenes could be also treated by a simple extension of the present calculations, with which we will not further deal in this Chapter.

Let us treat here some of the usual cycloadditions with our formulation for the sake of comparison. In the case of the (4+2) cycloaddition, for instance, the triene is divided into a diene and an olefin and thus the conjugation between C_2 and C_3 are cut off as shown in Figure 1(A). In this case, the amplitudes of the frontier orbitals on C_1, C_2, C_3, and C_6 are large and the orbital energy differences among them are small as a matter of fact, so $\Pi_{rs,tu}$ defined in Eq.(4) mainly depends on the expansion terms of (i,j)=(2,4) and (3,5) in the thermal

Table 1. Rotating Mode in Cross-bicyclization

polyene	[r,s/t,u]	Thermal	($\Pi_{rs,tu}$)	Photo-induced	($\Pi_{rs,tu}$)
diene	[1,3/2,4][a]	C, D	(-0.3578)	C, D	(-0.1789)
triene	[1,3/2,6][b]	A, B	(0.2352)	A, B	(0.0762)
	[1,3/2,4]	C, D	(-0.2906)	C, D	(-0.0694)
	[1,5/2,6]	C, D	(-0.3597)	C, D	(-0.1661)
	[3,5/2,4]	C, D	(-0.0274)	C, D	(-0.2072)
tetraene	[1,3/2,4]	C, D	(-0.2659)	C, D	(-0.0410)
	[1,3/2,6]	A, B	(0.2013)	A, B	(0.0053)
	[1,3/2,8][c]	C, D	(-0.1809)	C, D	(-0.0029)
	[1,5/2,6]	C, D	(-0.2998)	C, D	(-0.1269)
	[1,5/2,8]	A, B	(0.2359)	A, B	(0.0725)
	[1,5/4,6]	A, B	(0.1863)	A, B	(0.0830)
	[1,5/4,8][d]	C, D	(-0.1685)	C, D	(-0.1135)
	[1,7/2,8]	C, D	(-0.3548)	C, D	(-0.1965)
	[3,5/4,6]	C, D	(-0.2270)	C, D	(-0.0878)
	[3,5/2,4]	C, D	(-0.0311)	C, D	(-0.1626)
	[3,7/2,6]	C, D	(-0.0515)	C, D	(-0.1649)
	[3,7/2,4]	A, B	(0.0054)	A, B	(0.0801)

a, *b*, *c*, and *d* have been classified into (2+2), (4+2), (6+2), and (4+4) cycloaddition, respectively, up to now.

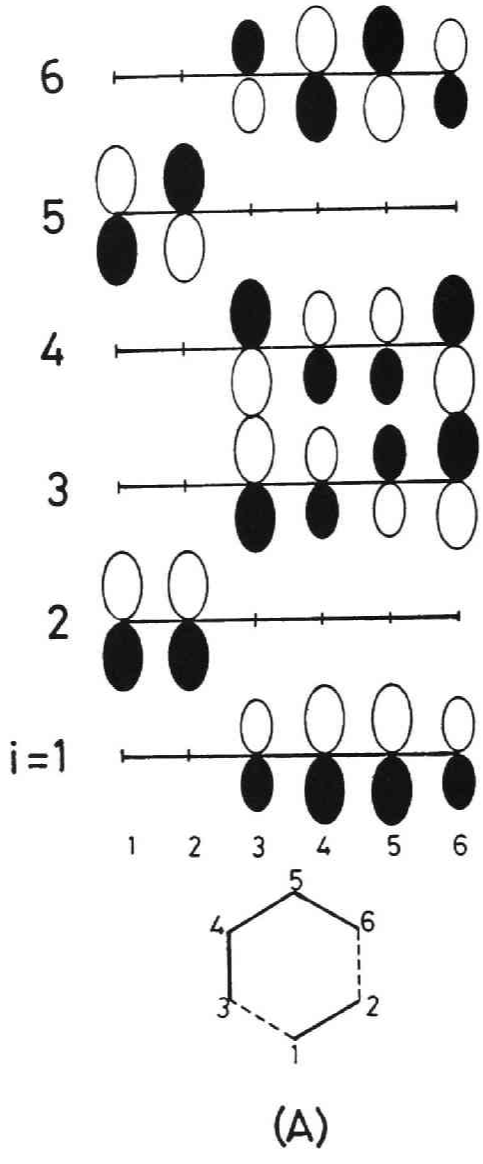

Figure 1. Orbital patterns of the systems composed of (A) an olefin and a diene, and (D) a triene. (B) and (C) show the frontier orbital interactions in (A) in thermal and photo-induced **processes**, respectively. It should be noted that σ bond between C_2 and C_3 may remain in (A).

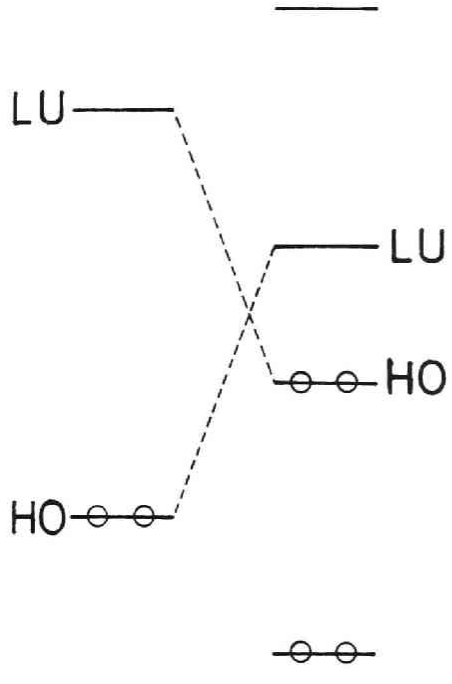

(B)

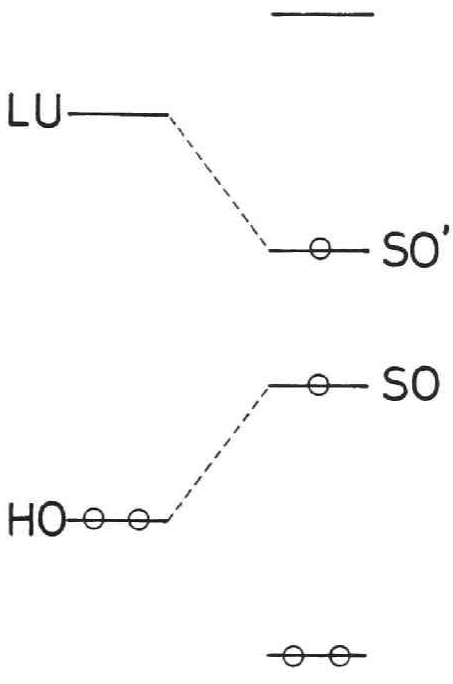

(C)

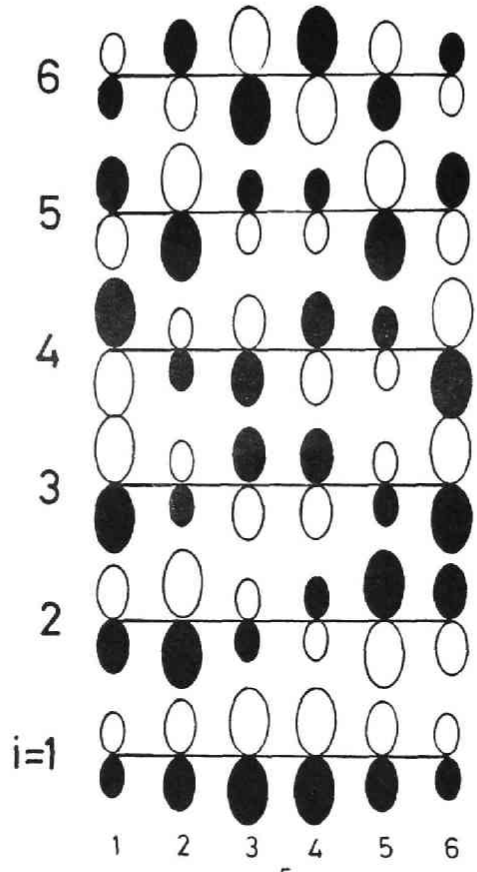

(D)

process, while of (i,j)=(2,3) and (4,5) in the photo-induced process. In other words, the HOMO-LUMO interactions in the former process and the HOMO-SOMO and the SO'MO-LUMO interactions in the latter between a diene and an olefin shown in Figures 1(B) and (C), respectively, are essentially important in order to predict the distinct stereoselective mode in each process of the cycloaddition. On the contrary, in the case of the cross-bicyclization in a triene, the same criterion would no longer serve because of the alterations of the amplitudes in the MO's with i=2, 3, 4, and 5 on the concerned carbons as shown in Figure 1(D). In this sense one can not expect a conspicuous difference of the stereoselective mode between the thermal and photo-induced processes and has to sum up extending over all MO's such as in Eq.(4) in order to judge the signs of the $\Pi_{rs,tu}$'s in the cross-bicyclization apart from the cycloaddition.

The values of $\Pi_{rs,tu}$ along with the contributing terms arising from the frontier orbital interactions and the predicted stereoselective modes in thermal and photo-induced cycloadditions for the cases of (2+2), (4+2), (6+2), and (4+4) are listed in Table 2, where $\Pi_{rs,tu}$'s are formally evaluated with setting the resonance integrals at the concerned positions to be zero in Eq.(1). In photo-induced (2+2) and (4+4) cases, the degeneracies between the HOMO and the SOMO and be-

Table 2. Stereoselective Mode in Cycloaddition through the Treatment of the Present Formulation

Type of Cycloaddition	Thermal ($\Pi_{rs,tu}$; its main term[a])	Photo-induced ($\Pi_{rs,tu}$; its main term[b])
2+2	C, D (-0.5000; -0.5000) (2_s+2_a or 2_a+2_s)	A, B ($+\infty$; $+\infty$) (2_s+2_s or 2_a+2_a)
4+2	A, B (0.3416; 0.4472) (2_s+4_s or 2_a+4_a)	C, D (-0.8292; -0.9472) (2_s+4_a or 2_a+4_s)
6+2	C, D (-0.2588; -0.3759) (2_s+6_a or 2_a+6_s)	A, B (0.4185; 0.4893) (2_s+6_s or 2_a+6_a)
4+4	C, D (-0.2683; -0.4236) (4_s+4_a or 4_a+4_s)	A, B ($+\infty$; $+\infty$) (4_s+4_s or 4_a+4_a)

[a] Contribution to $\Pi_{rs,tu}$ from the HOMO-LUMO interactions between two separate polyene parts.

[b] Contribution to $\Pi_{rs,tu}$ from the HOMO-SOMO and the SO'MO-LUMO interactions between two separate polyene parts.

tween the SO'MO and the LUMO invalidate to evaluate the required $\Pi_{rs,tu}$. Actually, however, these degeneracies would be reduced by the energetical splittings between these MO's on account of the presence of the electron correlation as illustrated in Figure 2.[12] Therefore, we tentatively set here the values of $(x_{HO}-x_{SO})$ and $(x_{SO'}-x_{LU})$ in Eq.(4) to be infinitely small positive, from which the concerned $\Pi_{rs,tu}$'s are positive infinite. This means that photo-induced [1,3/2,4] cross-bicyclization of diene or [1,5/4,8] case of tetraene might rather favour the (2+2) or (4+4) cycloaddition, respectively, from the viewpoint of the energetical stabilization, as will be seen in the next section.

IV. Application

(i) [1,3/2,4] Cross-bicyclization of Diene

Dauben and Ritscher have early obtained the photoproducts (9), (11), and (12) from ethylidenecyclooctenes (8) and (10).[5]

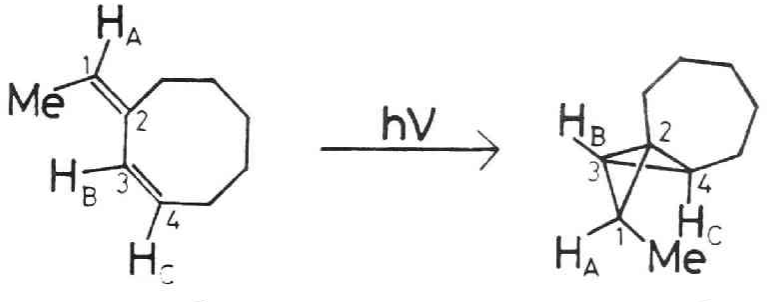

8 9

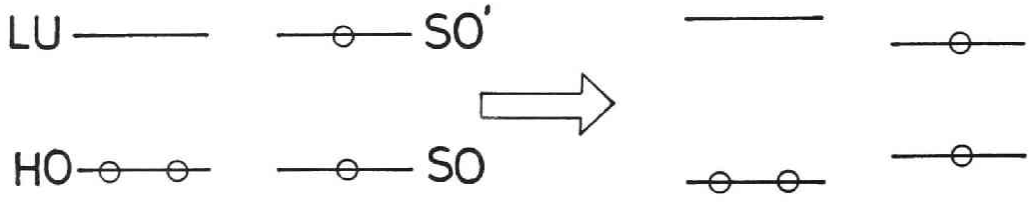

Figure 2. The splittings of the levels between the HOMO and the SOMO and between the SO'MO and the LUMO.

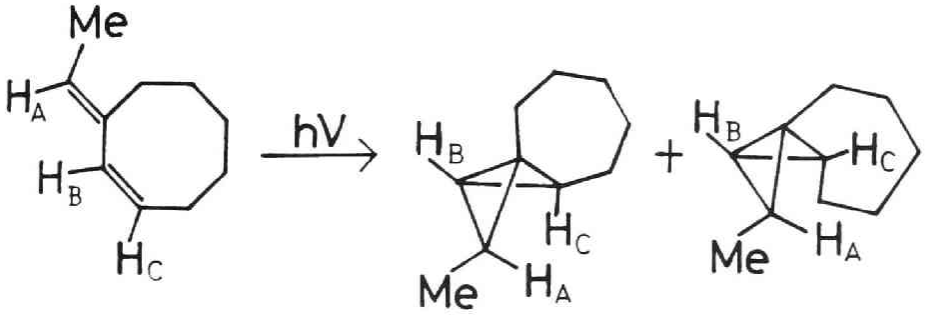

10 11 75% 12 25%

Both (9) and (11) are the results of mode B and compatible with the usual (2_a+2_a) cycloaddition. However, (12) is the result of the disfavoured mode C or D ((2_s+2_a) or (2_a+2_s)), so they have supposed an anomalous concerted reaction from a vibrationally relaxed singlet having an electronic configuration composed of an allyl anion and a methyl cation. While, from a standpoint of the cross-bicyclization, (12) is a reasonable product but (9) and (11) are not. The reason why these reactions rather favour these products can be explained by not a little energetical stabilizations in the photo-induced (2+2) cycloadditions as has been stated above. Furthermore, some steric hindrance in connection with the cyclooctene ring might play a role in separating the C_2-C_3 conjugation. Therefore, photo-induced [1,5/4,8] case of tetraene, which has not

been reported, would be also of interest because of the possibility of the competition with (4+4) cycloaddition.

(ii) [1,3/2,6] Cross-bicyclization of Triene

In photo-induced [1,3/2,6] case of triene, mode A or B is favoured, which predicts exactly the products from (3), (4), and (5) provided by Courtot *et al.*[4] The products from (1) and (2) by Padwa *et al.*,[3] however, show the opposite mode of stereoselection in the sense of the cross-bicyclization. In order to examine these discrepancies, we have evaluated $\Pi_{13,26}$ values as functions of the resonance integrals between C_2 and C_3 (β_{23}) of 1,5,6-triphenylhexatriene, (1) or (2), and 1,5-diphenylhexatriene, (3), (4), or (5), in their first excited configurations as listed in Table 3. It is evidently seen that the $\Pi_{13,26}$ of (3), (4), or (5) used by Courtot *et al.* is less sensitive to the weakening of β_{23}, while that of (1) or (2) by Padwa *et al.* is the smaller at $\beta_{23}=\beta$ and changes its sign at $\beta_{23}=0.6\beta$. That is, the stereoselective modes in photo-induced [1,3/2,6] cases of (1) and (2) will more easily change into that issued from the (4+2) cycloaddition than those of (3), (4), and (5), according to the weakening of the conjugation between C_2 and C_3, if it takes place for some reason. We infer that these situations are reflected in the reactions of Padwa *et al.* to a certain extent, although more de-

Table 3. The Values of $\Pi_{13,26}$ as Functions of β_{23} in 1,5,6-Triphenylhexatriene, (1) or (2), and 1,5-Diphenylhexatriene, (3), (4), or (5), in Their First Excited Configurations

β_{23}	(1) (2)	(3) (4) (5)
β	0.0382	0.0859
0.7β	0.0042	0.0822
0.6β	-0.0219	0.0686
0.5β	-0.0599	0.0391

tailed calculation including σ electrons is requisite to provide a definite information on this species. An example as to the hexatriene free from the conjugated substituents has also been shown. Dauben and Kellogg have obtained the photoproduct via (4_a+2_a) cycloaddition from 1,3,5-cycloundecatriene, 6)

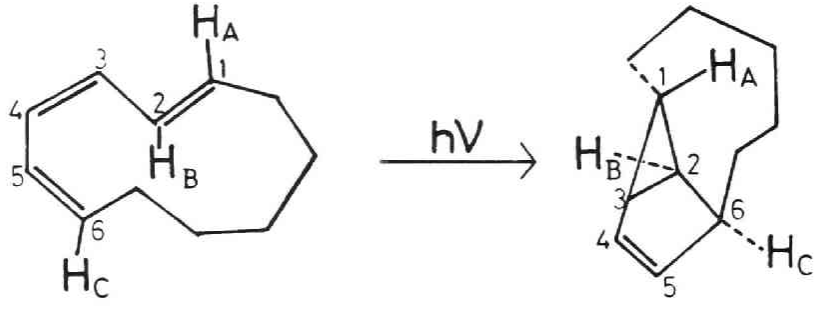

and supposed that the cyclization is initiated from the vibrationally relaxed first excited singlet state like the above case of ethylidenecyclooctene. But this stereoselective mode is easily explained by the cross-bicyclization of triene.

There have been other examples of the cross-bicyclizations that are found out in the photoisomerizations of benzohexatrienes reported by Seeley,[7)]

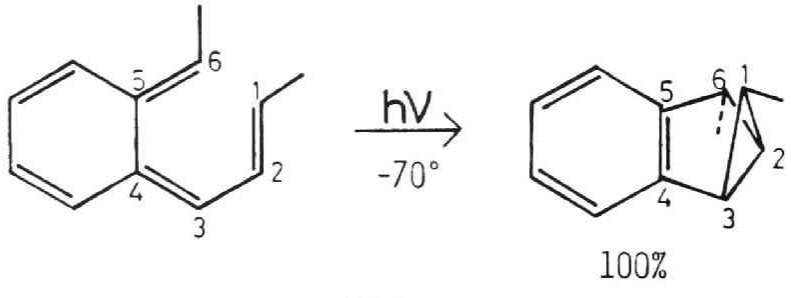

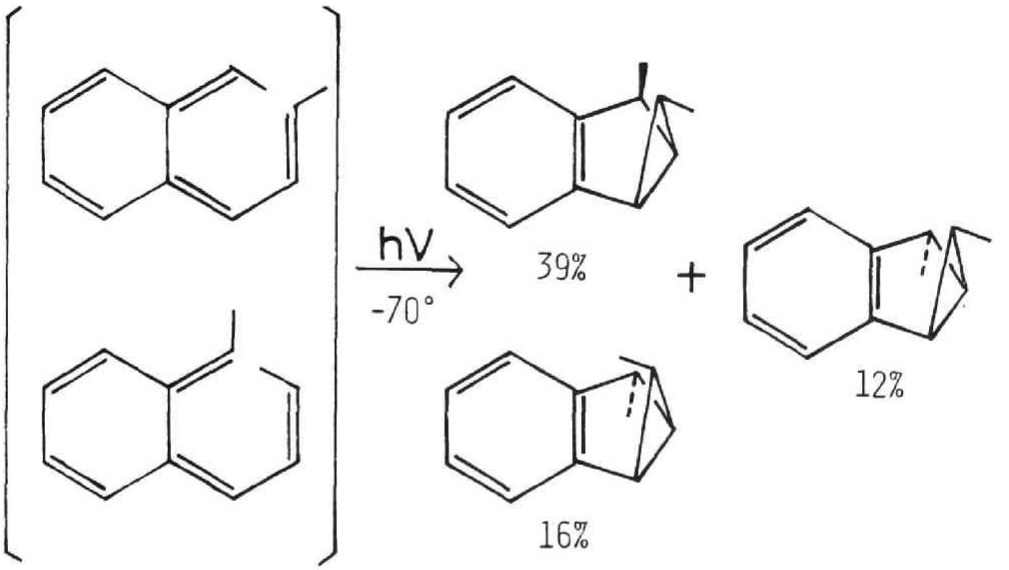

and by Sieber *et al.*[8)]

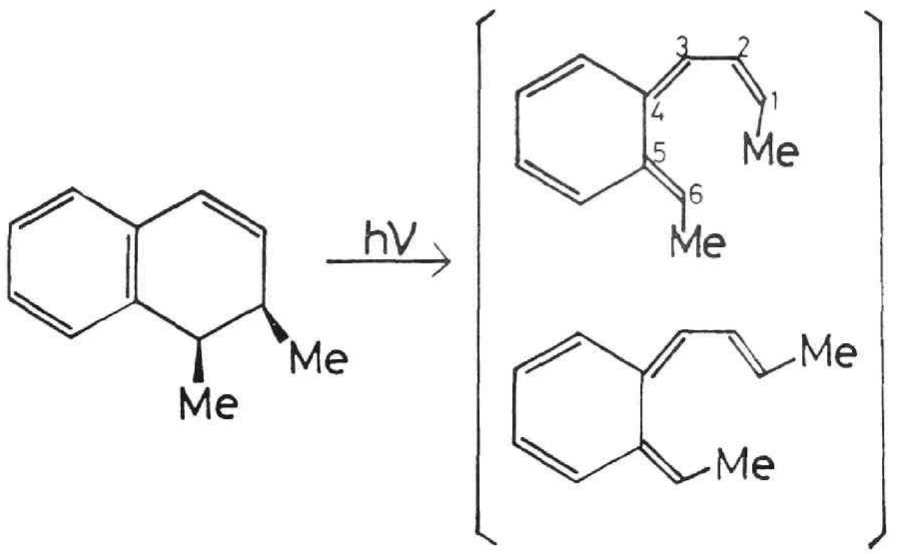

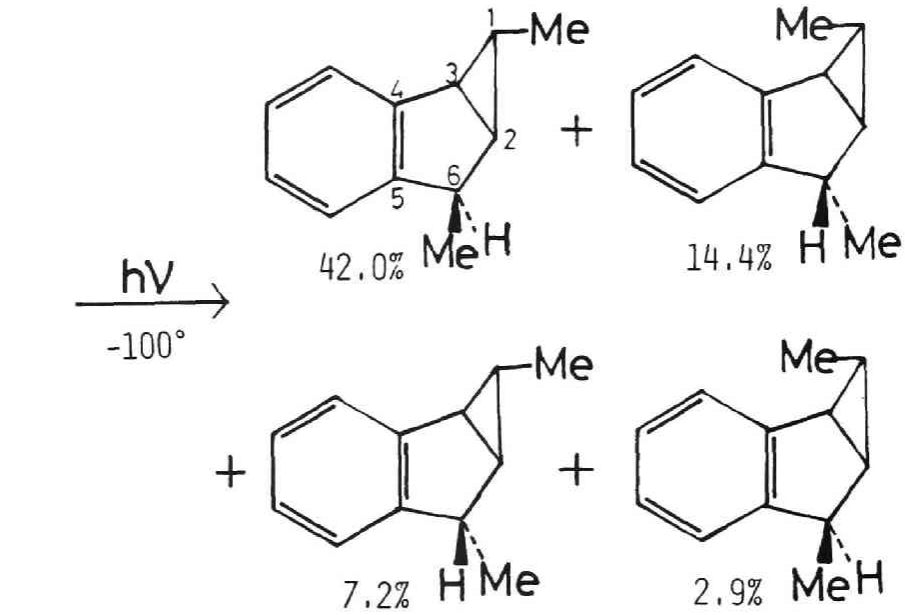
hV
-100°
Me
H
42.0%
14.4%
7.2%
2.9%

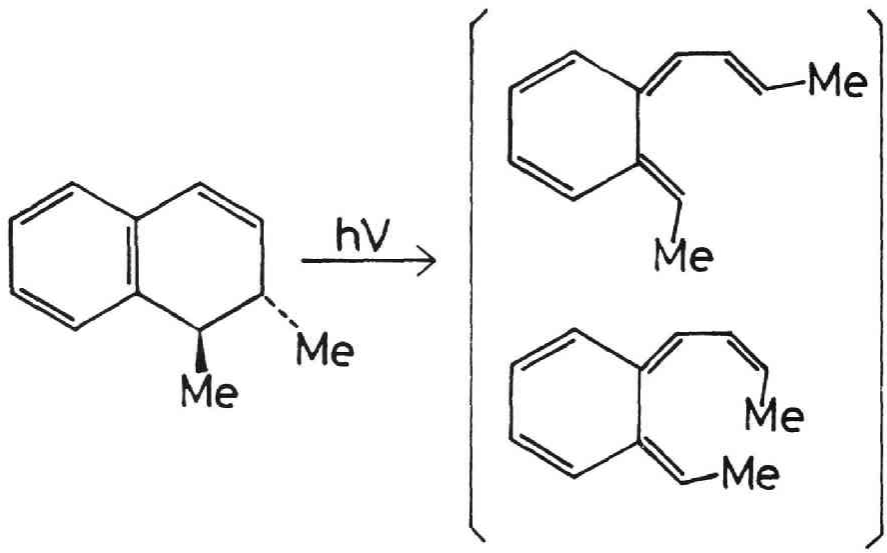
hV
Me
Me
Me
Me
Me

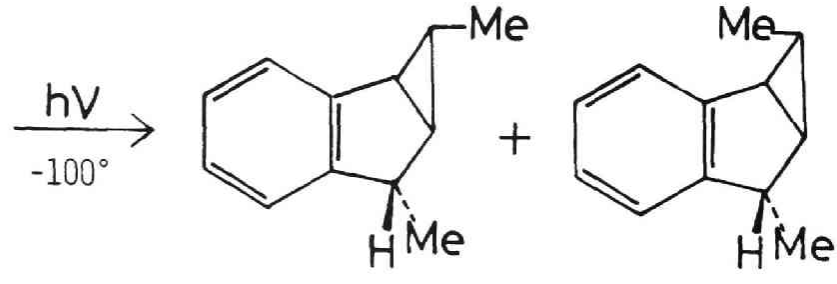
hV
-100°
Me
H
36.9%
12.3%

Since the major products of these reactions are not controlled by the stereoselective modes from the cycloaddition, these authors have ascribed these results to non-concerted reactions. But we are now in a position to tell that these reactions are concerted as well with the aid of the concept of the cross-bicyclization. It is also interesting that the result of the thermal [1,3/2,6] case of triene (Mode A or B) is equivalent to that of (4+2) cycloaddition ((4_s+2_s) or (4_a+2_a)), so that the theory of the usual cycloaddition has not had a trying experience in thermal case.

V. Conclusion

We have defined the concept of the cross-bicyclization complementary to that of the cycloaddition and pointed out the essential difference between these two. The predicted stereoselective modes from the cross-bicyclization are in reasonable agreement on the whole with the experimental observations that have been discarded from the category of the concerted reactions because of the faith in the cycloaddition rules. However, one should pay attention to the application of the rules to photo-induced [1,3/2,4] case of diene or [1,5/4,8] case of tetraene as well as to the case of polyene with conjugated substituents. To the author's knowledge, any

stereospecific bicyclizations in a conjugated polyene treated by the concept of the cycloaddition up to the present have been probed in this study.

It is also an important conclusion, at least in diene, triene, and tetraene, that the thermal and photo-induced processes yield identical results and that there occurs a distinct difference in the stereoselective mode according as (s-r)+(u-t) is equal to 4m+2 or 4m. A simple calculation of $\Pi_{rs,tu}$ is requisite at present to make use of the stereoselective rules in the cross-bicyclization apart from the cycloaddition, but more concise rules without resorting to calculations would be hoped and further experimental observations are desirable in order to assess the utility of the present concept of the cross-bicyclization.

References and Notes

1) (a) R. Hoffmann and R. B. Woodward, J. Am. Chem. Soc., 87, 2046(1965); (b) R. Hoffmann and R. B. Woodward, Acc. Chem. Res., 1, 17(1968); (c) R. B. Woodward and R. Hoffmann, Angew. Chem., 81, 797(1969); (d) R. B. Woodward and R. Hoffmann, "The Conservation of Orbital Symmetry," Academic Press, New York (1969).

2) (a) K. Fukui, Acc. Chem. Res., 4, 57(1971); (b) K. Fukui, "Theory of Orientation and Stereoselection," Springer-Verlag, Berlin (1975).

3) (a) A. Padwa and S. Clough, J. Am. Chem. Soc., 92, 5803 (1970); (b) A. Padwa, L. Brodsky, and S. Clough, J. Am. Chem. Soc., 94, 6767(1972).

4) P. Courtot, J. Salaün, and R. Rumin, Tetrahedron Lett., 1976, 2061.

5) W. G. Dauben and J. S. Ritscher, J. Am. Chem. Soc., 92, 2925(1970).

6) W. G. Dauben and M. S. Kellogg, J. Am. Chem. Soc., 94, 8951(1972).

7) D. A. Seeley, J. Am. Chem. Soc., 94, 4378(1972).

8) W. Sieber, H. Heimgartner, H. J. Hansen, and H. Schmid, Helv. Chim. Acta, 55, 3005(1972).

9) (a) C. A. Coulson and H. C. Longuet-Higgins, Proc. Roy.

Soc.(London), A191, 39(1947); (b) A192, 16(1947); (c) A193, 447(1948).

10) K. Fukui, Bull. Chem. Soc. Jpn., 39, 498(1966).

11) (a) K. Fukui, C. Nagata, T. Yonezawa, H. Kato, and K. Morokuma, J. Chem. Phys., 31, 287(1959); (b) K. Fukui, K. Morokuma, T. Yonezawa, and C. Nagata, Bull. Chem. Soc. Jpn., 33, 963(1960).

12) For example, see p.48 of Ref. 2(b) and references therein.

Chapter 5

Interactions in Biradicals

I. Introduction

In a chemical sense, the word "biradical" makes us think of a species such as one having an odd electron on each of two sites of a molecule. This conforms to the interpretation of a biradical in the triplet state. However, problems may arise in the case of a singlet biradical.

The conversion of biradical species along the path of ground- and excited-state reactions has been treated theoretically.[1-4] Salem *et al.* discussed the nature of a singlet biradical by taking ionic states into account and explained a number of experimental results in regard to various reaction intermediates in photochemistry.[5-10] The present work gives some new material.

II. Stabilization of Singlet Biradical by a Correlated Motion of Electrons

Consider a pair of two independent normalized one-electron space functions a and b whose overlap integral is s.

In the case of biradical problems these two orbitals can be made to represent the two "unpaired"-electron orbitals essentially localized at each radical site. The following three configurations are here taken into consideration to treat the problem as a two-electron system:

$$\Phi_1(1,2) = \frac{1}{\sqrt{2+2s^2}}\{a(1)b(2) + b(1)a(2)\}$$

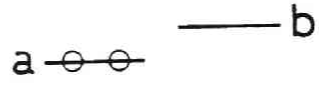

$$\Phi_2(1,2) = a(1)a(2)$$

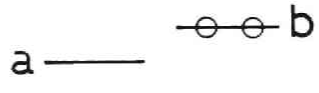

$$\Phi_3(1,2) = b(1)b(2)$$

(1)

It is assumed that orbitals a and b are real and their signs are chosen in such a way that s becomes positive.

The electronic states of this two-electron system are then given by

$$\Psi = \frac{1}{\sqrt{N}}(C_1\Phi_1 + C_2\Phi_2 + C_3\Phi_3) \ , \qquad (2)$$

where C_1, C_2, and C_3 can be obtained by solving the eigenvalue problem of the Hamiltonian matrix, and $1/\sqrt{N}$ is the normalization factor. They are the usual energy-extremized wavefunctions in which the effect of correlation in electron motion is taken into account.

Direct consideration of the correlated motion of electrons might also be considered. The extent of correlation in orbital motion could roughly be represented by the averaged reciprocal interelectronic distance,

$$\overline{\frac{1}{r_{12}}} = \frac{2}{\nu(\nu-1)}\iint \rho(1,2|1,2)\frac{1}{r_{12}}dv(1)dv(2) \ , \qquad (3)$$

(ν: number of electrons)

where r_{12} is the distance of **electrons** 1 and 2, and

$$\rho(1',2'|1,2) = \frac{\nu(\nu-1)}{2}\int \Psi^*(\underline{r}_1'\sigma_1, \underline{r}_2'\sigma_2, \underline{r}_3\sigma_3, \cdots\cdots)$$

$$\cdot\Psi(\underline{r}_1\sigma_1, \underline{r}_2\sigma_2, \underline{r}_3\sigma_3, \cdots\cdots)d\sigma_1 d\sigma_2 d\underline{r}_3 d\sigma_3\cdots\cdots , \tag{4}$$

is the second-order spinless density matrix. For the present two-electron problem, we have

$$\gamma \equiv \overline{\frac{1}{r_{12}}} = \int\int \Psi^*(1,2)\frac{1}{r_{12}}\Psi(1,2)dv(1)dv(2) . \tag{5}$$

The extremization of $\overline{1/r_{12}}$ is achieved by obtaining the stationary values satisfying

$$\delta\gamma = 0 . \tag{6}$$

The variation with respect to C_1, C_2, and C_3 leads to the secular equation,

$$\begin{vmatrix} \gamma_{11}-\gamma & \gamma_{12}-S_{12}\gamma & \gamma_{13}-S_{13}\gamma \\ \gamma_{21}-S_{21}\gamma & \gamma_{22}-\gamma & \gamma_{23}-S_{23}\gamma \\ \gamma_{31}-S_{31}\gamma & \gamma_{32}-S_{32}\gamma & \gamma_{33}-\gamma \end{vmatrix} = 0 , \tag{7}$$

where

$$\gamma_{jk} = \iint \Phi_j^*(1,2) \frac{1}{r_{12}} \Phi_k(1,2) dv(1) dv(2) \ ,$$

and

$$S_{jk} = \iint \Phi_j^*(1,2) \Phi_k(1,2) dv(1) dv(2) \qquad (j, k = 1, 2, \text{and } 3).$$

The coefficient of Φ_j in Eq.(2) can be obtained simultaneously, giving correlation-extremized wavefunctions $\{\Psi^{(i)}\}$ which are always mutually orthogonal. Both energy-extremization and correlation-extremization give wavefunctions with an essentially parallel trend in nonpolar species.[11] Thus in such favourable cases, we can use correlation-extremized wavefunctions as an approximate substitute of the usual energy-extremized functions. Such a consideration of the interaction of at least three configurations as mentioned above is essential in the theoretical interpretation of biradicals.

III. Bonding Character between Two Radical Sites

The bonding character between two radical sites each containing essentially one electron can be discussed by using Ψ of Eq.(2). A most reasonable scale of bonding character[12] might be the magnitude of accumulation of electron population in the intermediate region between two radical sites.[13-15]

The distribution of electron density is given by

$$\rho(1) = 2\int \Psi^{*}(1,2)\Psi(1,2)dv(2) \quad . \tag{8}$$

The density $\rho(1)$ is divided into three terms as

$$\rho(1) = A_{11}a(1)^{2} + 2A_{12}a(1)b(1) + A_{22}b(1)^{2} \quad . \tag{9}$$

The bonding strength can be determined by the second term of r.h.s. since the coefficient A_{12} of the cross term $a(1)b(1)$ contributes to the accumulation of electrons in the intermediate region.

It follows from Eq.(2) that

$$A_{12} = \frac{1}{N}\left\{\frac{s}{1+s^{2}}C_{1}^{2} + \sqrt{\frac{2}{1+s^{2}}}C_{1}(C_{2} + C_{3}) + 2sC_{2}C_{3}\right\} \quad , \tag{10}$$

where

$$N = C_1^2 + C_2^2 + C_3^2 + \frac{2\sqrt{2}s}{\sqrt{1+s^2}} C_1(C_2 + C_3) + 2s^2 C_2 C_3 \quad .$$

In general, C_j may be complex. However, for the sake of simplicity, Eq.(9) is written for the real values of C_j. If we allow C_1, C_2, and C_3 of Eq.(2) to take *any* real values, the maximum and minimum values which A_{12} can take are $1/(1+s)$ and $-1/(1-s)$ corresponding to the wavefunctions

$$\left.\begin{aligned} \Psi^{(B)} &= \frac{1}{\sqrt{2}} \frac{1}{1+s}\{\sqrt{1+s^2}\,\Phi_1 + \frac{1}{\sqrt{2}}(\Phi_2 + \Phi_3)\} \quad , \\ \text{and} \qquad & \\ \Psi^{(AB)} &= \frac{1}{\sqrt{2}} \frac{1}{1-s}\{\sqrt{1+s^2}\,\Phi_1 - \frac{1}{\sqrt{2}}(\Phi_2 + \Phi_3)\} \quad , \end{aligned}\right\} \qquad (11)$$

respectively. Thus we see that the most bonding state ($\Psi^{(B)}$) or the most antibonding state ($\Psi^{(AB)}$) is obtained in the case of *moderate* mixing of three configurations Φ_1, Φ_2, and Φ_3. This implies that admixture of the ionic configuration Φ_2 or Φ_3 with the covalent configuration Φ_1, or the delocalization of each odd electron to the other radical site, serves as an effective origin of bonding character between two weakly interacting radical sites. The importance of such electron

delocalization in the bond formation between molecules or radicals was early pointed out.[16-19] In particular, special importance of a cross term arising from two configurations, corresponding in the present case to the terms of C_1C_2 or C_1C_3 in A_{12}, was stressed.[20-22]

The bonding character of a singlet biradical is thus represented by sA_{12}. In the light of the relation

$$A_{11} + 2sA_{12} + A_{22} = 2 \ ,$$

we can also measure the less bonding character by the quantity $1/2(A_{11}+A_{22})$.

IV. Polar Character of Two Radical Sites

The density $\rho(1)$ also provides information as to what extent the two radical sites are polar. Evidently, polarity parallels $|A_{11}-A_{22}|$. We tentatively define the polar character of a singlet biradical by means of

$$\pi = \left| \frac{A_{11} - A_{22}}{A_{11} + A_{22}} \right| \ , \qquad (12)$$

in which

$$A_{11} = \frac{1}{N}\left(\frac{1}{1+s^2}C_1^2 + \frac{2\sqrt{2}s}{\sqrt{1+s^2}}C_1C_2 + 2C_2^2\right), \qquad (13)$$

$$A_{22} = \frac{1}{N}\left(\frac{1}{1+s^2}C_1^2 + \frac{2\sqrt{2}s}{\sqrt{1+s^2}}C_1C_3 + 2C_3^2\right).$$

These are the coefficients of $a(1)^2$ and $b(1)^2$ terms in $\rho(1)$ of Eq.(9) which is derived from a wavefunction Ψ already *correlation-extremized* according to the procedure in previous section.

By this definition, we have

$$\pi(\Phi_1) = 0, \quad \pi(\Phi_2) = \pi(\Phi_3) = 1,$$

provided that Φ_1, Φ_2, and Φ_3 are correlation-extremized states.

A change in electron distribution can be expected to arise causing bonding stabilization through a moderate mixing of ionic structures. In this connection the work of Wulfman and Kumei,[23] who first pointed out the high possibility of polarization in singlet excited states of alkenes, is of interest.

V. Biradical Character of Singlet Biradicals

Since the bonding character between two radical sites becomes maximum only in the case of moderate admixing of ionic configurations with a covalent configuration, the less ionic character can not be adopted for the measure of biradical character.

We must take into account the following requisites which qualify a biradical:

1) The bonding character between two radical ends should be small since a species with too large bonding character might be called a molecule, but not a biradical. The value $1/2(A_{11}+A_{22})$ should not be small.

2) The polar character should not be large since a species with a strong inequality in electron density at the radical ends should be called a zwitterion. Namely, $(1-\mathcal{T})$ should not be small.

A conventional but reasonable definition of the biradical character $\mathcal{B}$ may therefore be given by

$$\mathcal{B} = \frac{1}{2}(A_{11} + A_{22})(1 - \mathcal{T}) = \frac{1}{2}(A_{11} + A_{22} - |A_{11} - A_{22}|)$$

$$= (\text{the smaller of } A_{11} \text{ and } A_{22}) . \qquad (14)$$

Thus, the maximum possible biradical character in a *bonding*

state is unity (=1/(1+s)), and the maximum biradical character in an *antibonding* state is larger than unity (=1/(1-s)). We also have,

$$\mathcal{B}(\Phi_1) = \frac{1}{1+s^2} \quad , \quad \mathcal{B}(\Phi_2) = 0 \quad , \quad \mathcal{B}(\Phi_3) = 0 \quad ,$$

in which Φ_1, Φ_2, and Φ_3 are the functions of Eq.(1), assuming that they are correlation-extremized ones.

The discussion is easily extended to the case of complex wavefunctions.

VI. Nonbonding Biradicals

It may happen that each odd electron occupies each of two orbitals orthogonal to each other so that the overlap integral s in Eq.(9) disappears. Hence, the maximal biradical character is unity.

An example is perpendicular ethylene in which two orthogonal radical orbitals a and b are $(2p_x)_A$ and $(2p_y)_B$, respectively, A and B denoting two carbon atoms. In this case, it follows from symmetry relations that

$$\gamma_{12} = \gamma_{13} = 0 \quad , \qquad S_{12} = S_{13} = 0 \quad ,$$

in Eq.(7). Thus, $\Phi_1=1/\sqrt{2}\{a(1)b(2)+b(1)a(2)\}$ is already a correlation-extremized wavefunction with which Φ_2 or Φ_3 of different symmetry does not mix. From the definition of Eq. (14), the state $\Psi^{(1)}=\Phi_1$ has the $\mathcal{B}$ value of unity and can be called "purely" biradical. The other two states ($\Psi^{(2)}=1/\sqrt{2}$ $(\Phi_2+\Phi_3)$ and $\Psi^{(3)}=1/\sqrt{2}(\Phi_2-\Phi_3)$) also have the $\mathcal{B}$ value of unity. Such a biradical species may be called a *nonbonding biradical*.

The level situation of three correlation-extremized states is given below, together with the value of γ. The result is qualitatively consistent with that of numerical calculations.[24)]

$\Psi^{(i)}$			γ
$\frac{1}{\sqrt{2}}\{a(1)a(2)+b(1)b(2)\}$	$^1A_1$	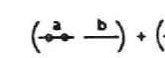	$(aa\|aa)+(ab\|ab)$ ~ 0.89120 (a.u.)
$\frac{1}{\sqrt{2}}\{a(1)a(2)-b(1)b(2)\}$	$^1B_2$		$(aa\|aa)-(ab\|ab)$ ~ 0.88969
$\frac{1}{\sqrt{2}}\{a(1)b(2)+b(1)a(2)\}$	$^1B_1$		$(aa\|bb)+(ab\|ab)$ ~ 0.39420
$\frac{1}{\sqrt{2}}\{a(1)b(2)-b(1)a(2)\}$	$^3A_2$		$(aa\|bb)-(ab\|ab)$ ~ 0.39268

It is to be noted that the level gap between $^1B_1$ and $^3A_2$ states is very small (*ca.* 1 kcal/mol) in this example. The small S-T separation is characteristic of nonbonding biradicals. From an energetic point of view, they are expected to interchange easily between singlet and triplet states.

VII. Biradical with Cyclic Orbitals

(i) Singlet Oxygen

Let two ($1\pi_g$) orbitals of oxygen molecule be

$$\phi_x = \frac{1}{\sqrt{2-2s}} \{(2p_x)_1 - (2p_x)_2\} ,$$

$$\phi_y = \frac{1}{\sqrt{2-2s}} \{(2p_y)_1 - (2p_y)_2\} ,$$

where O_1-O_2 axis is parallel to the z-axis and s is the overlap integral of $(2p_x)_1$ and $(2p_x)_2$ or that of $(2p_y)_1$ and $(2p_y)_2$. Three configurations are specified by

$$\Phi_1 = \frac{1}{\sqrt{2}} \{\pi^+(1)\pi^-(2) + \pi^-(1)\pi^+(2)\} ,$$

$$\Phi_2 = \pi^+(1)\pi^+(2) \ ,$$

$$\Phi_3 = \pi^-(1)\pi^-(2) \ ,$$

where

$$\pi^+ = \frac{1}{\sqrt{2}}(\phi_x + i\phi_y) \ ,$$

$$\pi^- = \frac{1}{\sqrt{2}}(\phi_x - i\phi_y) \ .$$

Φ_1, Φ_2, and Φ_3 of different symmetries are correlation-extremized wavefunctions corresponding to the stationary values of γ.

$\Psi(i)$		γ
$\Phi_1 = \frac{1}{\sqrt{2}}\{\phi_x(1)\phi_x(2)+\phi_y(1)\phi_y(2)\}$	$^1\Sigma_g^+$	$(xx\|xx)+(xy\|xy)$
$[\Phi_2, \Phi_3] = [\frac{1}{\sqrt{2}}\{\phi_x(1)\phi_x(2)-\phi_y(1)\phi_y(2)\},$	$^1\Delta_g$	$\frac{1}{2}(xx\|xx)+\frac{1}{2}(xx\|yy)$
$\frac{1}{\sqrt{2}}\{\phi_x(1)\phi_y(2)+\phi_y(1)\phi_x(2)\}]$		
$\left(\frac{1}{\sqrt{2}}\{\phi_x(1)\phi_y(2)-\phi_y(1)\phi_x(2)\}\right)$	$^3\Sigma_g^-$	$(xx\|yy)-(xy\|xy)$

((xy|xy), *etc.*, denote

$(\phi_x\phi_y|\phi_x\phi_y)$, *etc.*)

The uppermost level corresponds to $^1\Sigma_g^+$ excited singlet state and the lower degenerate level to $^1\Delta_g$ state. The former stands for the configuration

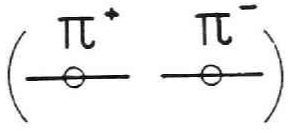

with $\mathcal{B}$ =1. The species can thus be called purely biradical.

In the latter state, the correlation-extremized wavefunctions consist of purely doubly-occupied configurations

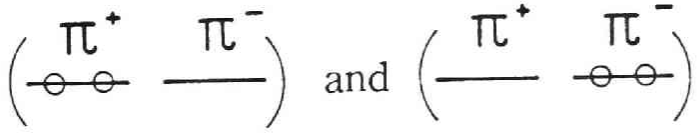

with $\mathcal{B}$ =0.

It should be noted that we have to employ the symmetry orbitals π^+ and π^- to construct wavefunctions with definite angular momenta.

Such cyclic orbitals, however, do not reflect the concept of radical site. The interpretation of $\mathcal{B}$-values in this case should be made with certain reservation.

(ii)Cyclobutadiene (Planar Square)

The orthogonal nonbonding orbitals can be taken as

$$\phi_1 = \frac{1}{\sqrt{2-2s'}} \{(2p_z)_4 - (2p_z)_2\} ,$$

$$\phi_2 = \frac{1}{\sqrt{2-2s'}} \{(2p_z)_1 - (2p_z)_3\} ,$$

where $(2p_z)_j$ (j=1, 2, 3, and 4) are the four $2p_z$ orbitals and s' is the overlap integral of $(2p_z)_1$ and $(2p_z)_3$. The three states are as follows.

$\Psi^{(i)}$		γ
$\frac{1}{\sqrt{2}}\{\phi_1(1)\phi_1(2)+\phi_2(1)\phi_2(2)\}$	$^1A_{1g}$	$(11\|11)+(12\|12)$
$\frac{1}{\sqrt{2}}\{\phi_1(1)\phi_1(2)-\phi_2(1)\phi_2(2)\}$	$^1B_{1g}$	$(11\|11)-(12\|12)$
$\frac{1}{\sqrt{2}}\{\phi_1(1)\phi_2(2)+\phi_2(1)\phi_1(2)\}$	$^1B_{2g}$	$(11\|22)+(12\|12)$
$\frac{1}{\sqrt{2}}\{\phi_1(1)\phi_2(2)-\phi_2(1)\phi_1(2)\}$	$^3A_{2g}$	$(11\|22)-(12\|12)$

($(11|22)$, *etc.*, denote $(\phi_1\phi_1|\phi_2\phi_2)$, *etc.*)

The level situation is consistent with the results of more elaborate calculations.[25)]

(iii) Singlet Planar Trimethylenemethane[26)]

The two orthogonal orbitals containing nonbonding electrons are written as

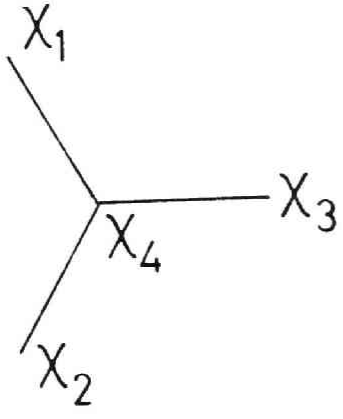

$$\phi_1 = \sqrt{\frac{2}{3(1-s')}}\{\chi_1 - \frac{1}{2}(\chi_2 + \chi_3)\} ,$$

$$\phi_2 = \frac{1}{\sqrt{2(1-s')}}(\chi_2 - \chi_3) ,$$

where χ_j (j=1, 2, 3, and 4) are the four $2p_z$ orbitals, and s' is the overlap integral of χ_1 and χ_2. The resulting three states are

$$^1A_1' \qquad \frac{1}{\sqrt{2}}\{\phi_1(1)\phi_1(2)+\phi_2(1)\phi_2(2)\}$$

$$^1E' \quad \begin{cases} \frac{1}{\sqrt{2}}\{\phi_1(1)\phi_2(2)+\phi_2(1)\phi_1(2)\} \\ \frac{1}{\sqrt{2}}\{\phi_1(1)\phi_1(2)-\phi_2(1)\phi_2(2)\} \end{cases}$$

$$\left(\quad {}^3A_2' \qquad \frac{1}{\sqrt{2}}\{\phi_1(1)\phi_2(2)-\phi_2(1)\phi_1(2)\} \quad \right)$$

The density of $^1E'$ ground state becomes

$$\rho(1) = \frac{2}{3(1-s')}\left[\{\chi_1(1)^2 + \chi_2(1)^2 + \chi_3(1)^2\} - \{\chi_1(1)\chi_2(1) + \chi_1(1)\chi_3(1) + \chi_2(1)\chi_3(1)\}\right] ,$$

showing that this is an antibonding biradical with $\mathcal{B}$ =1/(1 -s'). The antibonding character might primarily cause the nonplanar geometry of singlet ground-state trimethylenemethane. 27)

VIII. General Characterization of Biradicals

The correlation-extremization approach developed in previous section is convenient for grasping a qualitative feature, but it can not be used in polar species where the potential field is partial to either one of the two radical sites. In such cases, the usual energy-extremization procedure, *viz.*, the configuration interaction (CI) approach,

must be taken.

We use a CI wavefunction of n electron system $\Psi(1, 2, \cdots, n)$ to construct the density distribution $\rho(1)$, which is decomposed in such a way as

$$\rho(1) = A_{11}a(1)^2 + 2A_{12}a(1)b(1) + A_{22}b(1)^2 + 2\sum_j \{B_{aj}a(1) + B_{bj}b(1)\}\chi_j(1) + \sum_{j,k} B_{jk}\chi_j(1)\chi_k(1). \quad (15)$$

The set of orbitals, a, b, and χ_j, in principle atomic hybrids or usual atomic orbitals, are obtained by a relevant transformation of the set of valence-shell atomic orbitals in such a way that orbitals a and b are appropriately associated with essentially located radical sites.

The bonding character and polar character can be represented by sA_{12} and π of Eq.(12), respectively. We define a new concept, the delocalized character of a biradical, $\mathcal{D}$, by

$$\mathcal{D} = 2 - (A_{11} + 2sA_{12} + A_{22}) . \quad (16)$$

The biradical character of Eq.(14) can then be modified as

$$\mathcal{B} = \frac{A_{11}+A_{22}}{2-\mathcal{D}}(1-\pi)$$

$$= \frac{2}{2-\mathcal{D}} \cdot (\text{the smaller of } A_{11} \text{ and } A_{22}) \ . \qquad (17)$$

IX. Bonding Deformation of Singlet Biradicals

In the following examples, where the polar character π can be put equal to zero, the biradical character $\mathcal{B}$ depends only upon the overlapping between radical sites. Thus singlet biradicals stabilize with increasing overlapping between radical sites, which is in accordance with the direction of decreasing biradical character $\mathcal{B}$. In contrast, the triplet species tend to decrease overlapping to stabilize.[29,30]

A molecular deformation in singlet biradicals to raise overlapping may even take place when stabilization overcomes destabilization, if it arises, due to the deformation. It may happen that a triplet biradical with minimal overlapping shifts to the singlet state through intersystem crossing to cause stabilization by bonding deformation. Let us discuss the bonding deformation in the direction of decreasing $\mathcal{B}$ with regard to several examples of singlet biradicals.

The dependence of energy on the torsional angle θ in

perpendicular ethylene discussed in previous section is shown below.[24] The lowest singlet has a deformation-instability in addition to the triplet-instability near $\theta=\pi/2$. The $^3A_2$ ground state of perpendicular geometry once formed may tend towards the planar form through the intersystem crossing to produce ^1A_g ground-state ethylene.

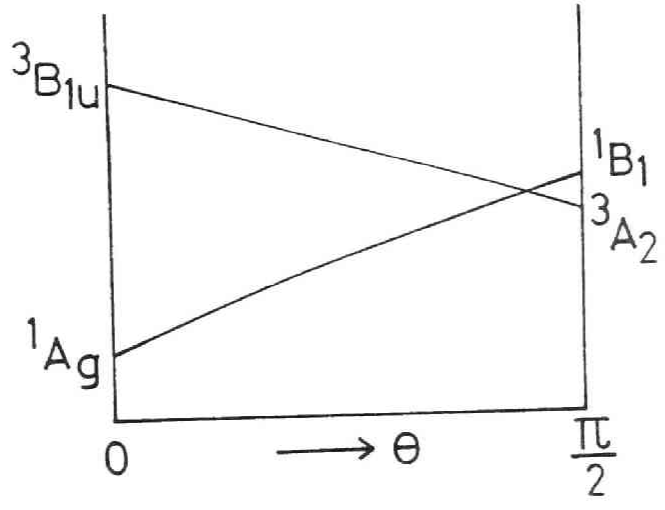

The direction of bonding deformation of perpendicular species is simply represented by the following orbital phase scheme.[28]

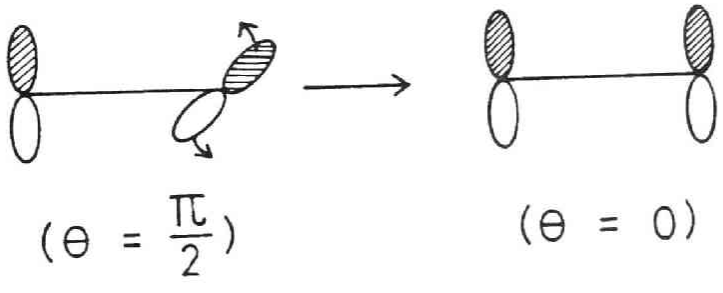

Similarly, the direction of deformation of square cyclobutadiene is given by the direction of in-phase overlapping of two odd-electron orbitals.

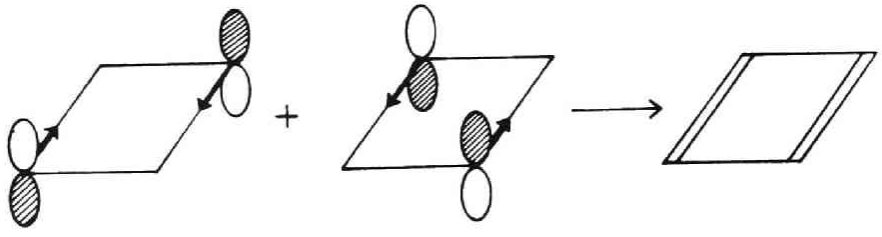

Also planar octagonal cyclooctatetraene will deform in the following way:

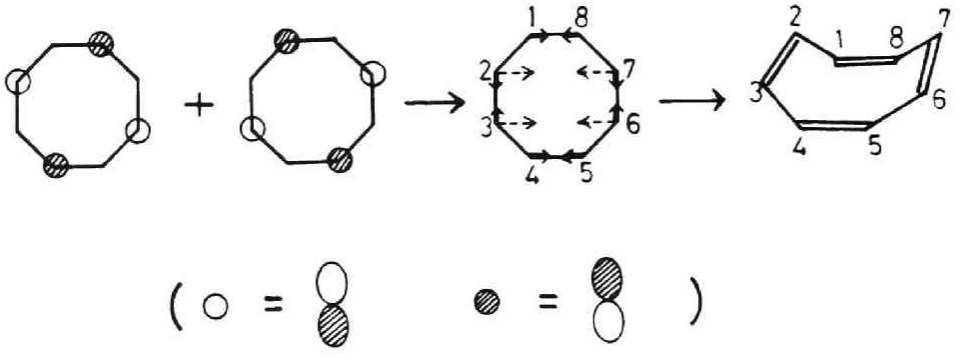

(○ = ● =)

The bonding deformation consideration is employed to predict the geometry of stable intermediates in singlet radical reactions.

methylenecyclopropane

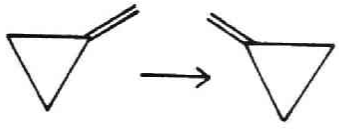

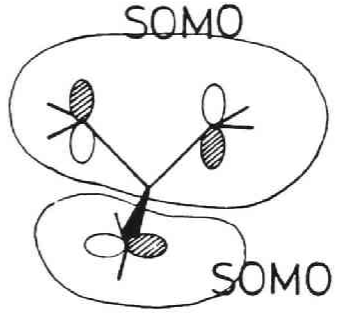

31)

methylenecyclobutane

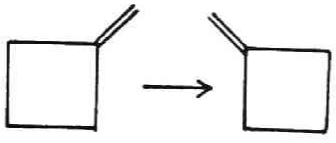

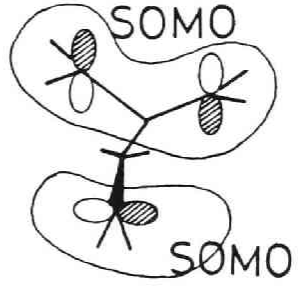

32)

1,2-dimethylenecyclobutane

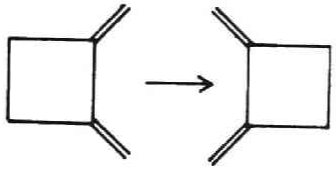

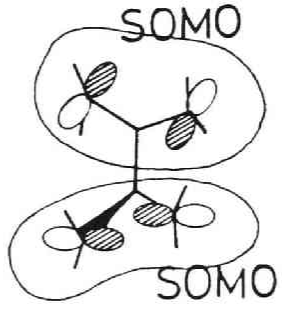

33)

SOMO denotes a singly occupied molecular orbital.

The bond alternation in carbon 2pπ chains can be explained by the following. The highest occupied (HO) and the lowest unoccupied (LU) MO's of a chain of equally distanced four p orbitals result approximately from the combination of

the following two orbitals a and b.

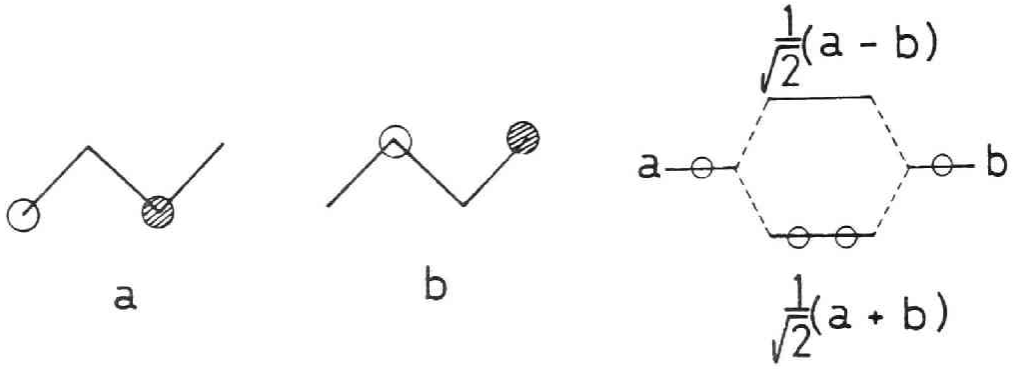

In this fictitious singlet biradical, the direction of deformation is also caused by the bonding overlapping of a and b to form a butadiene molecule, shown by

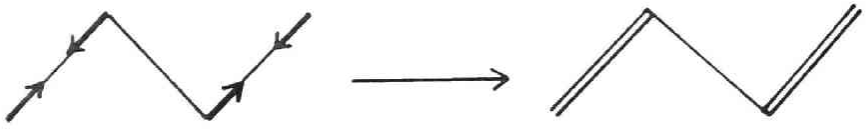

The lower occupied π orbital has hardly any connection with this deformation owing to its less nodal property.

Similarly, the difference in bond lengths in hexatriene, fulvene, naphthalene, *etc.*, is explained by considering the next HOMO's which contribute to the deformation less than HOMO because of their less nodal character.

An interesting application of the bonding deformation ap-

proach may be the prediction of the reaction path in excited states. In the π-π^* excited singlet state of hexatriene, the highest half-occupied orbital (a') and the lowest unoccupied orbital (b') are represented by

In order to consider bonding stabilization of the electron in orbital a', let us construct in the place of a' and b' the following quasiorthogonal orbitals.

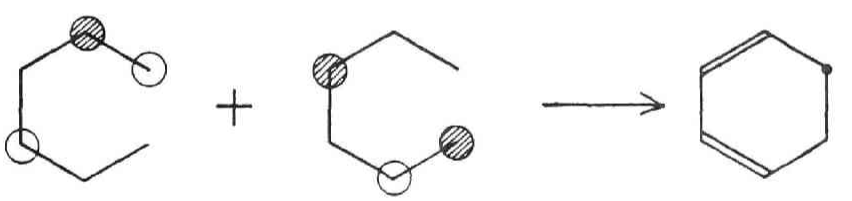

$\frac{1}{\sqrt{2}}(a'+b')$ $\frac{1}{\sqrt{2}}(a'-b')$

Combinations of these orbitals lead to orbitals a' and b', the former becoming occupied by a single electron to contribute to the bonding stabilization, and the direction of ring closure, if it occurs simultaneously, should be conrotatory. The conclusion is unchanged in the excited state with doubly occupied

a'. In contrast, in the excited butadiene, the direction of hypothetical 1,4-bonding would be disrotatory.

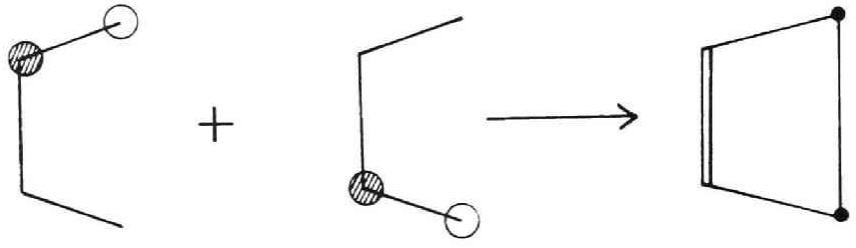

The lower singly occupied orbitals would contribute less by a similar discussion in terms of their less nodal properties.

The simple approach is useful since it can be applied to a rough estimation of the direction of bonding in higher excited singlet states of a known electron configuration. The configuration might have several SOMO's. The general procedure is as follows:

i) By a linear combination of the HOMO (singly or doubly occupied) and the LUMO, say a' and b', we construct two MO's, a and b, which are mutually orthogonal and spatially separated from each other to construct a fictitious singlet biradical species.

ii) The direction of maximal overlapping of a and b to decrease the biradical character $\mathcal{B}$, obtained by the usual procedure in the orbital interaction approach,[28] leads to a favourable reaction path.

In some cases, an excited state of the species before deformation may correlate to the ground state of the species after deformation, as in the following,

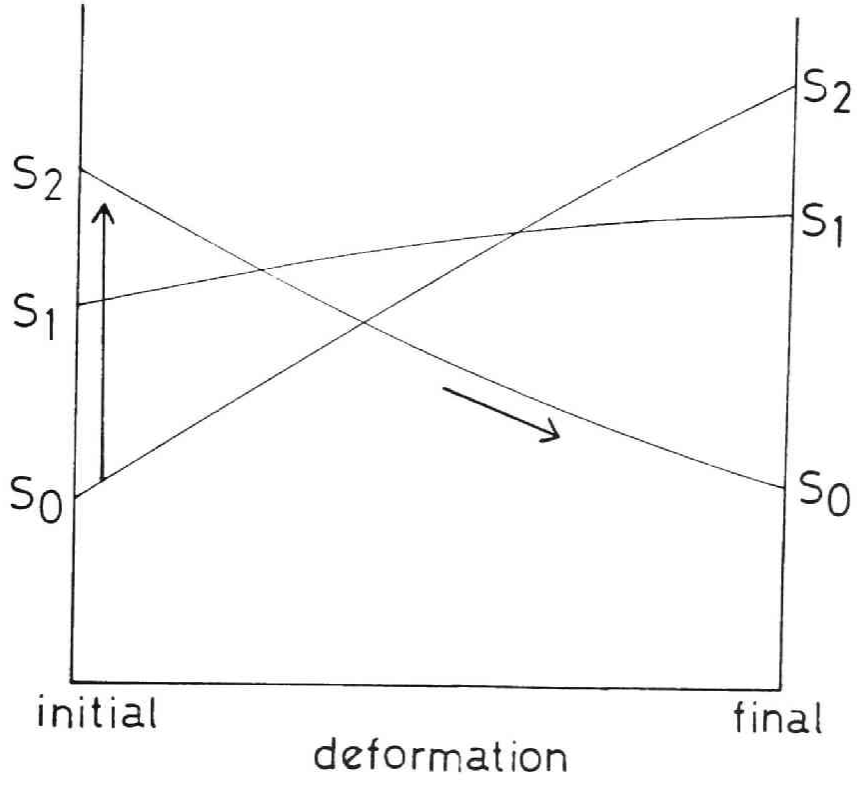

An example is the hypothetical disrotatory cyclization of S_2 excited butadiene to S_0 cyclobutene in the Longuet-Higgins-Abrahamson state correlation diagram.[34] The direction of such processes can be discussed by the method mentioned above.

X. Unpaired-Electron Isolating Deformation or Bonding in Triplet Biradicals

Once a triplet state is formed photochemically or thermally, a deformation or bond formation may be liable to take place to acquire stabilization in such a way that each of the two unpaired-electrons enters each of two orthogonal orbitals, or they become separated from each other by the newly formed bond as far away as possible.[9,30] In this connection Michl's conception of "loose" and "tight" biradicaloids is useful.[30c] The following examples are given for illustration.

Consider a π-π^* triplet hexatriene molecule. Twisting of the carbon chain would certainly diminish the overlapping of the two unpaired-electron orbitals. Two possibilities exist in regard to the twisting.

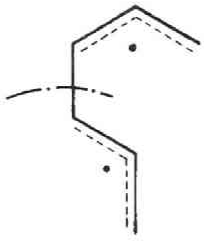

(I)

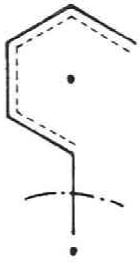

(II)

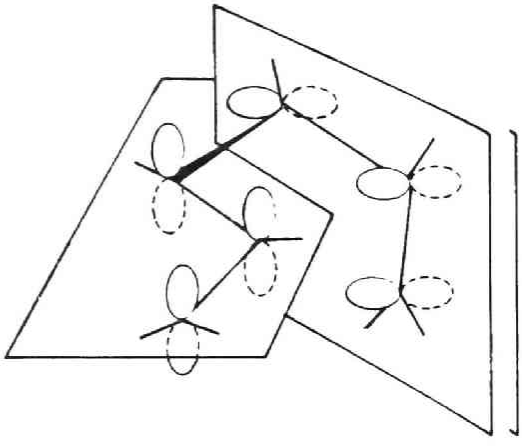

(III)

The sum of conjugation stabilization in the two separated parts in (I) is greater than in (II). The resulting geometry is shown in (III). Courtot and Salaün[35a] showed that sensitized photoreactions of hexatrienes preferentially cause the cis-trans isomerization of the *central* double bond, and that the singlet reaction causes isomerization of the terminal double bonds. The results are consistent with the theoretical prediction by Baird and West[35b] that the twisting of inner bonds should be preferred in the lowest triplet excited state of polyenes. In the singlet reaction a structure essentially like

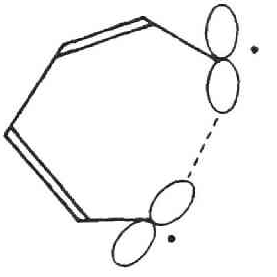

may be prevalent on account of the bonding nature of singlet biradicals, which will favour the terminal bond isomerization.

Geometries in which the planes associated with two unpaired-electron orbitals are perpendicular to each other might be expected more widely.[35c]

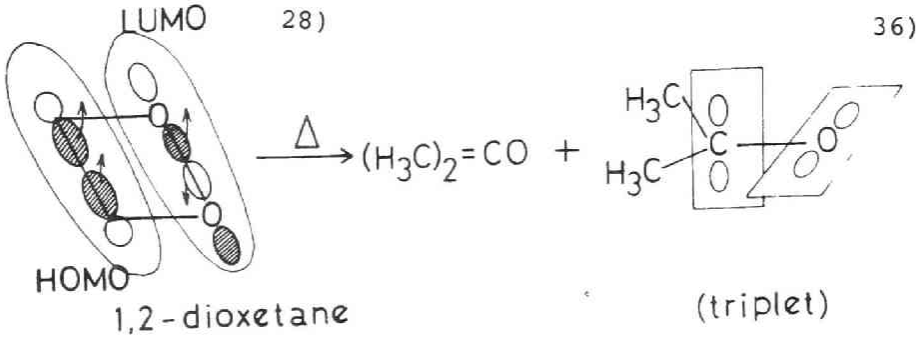

(Similar reactions are considered in chemiluminescent decomposition of 1,2-dioxetanone derivatives.[37])

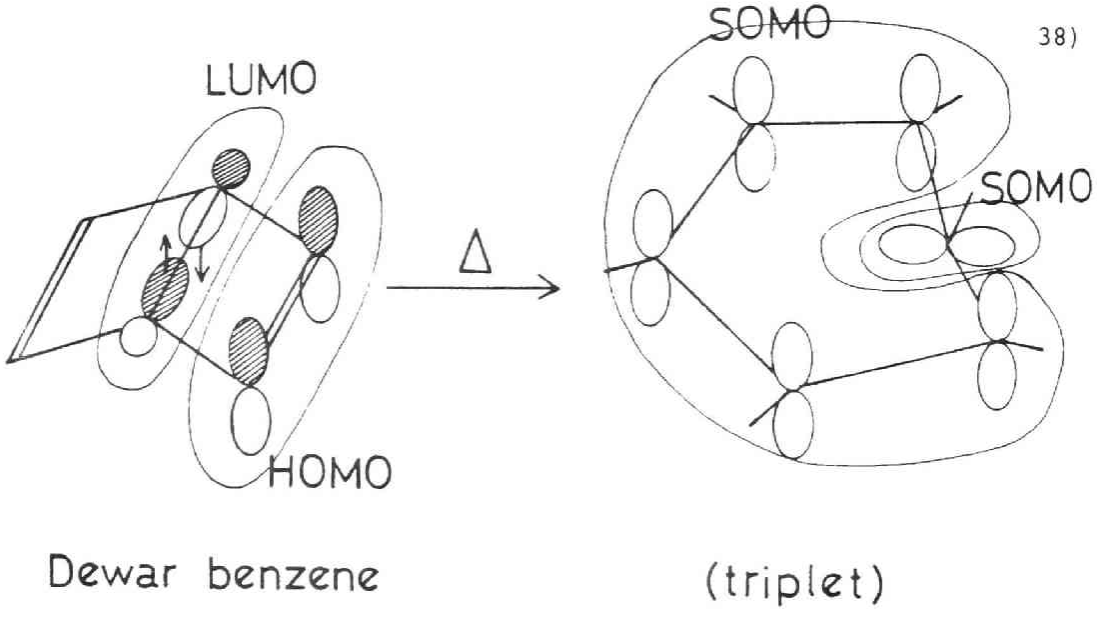

39)

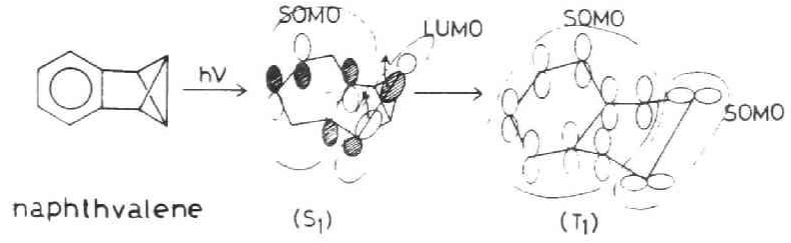

The above are examples of the separation of unpaired-electron orbitals by deformation. The isolation of unpaired-electrons also takes place by the formation of separating bonds.

40)

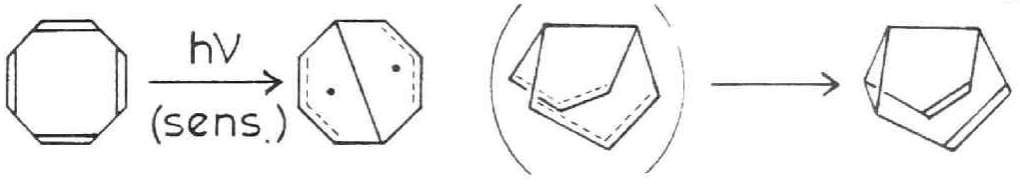

41)

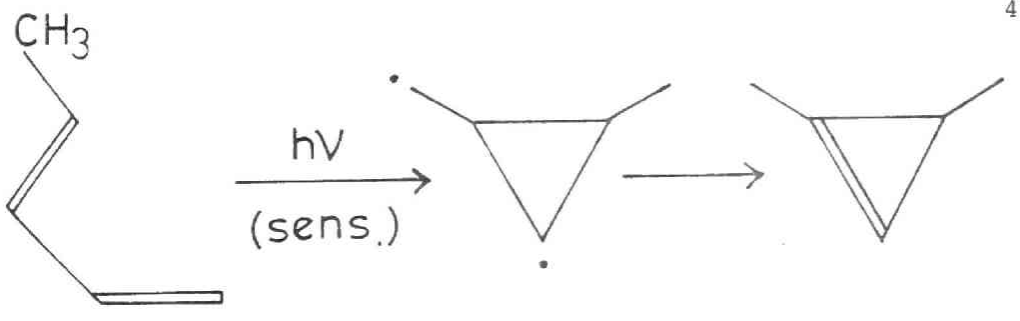

In the singlet-state reaction, a similar reaction takes place. In this case a certain concertedness may be mixed in the mech-

anism.[28]

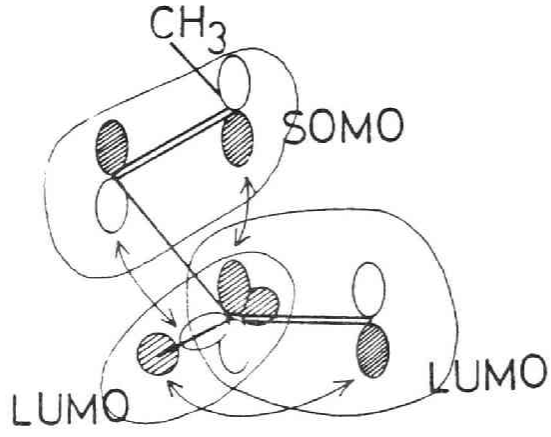

It appears that combination of the principle of unpaired-electron isolation in the triplet state with that of bonding deformation in the singlet state brings about a plausible mechanism occasionally prevalent in photochemical processes in which biradicaloid intermediates play an important role.

Suppose that the lowest triplet state (T_1) is produced, in some cases from higher excited singlet states (S_n) via S_1, through radiationless (triplet biradical formation by a non-sensitized photoprocess). A possible deformation path might be composed of stages (I) and (II) as shown in Figure 1.

Stage (I) involves separation of unpaired-electron orbitals by orthogonally twisting deformation or bond formation, occuring in the first triplet state. Stage (II) is that of bonding deformation or bond formation in the singlet ground

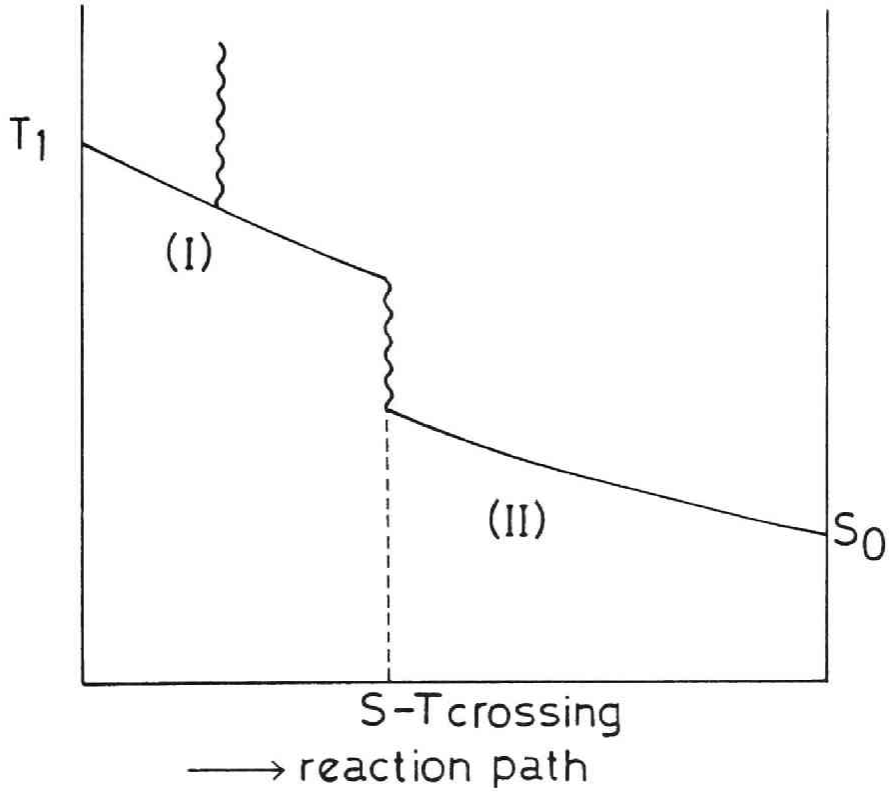

Figure 1. A possible reaction path. (S_0: singlet ground state; T_1: first triplet state; ~~~~ : radiationless transition)

state, S_0.

By considering intermediate T_1, stereoselective phenomena can be explained by the augmenting chance to undergo further conversion due to the long lifetime of the triplet state.

This mechanism of the intermediation of triplet state is supported by Kushick and Rice[42] as regards the effectuation of the S-T transition by dynamical coupling of the torsional motion around the C_1-C_2 bond in the cis-trans photoisomerization of butadiene.

Let us consider excited-state reactions of benzene, six π MO's of which are given below.

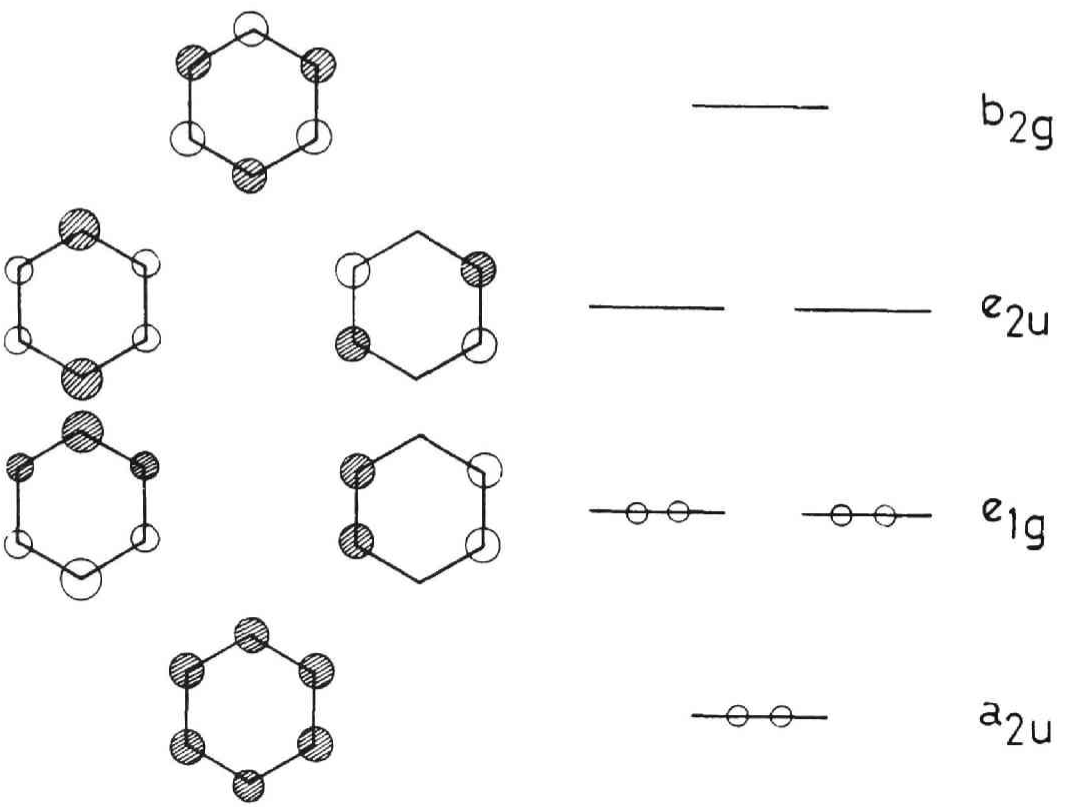

Then, Dewar benzene might be produced from $e_{1g} \rightarrow e_{2u}$ excited singlet ($^1B_{1u}$),[43a]

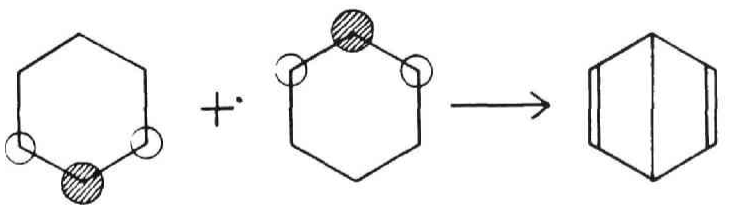

Dewar benzene

and the formation of benzvalene, prismane, and Dewar benzene would be favoured by triplet intermediation.

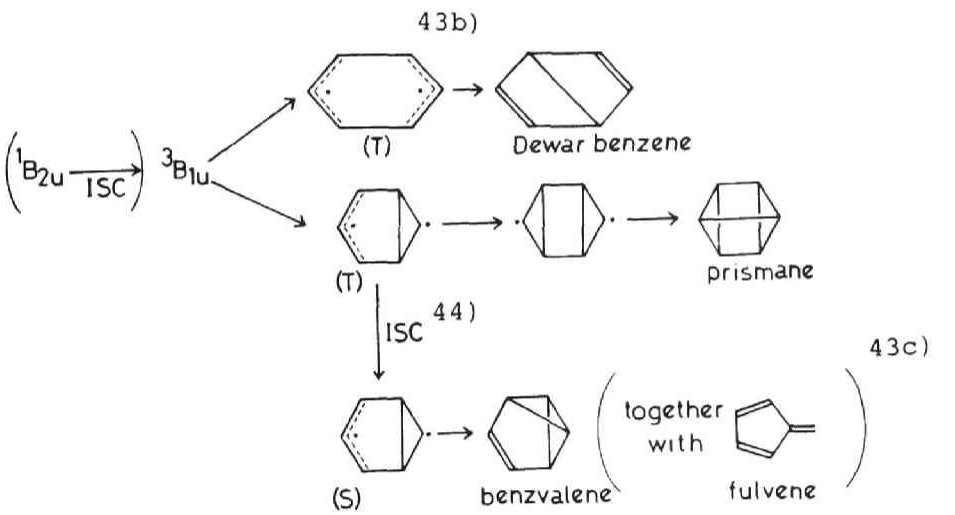

The mechanism involved might control the direction of reaction, giving a new principle of orientation or stereoselection in excited-state reactions.

References and Notes

1) R. B. Woodward and R. Hoffmann, Angew. Chem. Intern. Ed. Engl., 8, 781(1969).

2) J. A. Berson and L. Salem, J. Am. Chem. Soc., 94, 8917 (1972).

3) M. J. S. Dewar, S. Kirschner, and W. H. Kollmar, J. Am. Chem. Soc., 96, 7579(1974).

4) D. R. Roberts, J. Chem. Soc., Chem. Commun., 1974, 683.

5) L. Salem and C. Rowland, Angew. Chem. Intern. Ed. Engl., 11, 92(1972); L. Salem, Pure Appl. Chem., 33, 317(1973); L. Salem, W. G. Dauben, and N. J. Turro, J. Chim. Phys., 70, 694(1973); L. Salem, J. Am. Chem. Soc., 96, 3486(1974).

6) L. Salem, C. Leforestier, G. Segal, and R. Wetmore, J. Am. Chem. Soc., 97, 479(1975).

7) V. Vonačić-Koutecký, P. Bruckmann, P. Hiberty, J. Koutecký, C. Leforestier, and L. Salem, Angew. Chem. Intern. Ed. Engl., 14, 575(1975).

8) W. G. Dauben, L. Salem, and N. J. Turro, Acc. Chem. Res., 8, 41(1975).

9) L. Salem and P. Bruckmann, Nature, 258, 526(1975).

10) L. Salem, Science, 191, 822(1976).

11) The word "extremized" is used here only in the category

of the present two-electron, two-orbital approximation. The parallel trend mentioned is evident for the systems with equivalent radical centres (see text). However, it is not necessarily guaranteed for general cases.

12) K. Ruedenberg, Rev. Mod. Phys., 34, 326(1962).

13) H. Fujimoto, S. Yamabe, and K. Fukui, Bull. Chem. Soc. Jpn., 44, 2936(1971).

14) K. Fukui, XXIIIrd Intern. Congress of Pure and Applied Chemistry, Vol. 1, Butterworths, London (1971), p.65.

15) H. Fujimoto, S. Yamabe, and K. Fukui, Tetrahedron Lett., 1971, 443.

16) S. Yamabe, T. Minato, H. Fujimoto, and K. Fukui, Theoret. Chim. Acta(Berl.), 32, 187(1974).

17) S. Yamabe, S. Kato, H. Fujimoto, and K. Fukui, Bull. Chem. Soc. Jpn., 46, 3619(1973).

18) H. Fujimoto, S. Yamabe, T. Minato, and K. Fukui, J. Am. Chem. Soc., 94, 9205(1972).

19) K. Fukui, S. Kato, and H. Fujimoto, J. Am. Chem. Soc., 97, 1(1975).

20) H. Fujimoto and K. Fukui, Advances in Quantum Chemistry, 6, 177(1972).

21) H. Fujimoto and K. Fukui, in "Chemical Reactivity and Reaction Paths," ed. by G. Klopman, John Wiley & Sons, Inc., New York(1974), p.23.

22) S. Yamabe, S. Kato, H. Fujimoto, and K. Fukui, Bull. Chem. Soc. Jpn., 48, 1(1975).

23) C. E. Wulfman and S. Kumei, Science, 172, 1061(1971).

24) R. J. Buenker, S. D. Peyerimhoff, and H. L. Hsu, Chem. Phys. Lett., 11, 65(1971).

25) For example, D. P. Craig, Proc. Roy. Soc.(London), A202, 498(1950).

26) cf. W. T. Borden, J. Am. Chem. Soc., 98, 2695(1976).

27) M. J. S. Dewar and J. S. Wasson, J. Am. Chem. Soc., 93, 3081(1971); D. R. Yarkony and H. F. Schaefer III, J. Am. Chem. Soc., 96, 3754(1974); W. J. Hehre, L. Salem, and M. R. Wilcott, J. Am. Chem. Soc., 96, 4328(1974).

28) K. Fukui, "Theory of Orientation and Stereoselection," Springer-Verlag, Berlin (1975).

29) See p.81 of Ref. 28.

30) (a) S. Kita and K. Fukui, Bull. Chem. Soc. Jpn., 42, 66 (1969); (b) K. Fukui, Acc. Chem. Res., 4, 57(1971); (c) J. Michl, J. Am. Chem. Soc., 93, 523(1971); Mol. Photochem., 4, 257(1972); "Chemical Reactivity and Reaction Paths," ed. by G. Klopman, John Wiley & Sons, Inc., New York (1974), p.301; (d) H. E. Zimmerman and G. A. Epling, J. Am. Chem. Soc., 94, 3647(1972).

31) E. F. Ullman, J. Am. Chem. Soc., 82, 505(1960); J. J. Gajewski, J. Am. Chem. Soc., 93, 4450(1971); W. von E.

Doering and H. D. Roth, Tetrahedron, 26, 2825(1970); W. von E. Doering and L. Birladeanu, Tetrahedron, 29, 499 (1973).

32) W. von E. Doering and J. C. Gilbert, Tetrahedron Suppl., 7, 397(1966).

33) J. J. Gajewski and C. N. Shih, J. Am. Chem. Soc., 89, 4532(1967); W. von E. Doering and W. R. Dolbier, Jr., J. Am. Chem. Soc., 89, 4534(1967).

34) H. C. Longuet-Higgins and E. W. Abrahamson, J. Am. Chem. Soc., 87, 2045(1965).

35) (a) P. Courtot and J. Y. Salaün, J. Chem. Soc., Chem. Commun., 1976, 124; (b) N. C. Baird and R. M. West, J. Am. Chem. Soc., 93, 4427(1971); (c) W. G. Dauben and J. S. Ritscher, J. Am. Chem. Soc., 92, 2925(1970).

36) N. J. Turro and P. Lechtken, J. Am. Chem. Soc., 95, 264 (1973); N. J. Turro, H. C. Steinmetzer, and A. Yetka, J. Am. Chem. Soc., 95, 6468(1973); N. J. Turro and P. Lechtken, Pure Appl. Chem., 33, 363(1973); M. J. S. Dewar and S. Kirschner, J. Am. Chem. Soc., 96, 7578(1974); N. J. Turro, P. Lechtken, N. E. Schore, G. Schuster, H. C. Steinmetzer, and A. Yetka, Acc. Chem. Res., 7, 97(1974).

37) T. Goto and Y. Kishi, Angew. Chem. Intern. Ed. Engl., 7, 407(1968); W. D. McElroy, H. H. Seliger, and E. H. White, Photochem. Photobiol. 10, 153(1969); E. H. White, J. D.

Miano, C. J. Watkins, and E. J. Breaux, Angew. Chem., 86, 292(1974).

38) P. Lechtken, R. Breslow, A. H. Schmidt, and N. J. Turro, J. Am. Chem. Soc., 95, 3025(1973).

39) N. J. Turro, P. Lechtken, A. Lyons, R. R. Hautala, E. Carnahan, and T. J. Katz, J. Am. Chem. Soc., 95, 2035 (1973).

40) H. E. Zimmerman and H. Iwamura, J. Am. Chem. Soc., 90, 4763(1968).

41) S. Boué and R. Srinivasan, J. Am. Chem. Soc., 92, 3226 (1970).

42) J. N. Kushick and S. A. Rice, J. Chem. Phys., 64, 1612 (1976).

43) (a) I. Haller, J. Chem. Phys., 47, 1117(1967); (b) A. A. Gwaiz, M. A. El-Sayed, and D. S. Tinti, Chem. Phys. Lett., 9, 454(1971); (c) H. R. Ward and J. S. Wishnok, J. Am. Chem. Soc., 90, 5353(1968).

44) The possibility of the triplet intermediation in non-sensitized photolysis should be further examined. The sudden polarization of singlet biradicals[23] could be combined with the intersystem crossing $T_1 \rightarrow S_1$. The molecular geometry having minimum energy in the excited state is one with which the state T_1 has minimum energy. Such T_1 geometry would play some role in excited-state

reactions (*e.g.*, see K. Yamaguchi, T. Fueno, and H. Fukutome, Chem. Phys. Lett., 22, 466(1973)).

Chapter 6

Electronic Structures of an Infinite Polyene under Local Perturbations

I. Introduction

In the last decade, there has been a considerable progress in the quantum chemical treatment of the electronic structures of one-dimensional polymers based on Bloch's tight-binding LCAO-MO (BMO) method.[1] It is, however, unfeasible to treat a non-periodical system, such as having local defects or impurities, within that scheme, since it is based on the Bloch theorem[2] which is applicable to polymers composed of an infinite repetition of unit cells.

Recently, a method to treat polymers with aperiodic arrangements of monomers has been proposed by Ladik and Seel,[3] but it still requires a periodicity with a repetition of arrangements of several monomers as units. On the other hand, simple models of the local chemisorption on the surface of solid have been discussed rather qualitatively using the Green function technique by Schrieffer and by Koutecký.[4,5] In this Chapter, we show a treatment of locally perturbed linear polymers employing the Wannier function[6] as localized MO

(LMO) of the unperturbed system similar to Schrieffer and Koutecký but in a more quantitative way.

II. Formulation

An LMO of the p-th level localized at the j-th cell is defined by the Wannier transformation from the BMO as following,

$$a_p(\underline{r}-j\underline{a}) = \frac{1}{\sqrt{2N+1}} \sum_{k}^{BZ} \exp[-ikj\underline{a}]\Phi_p(k,\underline{r}), \quad (j= 0, \pm1, \pm2,\cdots, \pm N) \qquad (1)$$

where $\Phi_p(k,\underline{r})$ is the BMO of the p-th level with wavenumber k, $\underline{a}$ is the unit vector of the translational symmetry along the chain, BZ represents the summation over the Brillouin zone, and (2N+1) means the number of unit cells. Each of $\Phi_p(k,\underline{r})$ is spread into the (2N+1) LMO's localized at each unit cell.

Now, provided that a perturbation is applied to the 0-th cell, it will influence only those LMO's, $a_p(\underline{r}-j\underline{a})$, which are localized at the unit cells near the centre of perturbation, causing the correction terms $\delta a_p(\underline{r}-j\underline{a})$. Generally j is in the range from 0 to $\pm M$, where M indicates the number of neighbouring LMO's still having a significant decaying tail of amplitude in the 0-th cell. Since BMO and LMO are connected by a uni-

tary transformation, the total energy, the electron density, and the bond order of the perturbed system can be obtained by the summation of the quantities evaluated from the perturbed LMO's ($a_p(\underline{r}-j\underline{a})+\delta a_p(\underline{r}-j\underline{a})$, $-M\leqq j\leqq M$) and from other unperturbed LMO's. In other words, the correction terms of these quantities owing to the perturbation are issued from nothing but the presence of $\delta a_p(\underline{r}-j\underline{a})$. Thus the local perturbation problem of polymers is reduced to the estimation of the correction terms of a rather small number of perturbed LMO's.

The change of the unperturbed LMO of the p-th level localized at the j-th cell ($\delta a_p(\underline{r}-j\underline{a})$), that of its orbital energy ($\delta\varepsilon_{p,j}$), and that of the total energy of the polymer (δE) by the perturbation V applied to the 0-th cell is described as follows using the notations $V_{qr,j}=\langle a_q(\underline{r}-j\underline{a})|V|a_r(\underline{r}-j\underline{a})\rangle$, and $V'_{qr,j}=\langle a_q(\underline{r}-j\underline{a})|V'|a_r(\underline{r}-j\underline{a})\rangle$, where $V'=V-V_{pp,j}$:

$$\delta a_p(r-ja) = \sum_{q(\neq p)}^{all} \frac{V_{qp,j}a_q(\underline{r}-j\underline{a})}{\varepsilon_{p,j}-\varepsilon_{q,j}} + \left[\sum_{q(\neq p)}^{all}\sum_{r(\neq p)}^{all} \frac{V'_{rq,j}V_{qp,j}a_r(\underline{r}-j\underline{a})}{(\varepsilon_{p,j}-\varepsilon_{q,j})(\varepsilon_{p,j}-\varepsilon_{r,j})} - \frac{1}{2}\sum_{q(\neq p)}^{all} \frac{V_{pq,j}V_{qp,j}a_p(\underline{r}-j\underline{a})}{(\varepsilon_{p,j}-\varepsilon_{q,j})^2} \right]$$

$$+\left[\sum_{q(\neq p)}^{all}\sum_{r(\neq p)}^{all}\sum_{s(\neq p)}^{all}\frac{V'_{sr,j}V'_{rq,j}V_{qp,j}a_s(\underline{r}-j\underline{a})}{(\varepsilon_{p,j}-\varepsilon_{q,j})(\varepsilon_{p,j}-\varepsilon_{r,j})(\varepsilon_{p,j}-\varepsilon_{s,j})}\right.$$

$$-\frac{1}{2}\sum_{q(\neq p)}^{all}\sum_{r(\neq p)}^{all}\frac{V_{pq,j}V_{qp,j}V_{rp,j}a_r(\underline{r}-j\underline{a})}{(\varepsilon_{p,j}-\varepsilon_{q,j})^2(\varepsilon_{p,j}-\varepsilon_{r,j})}$$

$$-\sum_{q(\neq p)}^{all}\sum_{r(\neq p)}^{all}\frac{V_{pr,j}V_{rp,j}V_{qp,j}a_q(\underline{r}-j\underline{a})}{(\varepsilon_{p,j}-\varepsilon_{r,j})(\varepsilon_{p,j}-\varepsilon_{q,j})^2}$$

$$\left.-\sum_{q(\neq p)}^{all}\sum_{r(\neq p)}^{all}\frac{V_{pq,j}V'_{qr,j}V_{rp,j}a_p(\underline{r}-j\underline{a})}{(\varepsilon_{p,j}-\varepsilon_{q,j})^2(\varepsilon_{p,j}-\varepsilon_{r,j})}\right]+\cdots, \tag{2}$$

$$\delta\varepsilon_{p,j}=V_{pp,j}+\sum_{q(\neq p)}^{all}\frac{V_{pq,j}V_{qp,j}}{\varepsilon_{p,j}-\varepsilon_{q,j}}+\sum_{q(\neq p)}^{all}\sum_{r(\neq p)}^{all}$$

$$\frac{V_{pq,j}V'_{qr,j}V_{rp,j}}{(\varepsilon_{p,j}-\varepsilon_{q,j})(\varepsilon_{p,j}-\varepsilon_{r,j})}+\cdots, \tag{3}$$

and

$$\delta E=2\sum_{j=0}^{+M}\sum_{p}^{occ}\delta\varepsilon_{p,j}, \tag{4}$$

where the interelectron potentials are neglected. The changes of the electron density and the bond order are also easily derived from $\delta a_p(\underline{r}-j\underline{a})$ by the summation with respect to j as indicated in Eq.(4).

III. Application to Infinite Polyene

Let us consider here three types of local perturbations toward an infinite polyene without bond alternation as shown in Figure 1 in the frame of the Hückel MO approach where the Coulomb integral of a carbon atom and the resonance integral between adjacent carbon atoms are denoted as α and β, respectively, in the unperturbed polyene.

First, when the carbon atom $C_1^{(0)}$ in Figure 1(A) is replaced with a heteroatom X, the Coulomb integral of that atom will become $\alpha+\delta\alpha$ (Case I), where $C_u^{(j)}$ means the u-th carbon atom in the j-th cell. Next is the case where the resonance integral β between $C_1^{(0)}$ and $C_2^{(0)}$ is increased by $\delta\beta$ with the change of the bond length between them (Case II). The third case is the infinite polyene perturbed by another carbon atom C_x through a weak bond with $C_1^{(0)}$ whose resonance integral is $\delta\gamma$ (Case III). Prior to the treatment of these examples, the unperturbed system should be examined. Neglecting all but the nearest neighbour atom interaction (Hückel approxima-

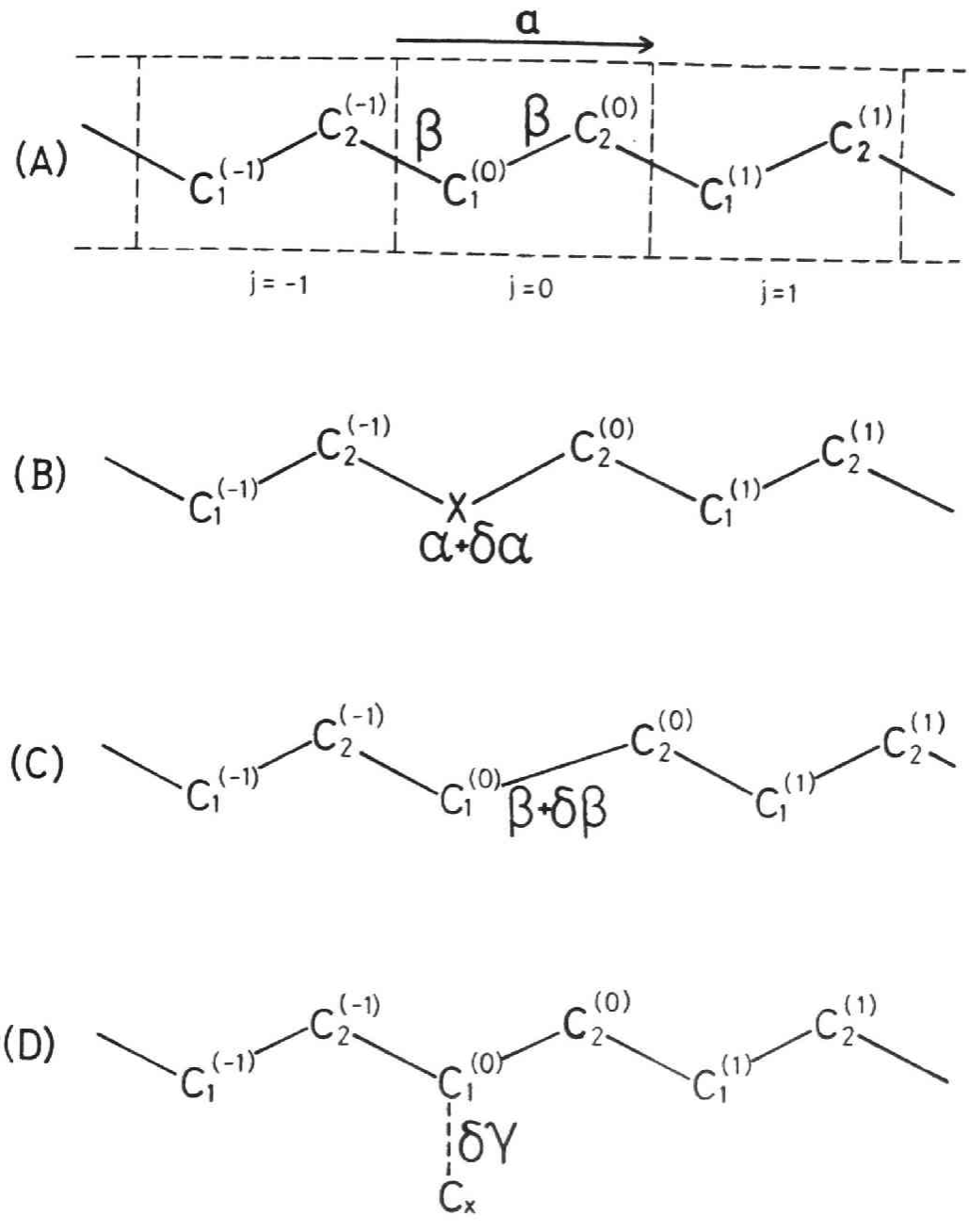

Figure 1. (A) Unperturbed polyene. The origin of the space coordinate $\underline{r}$ is fixed to $C_1^{(0)}$. (B), (C), and (D) are the perturbed systems designated as Cases I, II, and III, respectively.

tion), the occupied BMO of unperturbed polyene, $\Phi_1(k,\underline{r})$, the unoccupied $\Phi_2(k,\underline{r})$, and their orbital energies have been obtained as follows,[7)]

$$\Phi_1(k,\underline{r}) = \frac{1}{\sqrt{2N+1}} \sum_{j=0}^{+N} \exp[ikj\underline{a}]\{\frac{1}{\sqrt{2}}\chi_1(\underline{r}-j\underline{a}) + \frac{1}{\sqrt{2}}\exp[ik\underline{a}/2] \cdot \chi_2[\underline{r}-(j+\tfrac{1}{2})\underline{a}]\}, \quad (5\text{-A})$$

$$\Phi_2(k,\underline{r}) = \frac{1}{\sqrt{2N+1}} \sum_{j=0}^{+N} \exp[ikj\underline{a}]\{\frac{1}{\sqrt{2}}\chi_1(\underline{r}-j\underline{a}) - \frac{1}{\sqrt{2}}\exp[ik\underline{a}/2] \cdot \chi_2[\underline{r}-(j+\tfrac{1}{2})\underline{a}]\}, \quad (6\text{-A})$$

$$\varepsilon_1(k) = \langle\Phi_1(k,\underline{r})|H|\Phi_1(k,\underline{r})\rangle = \alpha + 2\beta\cos(k\underline{a}/2), \quad (5\text{-B})$$

$$\varepsilon_2(k) = \langle\Phi_2(k,\underline{r})|H|\Phi_2(k,\underline{r})\rangle = \alpha - 2\beta\cos(k\underline{a}/2), \quad (6\text{-B})$$

where χ_u specifies a $2p\pi$ AO of the u-th atom in the unit cell and H is the Hamiltonian of the system. The unit cell of the polyene is assumed to be composed of two carbon atoms. The occupied and the unoccupied LMO's localized at the 0-th cell are, respectively,

$$a_1(\underline{r}) = \sum_{j=0}^{\pm N} \frac{1}{2\pi} \left[\frac{\sqrt{2}\sin(j\pi)}{j} \chi_1(\underline{r}-j\underline{a}) + \frac{\sqrt{2}\sin\{(j+\frac{1}{2})\pi\}}{j+\frac{1}{2}} \cdot \chi_2[\underline{r}-(j+\tfrac{1}{2})\underline{a}] \right], \quad (7\text{-A})$$

$$a_2(\underline{r}) = \sum_{j=0}^{\pm N} \frac{1}{2\pi} \left[\frac{\sqrt{2}\sin(j\pi)}{j} \chi_1(\underline{r}-j\underline{a}) - \frac{\sqrt{2}\sin\{(j+\frac{1}{2})\pi\}}{j+\frac{1}{2}} \cdot \chi_2[\underline{r}-(j+\tfrac{1}{2})\underline{a}] \right], \quad (8\text{-A})$$

and shown in Figure 2. These correspond to the frontier orbitals in the finite molecule theory.[8] Similarly, their orbital energies are obtained as;

$$\varepsilon_{1,0} = \langle a_1(\underline{r}) | H | a_1(\underline{r}) \rangle = \alpha + \frac{4}{\pi}\beta , \quad (7\text{-B})$$

$$\varepsilon_{2,0} = \langle a_2(\underline{r}) | H | a_2(\underline{r}) \rangle = \alpha - \frac{4}{\pi}\beta . \quad (8\text{-B})$$

It should be noticed that the present LMO's $a_1(\underline{r})$ and $a_2(\underline{r})$ have no amplitude on $C_1^{(j)}$ $(j \neq 0)$, which allows us to treat rather simply the perturbation applied to $C_1^{(0)}$, since, in this case, M in Eq.(4) is equal to zero. The changes of theoretical quantities by the present types of perturbation

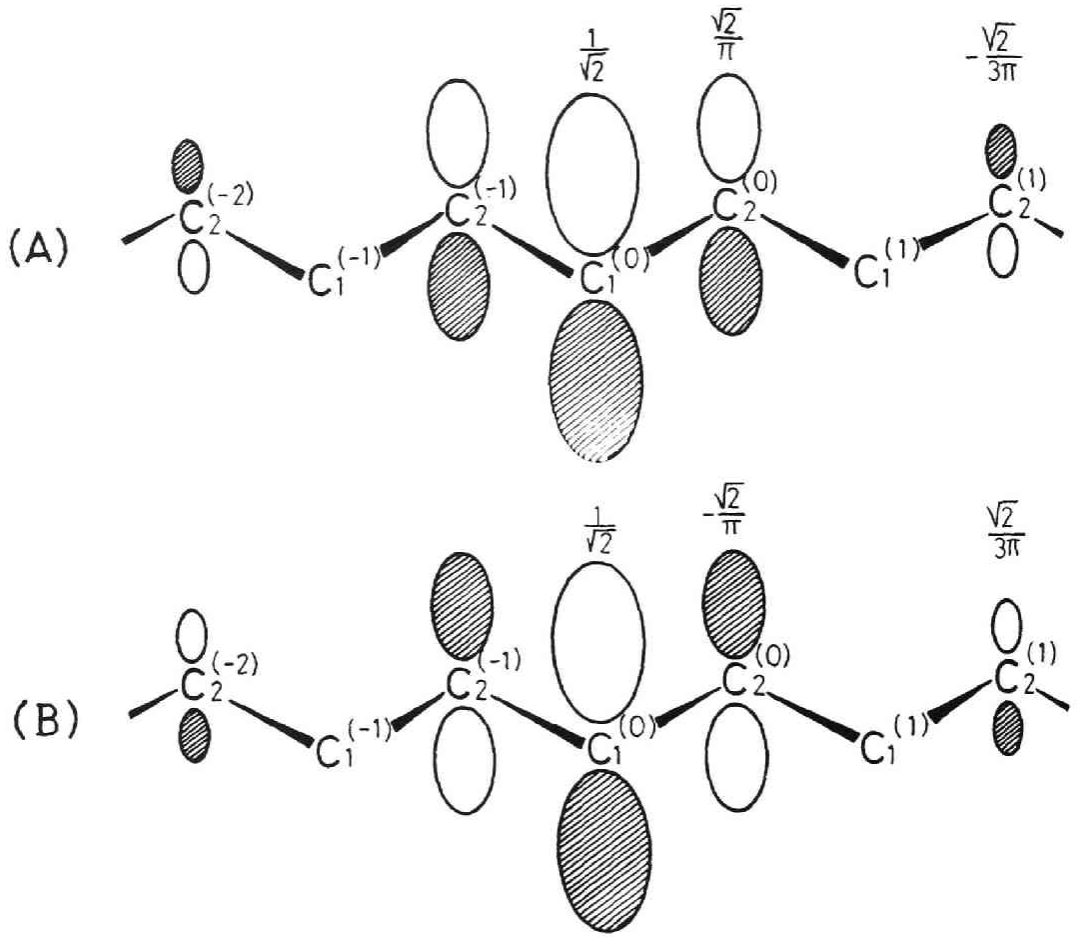

Figure 2. Amplitude of LMO's localized at the 0-th cell. (A) $a_1(\underline{r})$ (occupied); (B) $a_2(\underline{r})$ (unoccupied).

have already been formulated by Fukui *et al.*[9,10] for the finite molecule. Therefore, one has only to replace the unperturbed MO in their treatment by the LMO localized at the perturbed site.

The changes of $a_1(\underline{r})$ ($\delta a_1(\underline{r})$), $\varepsilon_{1,0}(\delta\varepsilon_{1,0})$, total energy of polyene (δE), bond order between arbitrary carbons in the polyene (δP_{uv}), electron density (δP_{uu}), created bond order between $C_1^{(0)}$ and C_X (δP_{1X}), electron density of C_X (δP_{XX}), and charge transfer from C_X to the polyene (δQ) are directly derived from the formulae in Ref. 10 for the present each case of perturbations.

In Case I, denoting $d_u^{\,i}$ as the coefficient of χ_u in $a_i(\underline{r})$,

$$\delta a_1(\underline{r}) = \frac{\pi}{16\beta}(\delta\alpha)a_2(\underline{r}) - \frac{\pi^2}{512\beta^2}(\delta\alpha)^2 a_1(\underline{r}) + o(\delta\alpha)^3, \quad (9\text{-A})$$

$$\delta\varepsilon_{1,0} = \frac{1}{2}(\delta\alpha) + \frac{\pi}{32\beta}(\delta\alpha)^2 , \quad (9\text{-B})$$

$$\delta E = \delta\alpha + \frac{\pi}{16\beta}(\delta\alpha)^2 , \quad (9\text{-C})$$

$$\delta P_{uv} = \frac{\pi}{8\beta}(d_u^{\,1}d_v^{\,2} + d_u^{\,2}d_v^{\,1})(\delta\alpha) + \frac{\pi^2}{128\beta^2}(d_u^{\,2}d_v^{\,2} - d_u^{\,1}d_v^{\,1})$$

$$\cdot(\delta\alpha)^2 + o(\delta\alpha)^3 , \quad (u=v \text{ or } u\neq v) \quad (9\text{-D})$$

where the third-order terms of $\delta\varepsilon_{1,0}$ and δE drop out because of the symmetries of $a_1(\underline{r})$ and $a_2(\underline{r})$. Likewise in Case II,

$$\delta a_1(\underline{r}) = 0 \ , \tag{10-A}$$

$$\delta\varepsilon_{1,0} = \frac{2}{\pi}(\delta\beta) \ , \tag{10-B}$$

$$\delta E = \frac{4}{\pi}(\delta\beta) \ , \tag{10-C}$$

$$\delta P_{uv} = 0 \ . \qquad (u=v \text{ or } u\neq v) \tag{10-D}$$

In the present case, $\delta a_1(\underline{r})$ and δP_{uv} as far as the third-order and the second- and the third-order terms of $\delta\varepsilon_{1,0}$ and δE drop out.

Furthermore, in Case III,

$$\delta a_1(\underline{r}) = \frac{\sqrt{2}\pi}{8\beta}(\delta\gamma)\chi_X + \frac{\pi^2}{64\beta^2}(\delta\gamma)^2(a_2(\underline{r}) - a_1(\underline{r})) + o(\delta\gamma)^3 \ , \tag{11-A}$$

$$\delta\varepsilon_{1,0} = \frac{\pi}{8\beta}(\delta\gamma)^2 + o(\delta\gamma)^4 \ , \tag{11-B}$$

$$\delta E = \frac{\pi}{4\beta}(\delta\gamma)^2 + o(\delta\gamma)^4 \ , \qquad \text{(11-C)}$$

$$\delta P_{uv} = \frac{\pi^2}{32\beta^2}(d_u^{\,2}d_v^{\,2} - d_u^{\,1}d_v^{\,1})(\delta\gamma)^2 + o(\delta\gamma)^3 \ , \quad (u=v \text{ or } u\neq v) \qquad \text{(11-D)}$$

$$\delta P_{1X} = \frac{\pi}{4\beta}(\delta\gamma) + o(\delta\gamma)^3 \ , \qquad \text{(11-E)}$$

$$\delta P_{XX} = o(\delta\gamma)^3 \ , \qquad \text{(11-F)}$$

$$\delta Q = o(\delta\gamma)^3 \ , \qquad \text{(11-G)}$$

where χ_X is $2p\pi$ AO of C_X. It is to be noted that δP_{uu}, δP_{XX}, and δQ are equal to zero, namely the electron densities of every carbon atom in the polyene and C_X remain unity, because of the symmetries of $a_1(\underline{r})$ and $a_2(\underline{r})$. The treatment of Case III can easily be extended to the system perturbed by another conjugated molecule instead of C_X, although it is omitted here for the sake of simplicity.

It has been shown that the formulations in the SCF-MO is quite similar to those in the Hückel MO for the finite molecule for Cases I and II.[11] Also the formulations of Bacon and Santry[12] may be available to the Case III for the SCF-MO treatment. Therefore, the present treatment of local pertur-

bation toward polymers within the Hückel MO approach would be basic as a starting point of the following approaches by non-empirical or semi-empirical Hartree-Fock theory.

References and Notes

1) For example, see "Electronic Structure of Polymers and Molecular Crystals," ed. by J. M. André and J. Ladik, Plenum Press, New York (1975).

2) F. Bloch, Z. Phys., 52, 555(1928).

3) J. Ladik and M. Seel, Phys. Rev., B13, 5338(1976).

4) J. R. Schrieffer, "Proc. 2nd International Congress of Quantum Chemistry," D. Reidel Publ. Co., Dordrecht-Holland (1976), p.305; also see: J. B. Danese and J. R. Schrieffer, Intern. J. Quant. Chem., S10, 289(1976).

5) J. Koutecký, "Proc. 2nd International Congress of Quantum Chemistry," D. Reidel Publ. Co., Dordrecht-Holland (1976), p.279; also see references therein.

6) G. H. Wannier, Phys. Rev., 52, 191(1937).

7) See p.9 and p.55 of Ref. 1.

8) K. Fukui, "Theory of Orientation and Stereoselection," Springer-Verlag, Berlin (1975).

9) K. Fukui, C. Nagata, T. Yonezawa, H. Kato, and K. Morokuma, J. Chem. Phys., 31, 287(1959).

10) K. Fukui, K. Morokuma, T. Yonezawa, and C. Nagata, Bull. Chem. Soc. Jpn., 33, 963(1960).

11) G. Diercksen and R. McWeeny, J. Chem. Phys., 44, 3554 (1966).

12) J. Bacon and D. P. Santry, J. Chem. Phys., 55, 3743(1971)..

Chapter 7

Orbital Interaction in the Dimerization of S_2N_2 into S_4N_4

In recent years, disulfur dinitride, S_2N_2, and tetrasulfur tetranitride, S_4N_4, shown in Figure 1 have been of much interest in that they are the precursors of polymeric sulfur nitride, $(SN)_x$,[1] which is a low-dimensional metallic conductor and even becomes a superconductor at 0.3°K.[2] On the other hand, it has been also reported that S_2N_2 rapidly dimerizes, in certain organic solvents with a trace of alkali, to S_4N_4,[3] which is known to have a geometry with coplanar N atoms from the X-ray diffraction analysis.[4] Then it would be an interesting problem to explain the process of the formation of S_4N_4 from S_2N_2 by using the consideration of orbital interaction.[5]

From the atomic arrangement of S_4N_4 and the principle of maximum overlap of the highest occupied (HO) MO and the lowest unoccupied (LU) MO between two S_2N_2 molecules, two kinds of S_2N_2 stacking interaction models (A) and (B) are considered as shown in Figure 2. They are of essentially different configurations to be stacked onto when S_2N_2 approaches each other. The HOMO and the LUMO of S_2N_2 employed in this Chapter are obtained with the use of the ASMO-SCF method.[6] The shape of

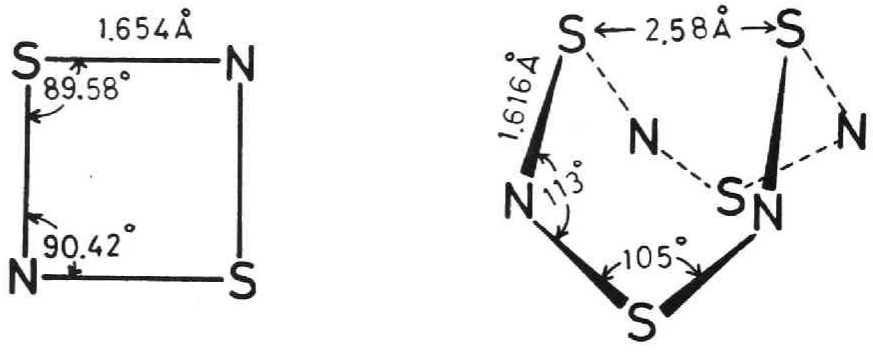

Figure 1. Geometries of S_2N_2[1a,1b] and S_4N_4.[4]

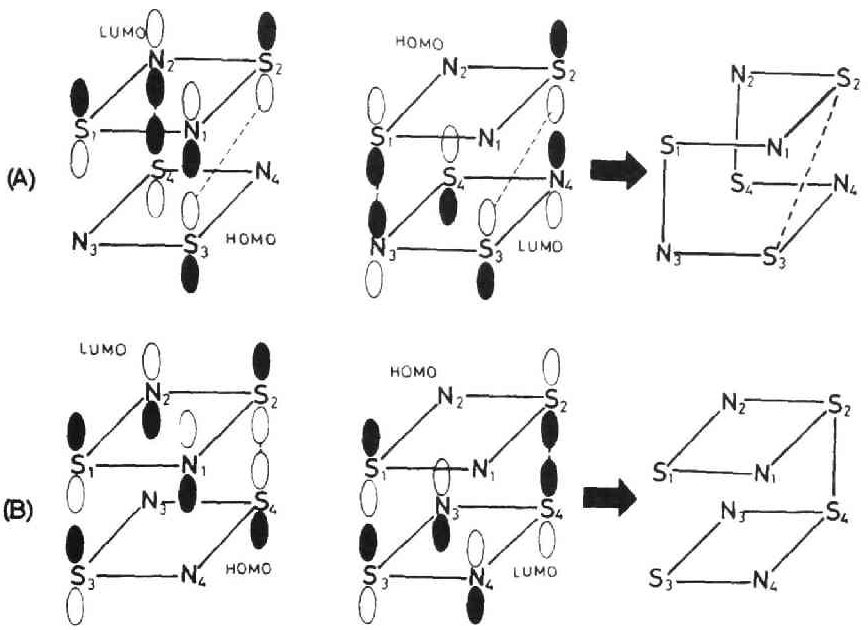

Figure 2. Two stacking interaction models (A) and (B) to form S_4N_4 by the dimerization of S_2N_2.

the HOMO is consistent with that analyzed by the photoelectron spectroscopic study[7] and the shape of the LUMO is the same with those obtained by other MO calculations under various versions.[8]

The HOMO-LUMO interactions of S_1-N_3 and N_2-S_4 are "bonding" in model (A), and thereby two new pσ type bonds are ready to be formed between them, accordingly as the π bonds of S_1-N_2 and N_3-S_4 are weakened. On the contrary, interactions of N_1-S_3 and S_2-N_4 are "antibonding" and, therefore, do not contribute to form new bonds. The intermediate-range interaction of S_2-S_3, which is favourable for bonding, should be taken into account even though the interaction is weak, since π AO of S diffuses and then the overlap of S_2-S_3 is not negligible.

On the other hand, following the stacking interaction in model (B), merely S_2-S_4 bond formation is favourable. This type of orbital interaction is disadvantageous to bring about the subsequent process of the dimerization, so model (B) could be discarded. It is to be noted that the way of stacking in model(B) coincides with that in S_2N_2 crystal along the b-axis.[1c]

Hence one can explain the process of the formation of S_4N_4 with coplanar N atoms with the use of model (A) as follows: the main bonds to be formed are S_1-N_3 and N_2-S_4 pσ bonds while the previous S_1-N_2 and N_3-S_4 cleavage along the formation of

new bonds as shown in Figure 2(A). In the framework of this dimerization model, the reaction proceeds quite easily only through bond interchange without large dislocation among nuclei and, therefore, without going over large potential barrier. Succeedingly a slight deformation may take place until the most stable geometry in Figure 1 is accomplished along S_2-S_3 bond which plays a role of fulcrum as illustrated in Figure 3. The most stable geometry is then expected to be completed when the weak S_1-S_4 bond is formed. The existence of these transannular S-S bonds has also been suggested by the MO calculations for S_4N_4 molecule itself.[8b,8c,9)]

Another geometry of S_4N_4 with coplanar S atoms which had been proposed by the IR and Raman spectroscopic analyses[10)] is denied at least in the present orbital interaction treatment on the direct dimerization of S_2N_2 into S_4N_4. The extended Hückel MO[9c)] and the CNDO/BW MO[9g)] calculations have also supported the geometry with coplanar N atoms from the viewpoint of the total energy of S_4N_4. However, there still may be a possibility of the interconversion of S_4N_4 between the geometries with coplanar N atoms and with coplanar S atoms making use of some appropriate vibrational modes each other. In this point, further investigation on these geometries taking also the vibrational analysis into account would be desirable.

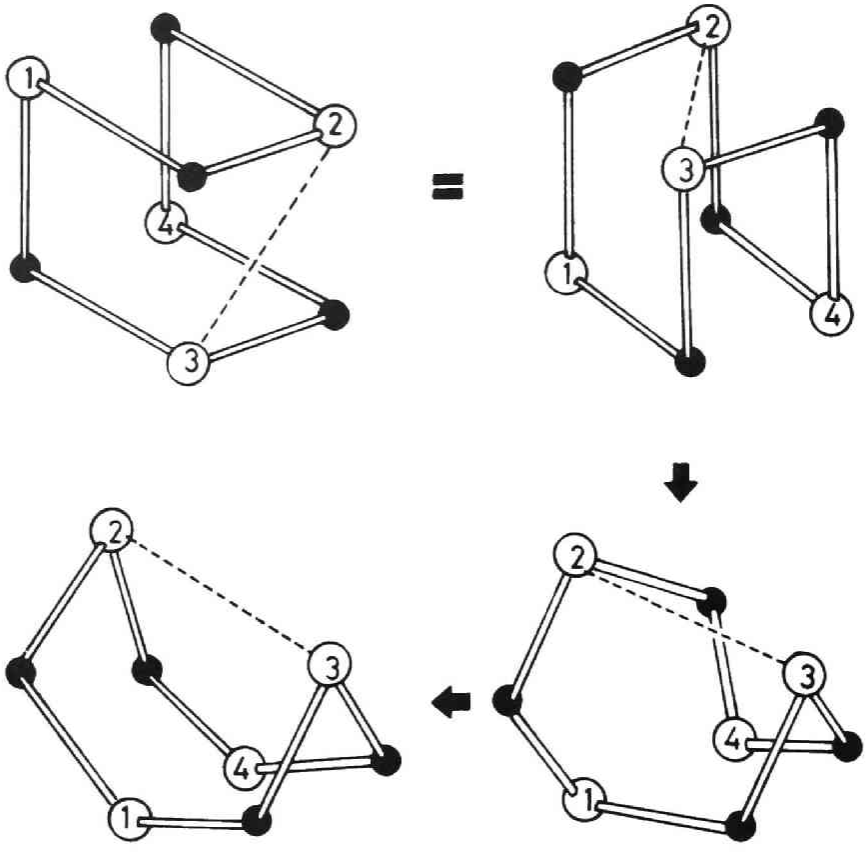

Figure 3. Topological mode of deformation from the S_2N_2 stacking model (A) to S_4N_4. White balls represent S atoms and black balls N atoms.

References and Notes

1) (a) A. G. MacDiarmid, C. M. Mikulski, P. J. Russo, M. S. Saran, A. F. Garito, and A. J. Heeger, J. Chem. Soc., Chem. Commun., 1975, 476; (b) C. M. Mikulski, P. J. Russo, M. S. Saran, A. G. MacDiarmid, A. F. Garito, and A. J. Heeger, J. Am. Chem. Soc., 97, 6358(1975); (c) M. J. Cohen, A. F. Garito, A. J. Heeger, A. G. MacDiarmid, C. M. Mikulski, M. S. Saran, and J. Kleppinger, J. Am. Chem. Soc., 98, 3844(1976).

2) R. L. Greene, G. B. Street, and L. J. Suter, Phys. Rev. Lett., 35, 1799(1975).

3) H. J. Emeléus, Endeavour, 32, 76(1973).

4) B. D. Sharma and J. Donohue, Acta Crystallogr., 16, 891 (1963).

5) K. Fukui, "Theory of Orientation and Stereoselection," Springer-Verlag, Berlin (1975).

6) T. Yonezawa, H. Konishi, and H. Kato, Bull. Chem. Soc. Jpn., 42, 933(1969); also see the next Chapter of this thesis.

7) D. C. Frost, M. R. LeGeyt, N. L. Paddock, and N. P. C. Westwood, J. Chem. Soc., Chem. Commun., 1977, 217.

8) (a) M. P. S. Collins and B. J. Duke, J. Chem. Soc., Chem. Commun., 1976, 701; (b) D. R. Salahub and R. P. Messmer,

J. Chem. Phys., 64, 2039(1976); (c) W. R. Salaneck, J. W-p Lin, A. Paton, C. B. Duke, and G. P. Ceasar, Phys. Rev., B13, 4517(1976); (d) J. A. Jafri, M. D. Newton, T. A. Pakkanen, and J. L. Whitten, J. Chem. Phys., 66, 5167 (1977).

9) (a) D. Chapman and T. C. Waddington, Trans. Faraday Soc., 58, 1679(1962); (b) F. S. Braterman, J. Chem. Soc., A, 2297(1965); (c) A. G. Turner and F. S. Mortimer, Inorg. Chem., 5, 906(1966); (d) J. B. Mason, J. Chem. Soc., A, 1567(1969); (e) R. Gleiter, J. Chem. Soc., A, 3174(1970); (f) P. Cassoux, J. F. Labarre, O. Glemser, and W. Koch, J. Mol. Struct., 13, 405(1972); (g) M. S. Gopinathan and M. A. Whitehead, Can. J. Chem., 53, 1343(1974).

10) E. R. Lippincott and M. C. Tobin, J. Chem. Phys., 21, 1559(1953).

Chapter 8

The Initial Stage of Polymerization from $(SN)_2$ Molecules to $(SN)_x$ Polymer

I. Introduction

There has recently been considerable interest in the covalent polymer, polymeric sulfur nitride, $(SN)_x$, since the discovery that it is a low-dimensional metallic conductor.[1,2] The theoretical treatment for $(SN)_x$ has also been carried out to reveal the metallic character of the $(SN)_x$ in its band structure.[3] Recently, MacDiarmid *et al.* have reported that the crystalline monomeric S_2N_2 polymerizes thermally in the solid state to form the $(SN)_x$ polymer.[4] They have also determined the structure of $(SN)_x$ as well as S_2N_2 shown in Figures 1(A) and (B) by X-ray diffraction. The initially colourless tabular monoclinic crystal of S_2N_2 turns intense blue-black and becomes paramagnetic giving a weak free radical signal at g=2.005. This substance then changes to golden-coloured, diamagnetic crystals of $(SN)_x$ polymer.

For the mechanism of the solid state polymerization, they have also proposed, particularly at the first step, the thermal opening (widening) of one of the S-N bonds in S_2N_2 to form a

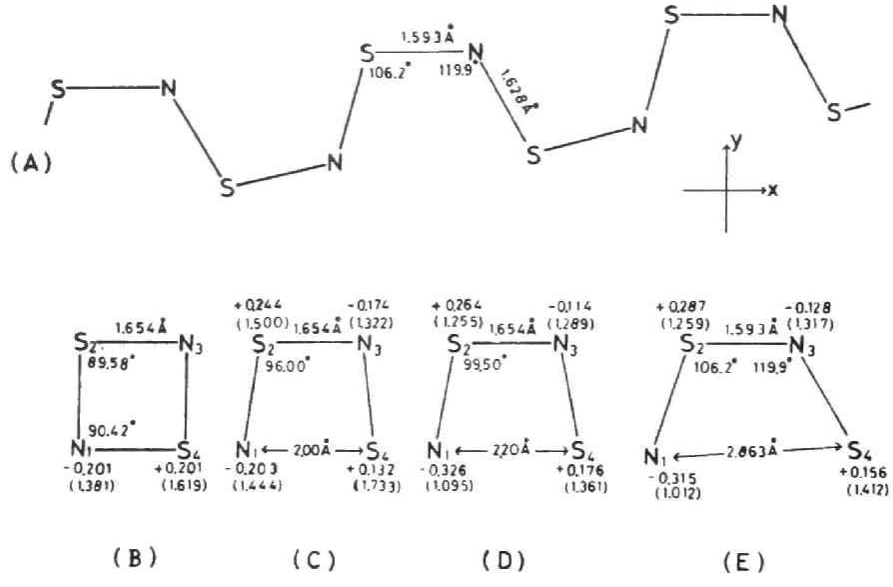

Figure 1. Geometries of the polymer $(SN)_x$ (A), the precursor S_2N_2 (B), and several deformed $(SN)_2$ molecules (C, D, and E) with atomic net charges and π electron densities (bracketed values). For (D) and (E), those of the triplet states are shown.

biradical species. This radical can then link up with another S_2N_2 molecule in the crystal to give the partly polymerized, paramagnetic $(SN)_2$ of blue-black colour, and finally the golden $(SN)_x$ polymer. Moreover, Baughman *et al.* have studied the polymerization including defect structures crystallographically.[5]

In this Chapter, we try to elucidate the polymerization reaction, particularly at the initial stage, and to confirm the mechanism proposed above by MO calculations. At first, the electronic structure of the precursor S_2N_2, and then, those of the several "deformed" structures of $(SN)_2$ as shown in Figure 1 are calculated and the thermal initiation reaction is investigated. The calculations are performed with the use of the semi-empirical INDO-type ASMO-SCF method for valence electrons including sulfur 3d orbitals,[6a] and the stability of the triplet state (open-shell) is examined by the sign of the transition energy from the lowest singlet state (closed-shell).[6b] This method has given fairly reasonable results, especially for the transition energies[6c-6e] because of good parametrization for Coulomb repulsion integrals.[7] Examined further are the electronic structures of the dimeric unit $(SN)_4$ and the trimeric unit $(SN)_6$.

II. Electronic Structure of S_2N_2

The molecular structure of S_2N_2 employed here is shown in Figure 1(B), which has been determined by MacDiarmid *et al.*[4a] This is square planar (D_{2h}) with 90° of the S-N-S angle[8] and almost equal bond lengths, 1.654Å.[9] The calculation of the electronic structure of S_2N_2 has been carried out by using the SCF-Xα-scattered wave method, which gives rather highly polar S-N bond ($S^{+0.48}$-$N^{-0.48}$).[10] This is probably because the method overestimates the contribution from the ionic structure.

The atomic net charges and π electron densities calculated here are also shown in Figure 1. This molecule has six π electrons - two π electrons from each sulfur atom and one π electron from each nitrogen atom. In consequence of the planar D_{2h} structure, the occupied orbitals are separated into σ and π orbitals. In the S-N bond, the charge densities of σ electrons are 4.180 and 3.820 on S and N, respectively, whereas those of π electrons are 1.619 and 1.381, respectively. This means that the charge transfer of π electrons from S to N (0.381) exceeds that of σ electrons from N to S (0.180). Consequently, the net charges on S and N are +0.201 and -0.201, respectively, as is usual for S-N bonds in other molecules[11] reflecting the fact that sulfur is less electronegative than nitrogen. As a matter of course, the highest occupied molecular orbital (HOMO) is of typical π MO, following another

π and two σ MOs close together as shown in Figure 2. It should be noticed here that there are two extraordinary low lying unoccupied MOs with negative eigenvalues and large S-N antibonding characters, *i.e.*, π^* and σ^* being very close each other. Such low lying σ^* MO may often induce bond-cleavages or drastic re-arrangement among MOs.

III. Electronic Structures of "Deformed" $(SN)_2$

According to the mechanism of the polymerization reaction proposed by MacDiarmid *et al.*, S_2N_2 is considered to be deformed thermally (near 0°C) at the first step to open one S-N bond, giving biradical character. In this section, how the biradical character appears according to the deformation is investigated. The geometries of $(SN)_2$ chosen here are shown in Figures 1(C), (D), and (E). In (C) and (D), the bond lengths of the sides opposite to the opened S-N bond are taken as being equal to the S-N bond length in the precursor, S_2N_2, (B), since shortening of them is unfavourable from the view point of nuclear repulsion as found in this calculation. (E) is employed from the fragment of the $(SN)_x$ polymer in structure (A). Sulfur 3d orbitals are requisite for the SCF convergence in the calculations for the open forms even though their contribution is not significant. As previously men-

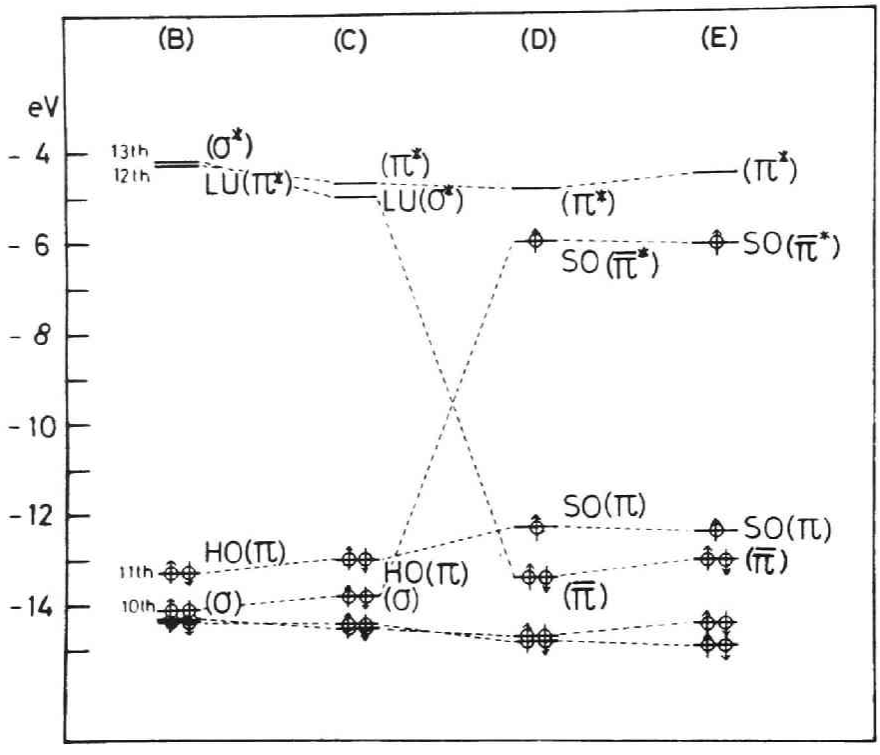

Figure 2. Orbital energy level correlation diagrams for deformed $(SN)_2$ (C, D, and E) together with the precursor, S_2N_2 (B). Changes of the orbital energy levels below the eighth MO are not essential and omitted here.

tioned, the possibility of the triplet biradical is investigated through examining the transition energy from the lowest singlet state to the triplet state in each structure.

In the cases of the precursor (B) and the slightly deformed (C), the ground states are, not unexpectedly, singlet, although the triplet π-π^* transition energy (Δ^3E_{π,π^*}) and the triplet π-σ^* transition energy (Δ^3E_{π,σ^*}) of the latter are positively small as shown in Table 1. Next, the case of a little more deformed structure (D) was examined. Δ^3E_{π,π^*} remains positive and almost the same value, while $\Delta^3E_{\pi,\bar{\pi}^*}$ is found to be negative. Hereafter, the signs π and $\bar{\pi}$ are defined to represent the π-type MO perpendicular to the molecular plane and that in the molecular plane, respectively. The above result means that the ground state of such a structure is a triplet formed from two singly occupied (SO) MOs, *i.e.*, π SOMO and $\bar{\pi}^*$ SOMO, as shown in Figure 2. The same result was obtained for the structure (E). Furthermore, these results were improved by the configuration interaction (CI) method including one electron excitations for the triplet states and pairing excitations for the singlet states within all the ranges from (HO-3)MO to (LU+3)MO. The situations are essentially not altered after CI as shown in Table 1. Thus, it is probable that the triplet state is energetically favourable for the ground state of such deformed structures rather than the sin-

Table 1. Transition Energies and the CI Improvements for the Stability of the Triplet States of the Deformed $(SN)_2$ (in eV)

Structure	Δ^3E_{π,π^*} (11th MO→13th MO)	Δ^3E_{π,σ^*} (11th MO→12th MO)	Δ^3E_{π,σ^*} (after CI)
(B)	1.922[a]	2.514[b]	2.867
(C)	1.401	1.223	1.627
(D)[c]	1.060	-0.693 ($\Delta^3E_{\pi,\bar{\pi}^*}$)	-0.068 ($\Delta^3E_{\pi,\bar{\pi}^*}$)
(E)[c]	1.876	-0.544 ($\Delta^3E_{\pi,\bar{\pi}^*}$)	-0.153 ($\Delta^3E_{\pi,\bar{\pi}^*}$)

[a] In this case, 11th MO→12th MO.

[b] In this case, 11th MO→13th MO.

[c] In these structures Δ^3E_{π,σ^*} is replaced by $\Delta^3E_{\pi,\bar{\pi}^*}$ because of the orbital crossing occurring in the deformation from (C) to (D) (see the text).

glet state. The atomic net charges and π electron densities of each structure are also shown in Figure 1, where the values of (D) and (E) are those of the triplet states. It is assumed here that the open-shell MOs in the triplet state are occupied with two more electrons of α spins. The α spin densities of the π MO and the $\bar{\pi}^*$ MO are shown in Table 2. As a whole, one can not find a large change of the atomic net charges even in the triplet states of (D) and (E). This implies that the transition from the singlet state to the triplet state is not due to the intramolecular charge transfer. On the other hand, such a transition would be expected to cause a drastic change of the number of π electrons from 6 to 5, as one of the π electrons is transferred from the π MO (11th) perpendicular to the molecular plane to the $\bar{\pi}^*$ MO (12th) in the plane in the biradicals of the structures (D) and (E). The large spin densities of both the π electrons and the $\bar{\pi}$ electrons are mainly on S_4 and on N_1. The $\bar{\pi}$ radical electron may be more reactive than π radical electron because the orbital energy of $\bar{\pi}^*$ SOMO is much higher than that of π SOMO. Interestingly, the dominant component of such $\bar{\pi}^*$ SOMO are p_x and as such are consistent with the direction of the polymerization as shown in Figure 1(A).

To understand such singlet-triplet transition in detail, the correlation diagrams of the orbital energy levels for each

Table 2. The α Spin Densities in $(SN)_2$ of the Structures (D) and (E)[a]

	Atom	s	p_x	p_y	$\bar{\pi}$ spin density	p_z	π spin density
(D)	N_1	0.000	0.272	0.000	0.273	0.187	0.187
	N_3	0.008	0.081	0.036	0.125	0.145	0.145
	S_2	0.001	0.069	0.005	0.092	0.036	0.082
	S_4	0.000	0.469	0.026	0.510	0.572	0.586
(E)	N_1	0.000	0.214	0.000	0.215	0.168	0.168
	N_3	0.009	0.067	0.098	0.175	0.171	0.171
	S_2	0.000	0.046	0.004	0.052	0.008	0.060
	S_4	0.000	0.364	0.172	0.559	0.584	0.601

[a] AO spin densities of 3d orbitals are of small values and hence omitted here. The values of $\bar{\pi}$ and π spin densities, however, contain the 3d contributions.

structure are given in Figure 2 and pictures of some of these MOs of both (C) and (D) in Figure 3. The 10th MO and the 12th MO in (C) are of bonding ($p\sigma$) and antibonding ($p\sigma^*$) character, respectively, to both the N_1-S_4 and the S_2-N_3 bonds, and are of antibonding ($p\bar{\pi}^*$) and bonding ($p\bar{\pi}$) character, respectively, to both the N_1-S_2 and the N_3-S_4 bonds. Thus, if the $p\bar{\pi}$ bond should be stronger than the $p\sigma$ bond by the elongation of the $p\sigma$ bond, there may be a possibility of level crossing between the 10th MO and the 12th MO. In fact, when the structure of $(SN)_2$ changes from (C) to (D), the occurrence of the level crossing between the 12th MO (σ^*) and the 10th MO (σ) is seen as shown in Figure 2. Namely, the 10th MO and the 12th MO in (C) are transformed to give bonding ($p\bar{\pi}$) and antibonding ($p\bar{\pi}^*$) character in (D), respectively, mainly with respect to the N_3-S_4 bond, and somewhat less with respect to the N_1-S_2 bond. These details are clarified by examining the values of the main Fock matrix elements, $C^{10}{}_r C^{10}{}_s \langle r|F|s\rangle$, where r and s are the component atomic orbitals (AOs) of the 10th MO, and C is the AO coefficient. It is seen from Table 3 that, in (C), the $N_1(2p_x)$-$S_4(3p_x)$ matrix element contributes to stabilization for the orbital energy, and that the $N_1(2p_x)$-$S_2(3p_x)$ and $N_3(2p_x)$-$S_4(3p_x)$ matrix elements contribute to destabilization. However, in (D), the $N_1(2p_x)$-$S_4(3p_x)$ element leads to less stabilization and the $N_3(2p_x)$-$S_4(3p_x)$ to stabilization. Since the orbital

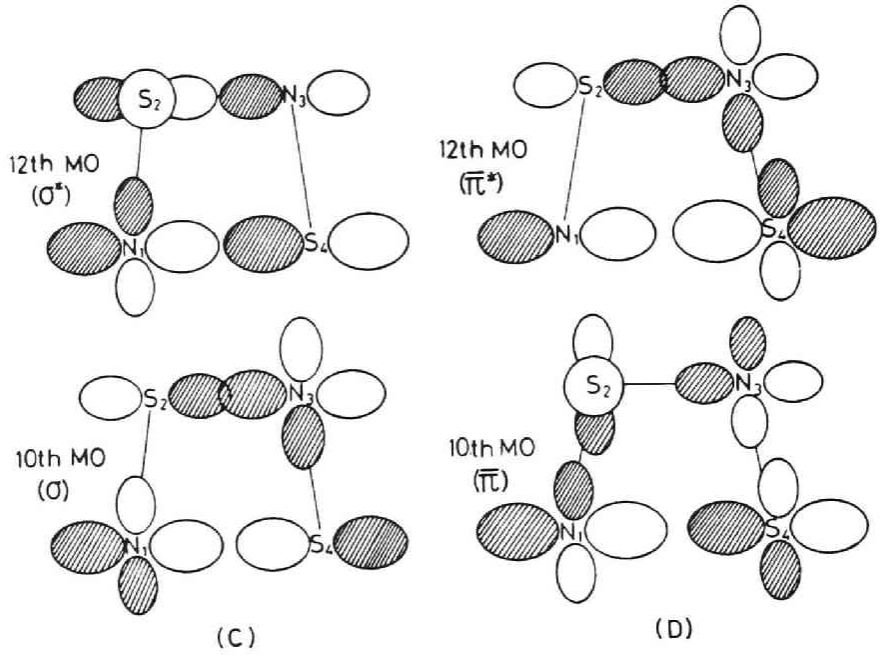

Figure 3. Pictures of 10th and 12th MOs of $(SN)_2$ having structures (C) and (D), respectively. Only the major AO components are depicted.

Table 3. The Values of Fock Matrix Elements Influencing 10th Orbital Energies of (C) and (D) (in eV)

r AO	s AO	(C) $C^{10}_r C^{10}_s \langle r\|F\|s\rangle$ [a]	(D) $C^{10}_r C^{10}_s \langle r\|F\|s\rangle$
N_1 $2p_x$	S_2 $3p_x$	0.373	-0.147
N_1 $2p_x$	S_4 $3p_x$	-1.461	-0.556
N_3 $2p_x$	S_4 $3p_x$	0.372	-0.439
N_3 $2p_y$	S_4 $3p_x$	-0.088	0.133

[a] See the text about the notations C^{10}_r and C^{10}_s.

level crossing in going from (C) to (D) is caused mainly by the changing of the sign of the $3p_x$ orbital on S_4 and the larger contribution of the 3s orbital on S_2, it would not be so difficult to bring about such a triplet transition, if the widening of the N_1-S_4 bond takes place easily.

In fact, according to the IR spectrum of the solid S_2N_2,[12] the strong bands at 476.2cm^{-1} and 785cm^{-1} are assigned to be B_{2u} and B_{3u} modes, respectively, which correspond to the widening of one of the S-N bonds (and hence shortening of the opposite S-N bond). These extraordinary low frequencies imply the shallow potential of the S-N bond for such vibrational modes and therefore the widening may easily be induced, even thermally, because, *e.g.*, 476.2cm^{-1} is equal to 1.36kcal/mol, which is the same order of RT at room temperature (*ca.* 0.6kcal /mol). This consideration leads that the polymerization may be accelerated by applying the appropriate IR ray.

Thus it is expected that, at the point where the level crossing occurs, the N_1-S_4 pσ bond vanishes and the N_3-S_4 p$\bar{\pi}$ bond prevails, and that the triplet state emerges in the course of the deformation probably due to the vibrational motion. Furthermore, it is attempted to estimate the mixing of the triplet configuration with the singlet closed-shell configuration for (C), and the mixing of the singlet (original closed-shell) configuration with the triplet (biradical) configuration

for (D) and (E) through spin-orbit coupling. Considering the perturbation correction,[13] the state function, required at present, $^{1(3)}\Phi_i$, is given by;

$$^{1(3)}\Phi_i = {}^{1(3)}\Phi_i^0 + \sum_k \frac{\langle {}^{1(3)}\Phi_i^0 | H_{SO} | {}^{3(1)}\Phi_k^0 \rangle}{\Delta^3 E_{i,k}} \, {}^{3(1)}\Phi_k^0 ,$$

where $^{1(3)}\Phi_i^0$ and $^{3(1)}\Phi_k^0$ are the unperturbed i-th singlet (triplet) ASMO and the unperturbed k-th triplet (singlet) ASMO, respectively. H_{SO} is usual spin-orbit coupling operator, and $\Delta^3 E_{i,k}$ is the energy difference. In the case of (C), $^1\Phi_i^0$ refers to the closed-shell configuration and $^3\Phi_k^0$ to the $\pi \rightarrow \sigma^*$ (11th MO$\rightarrow$12th MO) triplet configuration, whereas in (D) and (E), $^3\Phi_i^0$ refers to the $\pi \rightarrow \bar{\pi}^*$ (11th MO$\rightarrow$12th MO) triplet configuration and $^1\Phi_k^0$ to the original closed-shell configuration. These $^{3(1)}\Phi_k^0$ states seem to contribute mainly to the second term in the above correction rather than to other configurations, because the energy differences $\Delta^3 E_{\pi,\sigma^*}$ ($\Delta^3 E_{\pi,\bar{\pi}^*}$) are considerably smaller. The matrix element in the numerator is further reduced to $\langle \Psi^{11}_{\bar{\pi}} | H_{SO} | \Psi^{12}_{\sigma^*} \rangle$ ($\langle \Psi^{11}_{\pi} | H_{SO} | \Psi^{12}_{\bar{\pi}^*} \rangle$), where Ψ^{11}_{π} and $\Psi^{12}_{\sigma^*}$ ($\Psi^{12}_{\bar{\pi}^*}$) denote the 11th π MO and the 12th σ^* ($\bar{\pi}^*$) MO, respectively. Taking only one-centre terms into account as to the matrix element and em-

ploying the spin-orbit coupling constants ζ of $74.2cm^{-1}$ and $363cm^{-1}$ for nitrogen and sulfur, respectively,[14] one obtains;

$$^1\Phi_i = {}^1\Phi_i{}^0 + 0.009\ {}^3\Phi_k{}^0 \quad \text{for (C)},$$

$$^3\Phi_i = {}^3\Phi_i{}^0 - 0.019\ {}^1\Phi_k{}^0 \quad \text{for (D)},$$

and

$$^3\Phi_i = {}^3\Phi_i{}^0 - 0.006\ {}^1\Phi_k{}^0 \quad \text{for (E)}.$$

The orders of the mixing coefficients are considerably larger than those in usual organic hetero compounds[15] on account of the heavy atom (sulfur) effect. Moreover, the 11th π MO and the 12th σ^* ($\bar{\pi}^*$) MO are advantageous, considering the character of the orbital angular momentum operator involved in H_{SO}. Thus, in $(SN)_2$, the degree of mixing of the singlet state is essentially remarkable. In particular, the biradical resulting from the π-$\bar{\pi}^*$ triplet transition, would be easily formed from the singlet state. It should be stressed here that the energy difference between the triplet and the singlet state is small (approximately 1 kcal/mol) and hence it would not be unreasonable if the population of the singlet

state, even if it were energetically higher, should increase with increase of temperature according to the Boltzmann distribution. In this respect, it is interesting to note that the ESR spectrum of blue-black, partly polymerized $(SN)_2$ decreases in intensity with increase in the temperature at which it is measured, *e.g.*, -100°C *vs.* 25°C.[16]

IV. Electronic Structures of $(SN)_4$ and $(SN)_6$

In order to understand further steps of the polymerization, we calculated the electronic structures of linear $(SN)_4$ and $(SN)_6$. The geometries employed are those from appropriate fragments of the polymer in Figure 1(A). The calculated atomic net charges and π electron densities are shown in Figure 4 and the orbital energy diagram for these molecules are shown in Figure 5. It is seen that π electron densities are distributed less on N_1 and S_8 in $(SN)_4$, and on N_1 and S_{12} in $(SN)_6$, and that $(SN)_4$ and $(SN)_6$ have a total of 10π and 16π electrons, respectively. Furthermore the ground states of these molecules are found to be singlet rather than triplet states. The HOMO (σ) in $(SN)_4$ is considerably stabilized by the SOMO ($\bar{\pi}^*$)-SOMO ($\bar{\pi}^*$) interaction between two $(SN)_2$ biradicals. The (HO-1)MO (π) is almost unchanged from the original π MO in structure (E) and then, these two are nearly degener-

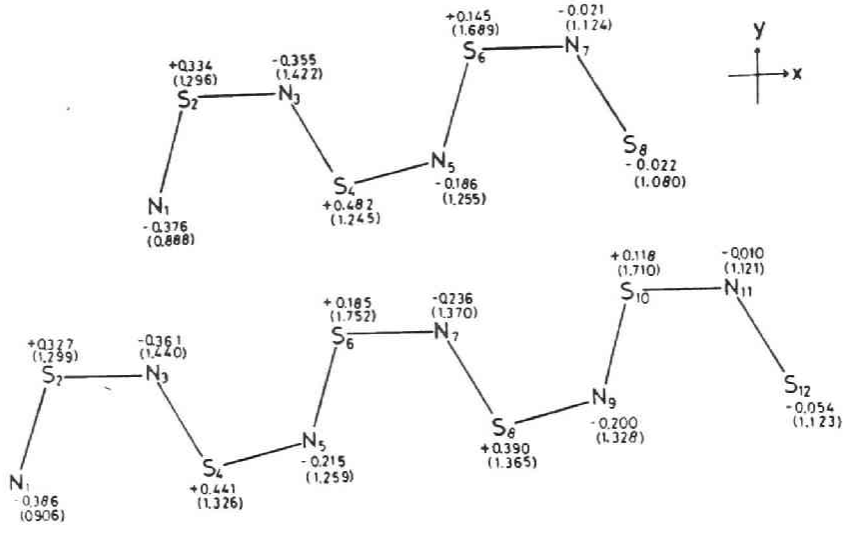

Figure 4. The calculated results for atomic net charges and π electron densities (bracketed values) of $(SN)_4$ and $(SN)_6$ molecules. Note that the total number of π electrons are 10 and 16, respectively, for these fragments.

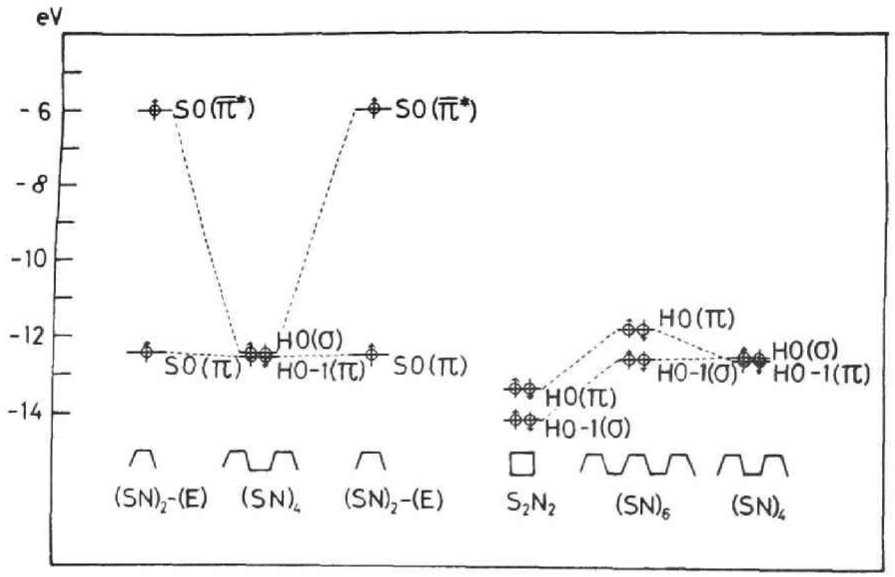

Figure 5. Orbital energy diagrams of S_2N_2, $(SN)_2$, $(SN)_4$, and $(SN)_6$.

ate. In $(SN)_6$, however, the HOMO (π) is somewhat separated from the (HO-1)MO (σ). These results and their HOMOs and (HO-1)MOs suggest that $(SN)_4$ is derived from two $(SN)_2$ molecules in the triplet state ($5\pi+5\pi$), and that $(SN)_6$ is derived from $(SN)_4$ and square S_2N_2 in the singlet state ($10\pi+6\pi$).

Thus from the results of these calculations, the paramagnetism is expected to vanish as the polymerization proceeds, which is in agreement with the experimental results.

V. Conclusion

The electronic structures of the square S_2N_2 molecule and several deformed $(SN)_2$ molecules, and of $(SN)_4$ and $(SN)_6$ molecules have been examined.

In the deformed $(SN)_2$, the triplet biradical nature begins to emerge as one of the S-N bonds opens. The appearance of the triplet state seems to correspond to the interaction of the opened S-N $p\sigma$ bond with the adjacent S-N $p\bar{\pi}$ bond in the molecular plane.

From a simple estimation of the spin-orbit coupling in the deformed $(SN)_2$ molecules, there appears to be considerable mixing of the singlet state with the triplet state or of

the triplet state with the singlet state. The opening of the S-N bond might be expected to occur easily, *i.e.*, thermally, in view of the IR spectroscopic data of the appropriate vibrational modes.

$(SN)_4$ and $(SN)_6$, however, do not show triplet ground states. $(SN)_4$ is believed to result through the dimerization of two $(SN)_2$ biradicals, whereas $(SN)_6$ may be regarded as being formed by the addition of singlet $(SN)_4$ to singlet S_2N_2. Analogous processes would then lead to higher polymers.

References and Notes

1) (a) V. V. Walatka, Jr., M. M. Labes, and J. H. Perlstein, Phys. Rev. Lett., 31, 1139(1973); (b) C. Hsu and M. M. Labes, J. Chem. Phys., 61, 4640(1974).

2) Some recent references are (a) R. L. Greene, P. M. Grant, and G. B. Street, Phys. Rev. Lett., 34, 89(1975); (b) A. A. Bright, M. J. Cohen, A. F. Garito, A. J. Heeger, C. M. Mikulski, P. J. Russo, and A. G. MacDiarmid, Phys. Rev. Lett., 34, 206(1975); (c) R. L. Greene, G. B. Street, and L. J. Suter, Phys. Rev. Lett., 34, 577(1975); (d) W. D. Gill, R. L. Greene, G. B. Street, and W. A. Little, Phys. Rev. Lett., 35, 1732(1975); (e) P. M. Grant, R. L. Greene, and G. B. Street, Phys. Rev. Lett., 35, 1743 (1975); (f) L. Ley, Phys. Rev. Lett., 35, 1796(1975); (g) P. Mengel, P. M. Grant, W. E. Rudge, B. H. Schechtman, and D. W. Rice, Phys. Rev. Lett., 35, 1803(1975); (h) L. Pintschovius, H. P. Geserich, and W. Möller, Solid St. Commun., 17, 477(1975); (i) C. H. Chen, J. Silcox, A. F. Garito, A. J. Heeger, and A. G. MacDiarmid, Phys. Rev. Lett., 36, 525(1976).

3) (a) D. E. Parry and J. M. Thomas, J. Phys., C8, L45 (1975); (b) W. E. Rudge and P. M. Grant, Phys. Rev. Lett., 35, 1799(1975); (c) W. I. Friesen, A. J. Berlinsky, B.

Bergersen, L. Weiler, and T. M. Rice, J. Phys., C8, 3549 (1975); (d) V. T. Rajan and L. M. Falicov, Phys. Rev., B12, 1240(1975); (e) A. Zunger, J. Chem. Phys., 63, 4854 (1975); (f) H. Kamimura, A. M. Glazer, A. J. Grant, Y. Natsume, M. Schreiber, and A. D. Yoffe, J. Phys. C9, 291 (1976); (g) A. A. Bright and P. Soven, Solid St. Commun., 18, 317(1976).

4) (a) A. G. MacDiarmid, C. M. Mikulski, P. J. Russo, M. S. Saran, A. F. Garito, and A. J. Heeger, J. Chem. Soc., Chem. Commun., 1975, 476; (b) C. M. Mikulski, P. J. Russo, M. S. Saran, A. G. MacDiarmid, A. F. Garito, and A. J. Heeger, J. Am. Chem. Soc., 97, 6358(1975).

5) R. H. Baughman, R. R. Chance, and M. J. Cohen, J. Chem. Phys., 64, 1869(1976).

6) (a) T. Yonezawa, H. Konishi, and H. Kato, Bull. Chem. Soc. Jpn., 42, 933(1969); (b) C. C. J. Roothaan, Rev. Mod. Phys., 23, 69(1951); (c) H. Konishi, H. Kato, and T. Yonezawa, Theoret. Chim. Acta(Berl.), 19, 71(1970);(d) H. Yamabe, H. Kato, and T. Yonezawa, Bull. Chem. Soc. Jpn., 44, 22(1971); (e) H. Yamabe, H. Kato, and T. Yonezawa, Bull. Chem. Soc. Jpn., 44, 611(1971).

7) The two-centre Coulomb repulsion integrals are calculated by the Ohno approximation (K. Ohno, Theoret. Chim. Acta (Berl.), 2, 219(1964)), and the one-centre exchange in-

tegrals are evaluated by the Slater-Condon parameters estimated by Hinze and Jaffé (J. Hinze and H. H. Jaffé, J. Chem. Phys., 38, 1834(1963)).

8) 90.42° and 89.58° for the S-N-S and the N-S-N angles, respectively.

9) 1.651Å and 1.657Å alternatively.

10) D. R. Salahub and R. P. Messmer, J. Chem. Phys., 64, 2039(1976).

11) D. B. Adams, A. J. Banister, D. T. Clark, and D. Kilcast, Intern. J. Sulfur Chem., 1, 143(1971).

12) J. Bragin and M. V. Evans, J. Chem. Phys., 51, 268(1969).

13) For example, see D. S. McClure, J. Chem. Phys., 20, 682 (1952).

14) M. Blume and R. E. Watson, Proc. Roy. Soc.(London), A271, 565(1963).

15) For example, see T. Yonezawa, H. Katô, and H. Kato, Theoret. Chim. Acta(Berl.), 13, 125(1969).

16) Unpublished observations, A. G. MacDiarmid and M. S. Saran.

Chapter 9

Electronic Structures of $(SN)_x$ and $(SCH)_x$ Polymers

I. Introduction

There have been considerable experimental and theoretical interests in low-dimensional metallic conductors such as tetracyanoquinodimethane (TCNQ) charge-transfer salts and $K_2[Pt(CN)_4]Br_{0.3}\cdot 3H_2O$ mixed valence complex.[1] Recently, the third member, polymeric sulfur nitride, $(SN)_x$, has been revealed as a low-dimensional metallic polymer,[2] which does not show the Peierls transition unlike the above two, and even becomes a superconductor at $\sim 0.3^\circ K$.[3]

The theoretical band structure calculations of $(SN)_x$ have been performed with the OPW method[4] and several non SCF-tight-binding techniques such as the extended Hückel method.[5] In these tight-binding MO calculations, however, the electron-electron interaction potential is not taken into account explicitly, and hence these methods would be only reliable on the non-polar polymers such as polyethylene.[6] Since the sulfur-nitrogen bond in $(SN)_x$ has been estimated experimentally to be of rather polar character,[7] it would be suitable to calculate the MO including the electron repulsion integrals for this

polymer. The SCF-tight-binding MO calculation including these repulsion integrals has been carried out only by Zunger and by Merkel and Ladik[8] for the one-dimensional structure of $(SN)_x$ in the crystal structure proposed by Boudeulle and Michel (Lyon structure)[9] based on the electron-diffraction analysis as shown in Figure 1(A). The band structures obtained by them clearly show the metallic nature of $(SN)_x$, and the possibility of the occurrence of the Peierls transition has been denied by the former.

More recently, however, the more reliable structure of $(SN)_x$ has been proposed by MacDiarmid *et al.* (Pennsylvania structure)[10] based on the X-ray diffraction analysis as shown in Figure 1(B). In this Chapter, the result of electronic structures of the one-dimensional Pennsylvania structure of $(SN)_x$ by the SCF-tight-binding MO calculation including the electron repulsion is presented, and, furthermore, the calculation for an assumed structure of $(SCH)_x$ polymer is made so as to study an isoelectronic system with the $(SN)_x$ polymer.

II. Method of Calculation

In order to avoid the complicated calculations of the all matrix elements by *ab initio* methods, the CNDO/2 approximation by Pople and Segal[11] is employed. The SCF iteration process

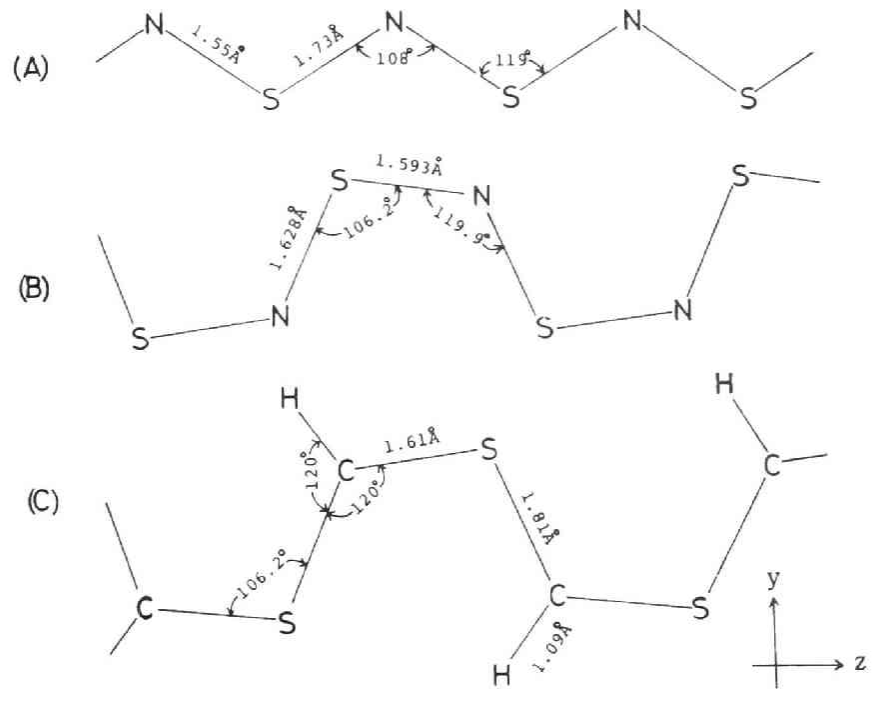

Figure 1. The structures of $(SN)_x$ and $(SCH)_x$; (A) the Lyon structure (Ref.9), (B) the Pennsylvania structure (Ref.10), and (C) an assumed structure for the calculation here (see text).

is accelerated by the density matrix method previously introduced by Imamura and Fujita to calculate biopolymers.[12] The formalism of the calculation has been described thoroughly in thier article, so the details will not be mentioned here again. All valence AOs and 3d orbitals for sulfur atom were considered since it has been pointed out that the contribution from 3d orbitals is not negligible for $(SN)_x$.[8] For the parametrizations were adopted those of spd set by Santry and Segal,[13] and the number of representative wave vector K was chosen as 21 at regular intervals ($\pi/10a$; a is the length of the unit cell) in the Brillouin zone.

The structure of $(SCH)_x$ analogous to that of the Pennsylvania structure of $(SN)_x$ was assumed as shown in Figure 1(C). The angle at sulfur was chosen as 106.2° after that in $(SN)_x$, and that at carbon as 120° after ordinary sp^2 hybridization. The two kinds of S-C distances, 1.81Å and 1.61 Å, are employed from the data for dimethyl disulfide[14] and thioformaldehyde,[15] respectively. The C-H bond distance, 1.09 Å, also from the latter. Each of SN and SCH units consists of 11 valence electrons and, hence, an open-shell structure. Since the $(SN)_x$ crystal, however, does not show paramagnetism,[10]) the system could be treated as a closed-shell system. In the MO calculation of the $(SN)_x$ polymer, $(SN)_2$ was employed as a unit cell. In the $(SCH)_x$ polymer, $(SCH)_2$ was assumed as well.

Since the polymer chains possess a two-fold screw rotation as a symmetry operation, all pairs of bands stick together at the edges of the Brillouin zone,[16] and, in this case, the highest occupied (HO) (π) and the lowest unoccpied (LU) (π^*) bands also degenerate there. At such points, it is, in principle, unreasonable to describe the system with a single Slater determinant. Thus the density matrix elements were extrapolated at $K=\pm 9\pi/10a$ and $\pm\pi/10a$ for the evaluations of those at $K=\pm\pi/a$ and 0, respectively. The values of overlap integrals between the central unit cell and the N-th nearest neighbouring cell rapidly decrease to 0 where $N=3\sim4$ ($9\sim13.5$Å from the central unit cell). But as those of electron repulsion (Coulomb) integrals slowly decrease, they were considered as far as the 7-th nearest neighbours (~31Å from the central unit cell).

III. Results and Discussion

The calculated results of AO densities, atomic net charges, and the total energies per unit cell are shown in Table 1 along those of the Lyon structure of $(SN)_x$. As the direction of the polymer chain is set along the Z-axis and the polymer plane is perpendicular to the X-axis, the π orbitals are of $2p_x$, $3p_x$, $3d_{xy}$, and $3d_{xz}$ AOs. Both of $(SN)_2$ and $(SCH)_2$ units have six π electrons, supplied two π electrons from the sulfur atom

Table 1. AO Densities, Atomic Net Charges, and the Total Energies of $(SN)_x$ and $(SCH)_x$

		$(SN)_x$: Pennsylvania structure		$(SN)_x$: Lyon structure[a]		$(SCH)_x$		
		S	N	S	N	S	C	H
AO	s	1.810	1.550	1.824	1.549	1.768	1.114	0.912
	p_x	1.407	1.218	0.714	1.163	1.478	1.135	
	p_y	0.822	1.235	0.784	1.315	0.923	0.962	
	p_z	0.728	1.228	1.497	1.153	0.929	0.964	
	d_{xz}	0.242		0.308		0.296		
	d_{xy}	0.133		0.219		0.091		
	d_{yz}	0.290		0.044		0.202		
	$d_{x^2-y^2}$	0.087		0.326		0.065		
	d_{z^2}	0.250		0.098		0.160		
π electron densities		1.782	1.218	1.947	1.153	1.865	1.135	
atomic net charges		+0.231	-0.231	+0.186	-0.186	+0.087	-0.175	+0.088
total energies per unit cell (in eV)		-1230.056 (-1218.220)[b] (-1227.731)[c]		-1228.562[d]		-1018.057 (-1005.877)[b]		

(to be continued on the next page)

a) Ref. 8. For this structure, p_z, d_{xz}, d_{yz}, and d_z2 AOs are the components of π orbitals.

b) The total energy of $(SN)_2$ or $(SCH)_2$ molecule with the same configuration of the unit cell in $(SN)_x$ or $(SCH)_x$, respectively.

c) The total energy of the most stable configuration (square form) of $(SN)_2$ molecule (Ref. 10).

d) The value calculated in the present **treatment** on the same basis for the Pennsylvania structure.

and one from the nitrogen or the carbon atom. In $(SN)_x$ calculated here, the densities of $3p_x$ and $2p_x$ AOs on S and N are 1.407 and 1.218, respectively, and the contribution from $3d_{xy}$ and $3d_{xz}$ AOs is totally 0.375, the magnitude of which is not negligible. The atomic net charge on S is +0.231, and it is somewhat larger than that estimated for the Lyon structure, +0.186,[8] but somewhat less than that estimated by XPS method, +0.30∿0.42.[7] In $(SCH)_x$, although the π electron densities on S and C are not so different from those on S and N in $(SN)_x$, the atomic net charge on S is +0.087 which is by far less than that in $(SN)_x$. This would be direct reflection of the electronegativity of each atom, namely S<C<N in order. It is also interesting that the atomic net charge on H is very close to that on S. It is clearly shown, from the difference in the total energies of a unit cell and isolated $(SN)_2$ molecules, that the polymeric state is more stable than the isolated molecules. Moreover, the comparison of the total energies per unit cell of the two structures of $(SN)_x$ definitely shows that the Pennsylvania structure is favourable. For $(SCH)_x$, it is similarly predicted that the polymeric state is stable in comparison with the isolated $(SCH)_2$ molecule.

The energy bands and the densities of states of the polymers are shown in Figures 2(A) and (B). The curves of the densities of states are obtained with the Brust's method[17] summing

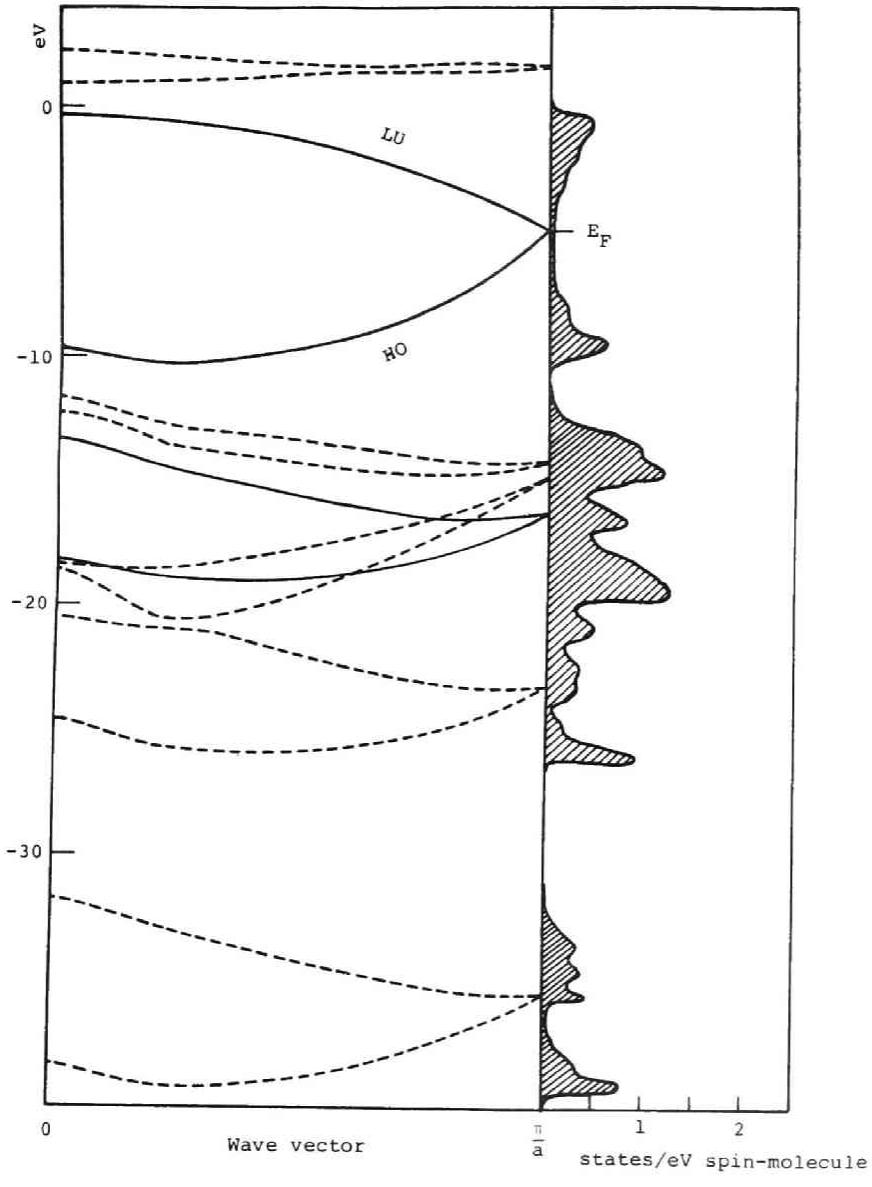

(A)

Figure 2. The band structures and the densities of states of (A)$(SN)_x$ and (B)$(SCH)_x$. Dotted lines and solid ones indicate σ bands and π bands, respectively. The upper several vacant bands and the densities of states of those which are upper than the LU bands are not essential and omitted here.

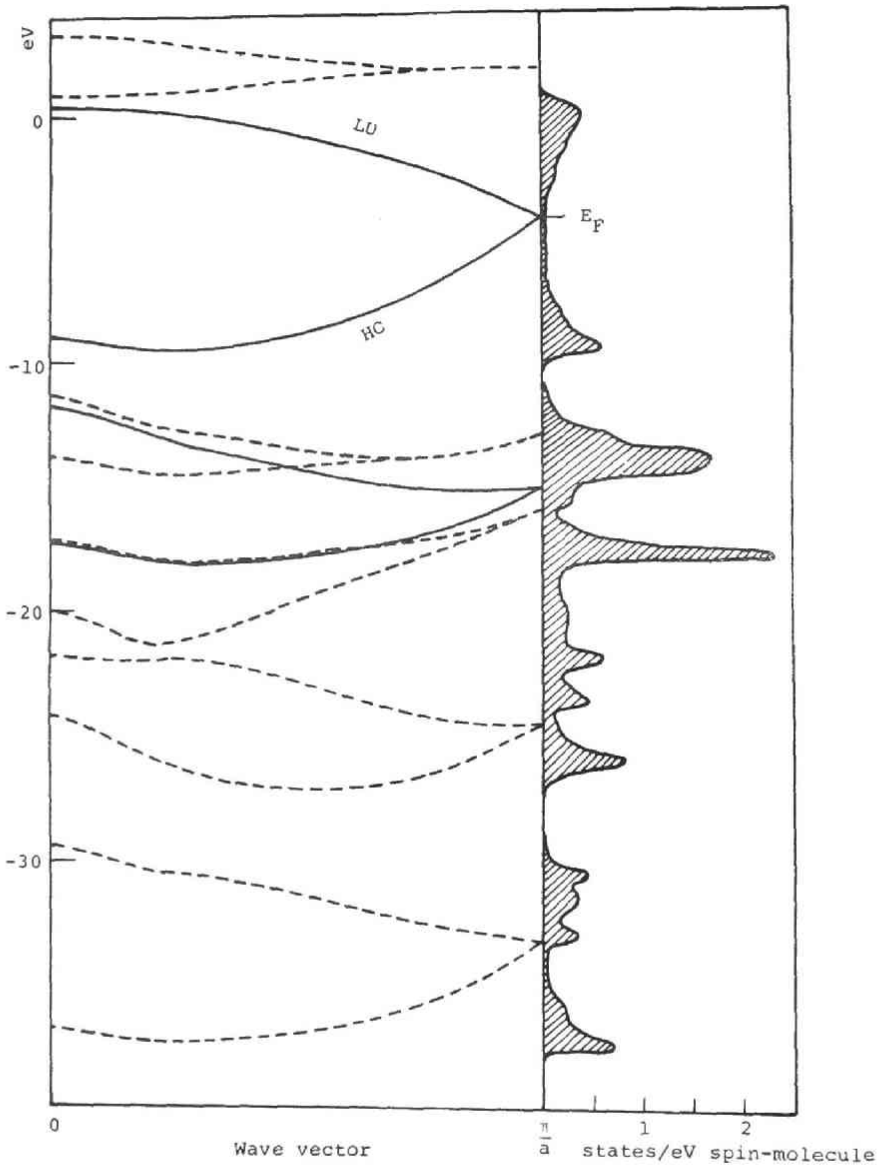
eV
0
-10
-20
-30
LU
HC
E_F
0
Wave vector
$\frac{\pi}{a}$
1
2
states/eV spin-molecule

(B)

over 300 points sampled in the Brillouin zone for each energy band. The valence bands consist of three π bands and eight σ bands, and the HO and the LU bands are of π natures mainly composed of sulfur $3p_x$ AO in both $(SN)_x$ and $(SCH)_x$. These energy bands of $(SN)_x$ and $(SCH)_x$ are seen to be of rather similar shape and the Fermi energies (E_F) are obtained as -4.996eV and -4.340eV, respectively. E_F of the Lyon structure of $(SN)_x$ has been reported to be -5.714eV.[8] The shape of the density of states of $(SN)_x$ agrees qualitatively with those obtained previously by ESCA spectroscopy.[7,18] The density of states at E_F ($D(E_F)$) is small but finite for $(SN)_x$, namely, 0.04states /eV spin-molecule, which shows the metallic nature of $(SN)_x$. Experimental value of $D(E_F)$ is 0.12∿0.18states/eV spin-molecule [18,19] which agrees quantitatively with the present result but is somewhat larger, showing perhaps the reflection of the actual three-dimensional structure of $(SN)_x$ crystal. For $(SCH)_x$, the shape of the density of states again resembles that of $(SN)_x$ but the peaks are more sharpened than in $(SN)_x$, and $D(E_F)$ is 0.06states/eV spin-molecule. This value encourages us that $(SCH)_x$ may become also a metallic conductor if it should be successfully synthesized, and unless any interference such as Peierls transition should occur to break down the metallic state of $(SCH)_x$.

The E_{AB} analyses in the scheme of the CNDO/2 method are

shown in Figure 3 for $(SN)_x$ and $(SCH)_x$. It is shown that N_1-S_4 in $(SN)_x$ and S_1-C_6 in $(SCH)_x$ are both attractive. Moreover, it should be noticed that, both in $(SN)_x$ and in $(SCH)_x$, S_2-S_4 and S_1-S_4 are considerably attractive, while N_1-N_3 and C_3-C_6 are weakly repulsive, and hence the skeleton of each unit cell is held rather tightly. This would cause interesting effects to the force constant of the lattice displacement and to the Debye frequency of the system.

It is also noticed that much attention should be paid to the description of the system at $K=\pm\pi/a$, since there occurs a degeneracy of the HO and the LU bands. In order to overcome such a situation, some appropriate linear combination of the Slater determinants (Configuration Interaction) should be adopted.

The possibility of the interaction between two $(SN)_x$ chains or the highly anisotropic two- or three-dimensionality of $(SN)_x$ crystal has also been pointed out from some experimental aspects.[10,20] The SCF-tight-binding calculation including two chains is desirable.

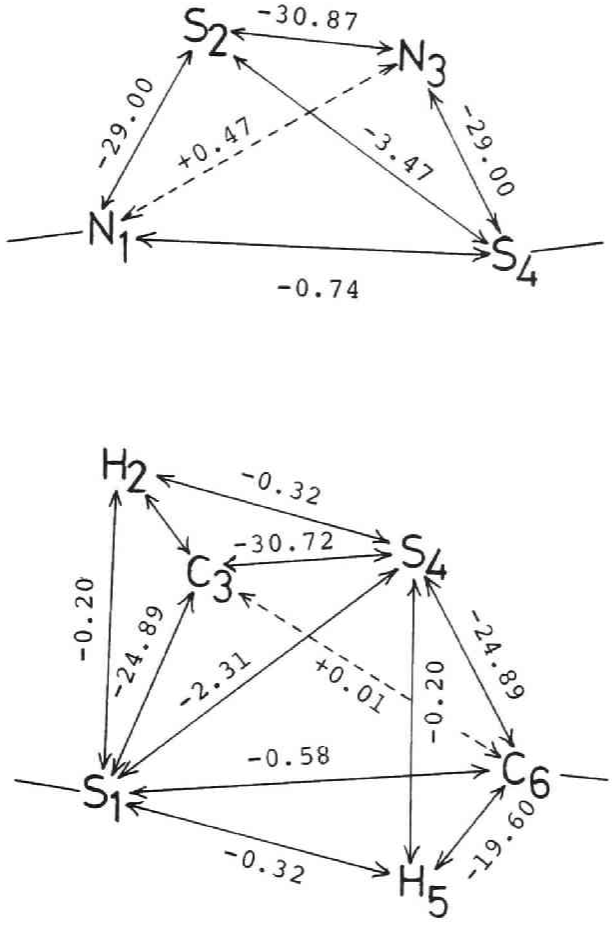

Figure 3. The E_{AB} analyses for the representative unit cells of $(SN)_x$ and $(SCH)_x$. The energies are shown in eV. Dotted lines and solid ones indicate the repulsive and attractive interactions, respectively.

References and Notes

1) For example, see H. J. Keller, "Low-Dimensional Cooperative Phenomena," Plenum Press, New York (1975).

2) V. V. Walatka, Jr., M. M. Labes, and J. H. Perlstein, Phys. Rev. Lett., 31, 1139(1973); C. Hsu and M. M. Labes, J. Chem. Phys., 61, 4640(1974); C. K. Chiang, M. J. Cohen, A. F. Garito, A. J. Heeger, C. M. Mikulski, and A. G. MacDiarmid, Solid St. Commun., 18, 1451(1976).

3) R. L. Greene, G. B. Street, and L. J. Suter, Phys. Rev. Lett., 34, 577(1975).

4) W. E. Rudge and P. M. Grant, Phys. Rev. Lett., 35, 1799 (1975).

5) D. E. Parry and J. M. Thomas, J. Phys., C8, L45(1975); W. I. Friesen, A. J. Berlinsky, B. Bergersen, L. Weiler, and T. M. Rice, J. Phys., C8, 3549(1975); V. T. Rajan and L. M. Falicov, Phys. Rev., B12, 1240(1975); H. Kamimura, A. M. Glazer, A. J. Grant, Y. Natsume, M. Schreiber, and A. D. Yoffe, J. Phys., C9, 291(1976); A. A. Bright and P. Soven, Solid St. Commun., 18, 317(1976).

6) H. Fujita and A. Imamura, J. Chem. Phys., 53, 4555(1970).

7) P. Mengel, P. M. Grant, W. E. Rudge, B. H. Schechtman, and D. W. Rice, Phys. Rev. Lett., 35, 1803(1975).

8) A. Zunger, J. Chem. Phys., 63, 4854(1975); C. Merkel and

J. Ladik, Phys. Lett., 56A, 395(1976).

9) M. Boudeulle and P. Michel, Acta Crystallogr., A28, S199 (1972).

10) A. G. MacDiarmid, C. M. Mikulski, P. J. Russo, M. S. Saran, A. F. Garito, and A. J. Heeger, J. Chem. Soc., Chem. Commun., 1975, 476; C. M. Mikulski, P. J. Russo, M. S. Saran, A. G. MacDiarmid, A. F. Garito, and A. J. Heeger, J. Am. Chem. Soc., 97, 6358(1975).

11) J. A. Pople and G. A. Segal, J. Chem. Phys., 44, 3289(1966).

12) A. Imamura and H. Fujita, J. Chem. Phys., 61, 115(1974).

13) D. P. Santry and G. A. Segal, J. Chem. Phys., 47, 158 (1967).

14) D. Sutter, H. Dreizler, and H. D. Rudolph, Z. Naturforsch., 20A, 1676(1965).

15) D. R. Johnson, F. X. Powell, and W. H. Kirchoff, J. Mol. Spectrosc., 39, 136(1971).

16) For example, see V. Heine, "Group Theory in Quantum Mechanics," Pergamon Press, London (1960), p.265.

17) J. Brust, "Methods of Computational Physics," Academic Press, New York (1968), Chap. 8.

18) L. Ley, Phys. Rev. Lett., 35, 1796(1975).

19) R. L. Greene, P. M. Grant, and G. B. Street, Phys. Rev. Lett., 34, 89(1975).

20) A. A. Bright, M. J. Cohen, A. F. Garito, A. J. Heeger, C. M. Mikulski, P. J. Russo, and A. G. MacDiarmid, Phys. Rev. Lett., 34, 206(1975); H. Kamimura, A. J. Grant, F. Levy, A. D. Yoffe, and G. D. Pitt, Solid St. Commun., 17, 49 (1975); L. Pintschovius, H. P. Geserich, and W. Möller, Solid St. Commun., 17, 477(1975).

Chapter 10

Interchain Interaction in $(SN)_x$ Polymer

The importance of interchain interaction in the low-dimensional metallic polymer $(SN)_x$ has been pointed out by several investigators[1-18] with a view that it would be a main cause to suppress a metal-insulator transition at low temperature. This kind of interaction has been discussed explicitly only by Messmer and Salahub,[19,20] who performed MO calculations with the use of the SCF-Xα-SW method on two interacting S_4N_4 units taken out from the original $(SN)_x$ crystal structure and two-dimensional band structure calculations with the use of the extended Hückel method on $(\bar{1}02)$ and (100) crystallographic planes. According to the shape of the band structure, they have inferred that the interchain interaction in the (100) plane would be important to the nature of the conduction band of $(SN)_x$. But their conclusion about the shortest interchain S-S and S-N interactions seems to be rather vague because of the finite cluster model they employed. In this Chapter, we will discuss on the interchain interaction in a more quantitative way on the basis of the one-dimensional tight-binding SCF-MO calculations of two chains of $(SN)_x$ in the $(\bar{1}02)$ and the (100)

crystallographic planes taken out from the data of the X-ray diffraction analysis[4] as shown in Figure 1. The CNDO/2 approximation[21] including 3d orbitals of sulfur atoms was employed and for the parametrizations were adopted those of spd-set by Santry and Segal.[22] This approximation has given reliable results on the interaction energies especially for polar molecules[23] as well as polar biopolymers such as poly-glycine[24] and poly-L-alanine,[21] although it has a tendency towards underestimation of the effect of the interatomic charge transfer.[23] The intercell interactions were considered as far as the 7th nearest neighbouring cell ($\sim$30Å from the central unit cell).

In Figure 2, the band structures and the densities of states of two interacting chains in the ($\bar{1}02$) and the (100) planes are illustrated along with those of the infinitely separated chains.[25] Owing to the one-dimensional model employed here, the highest occupied (HO) and the lowest unoccupied (LU) bands are split off at the Brillouin zone boundary in the ($\bar{1}02$) and the (100) cases lacking in the symmetry of a two-fold screw rotation such as in the infinitely separated case. The degree of this split, however, will become a measure of these two kinds of the interchain interactions. In the ($\bar{1}02$) and the (100) cases, the widths of HO-LU split are 0.040eV and 2.027eV, respectively. Furthermore, the density

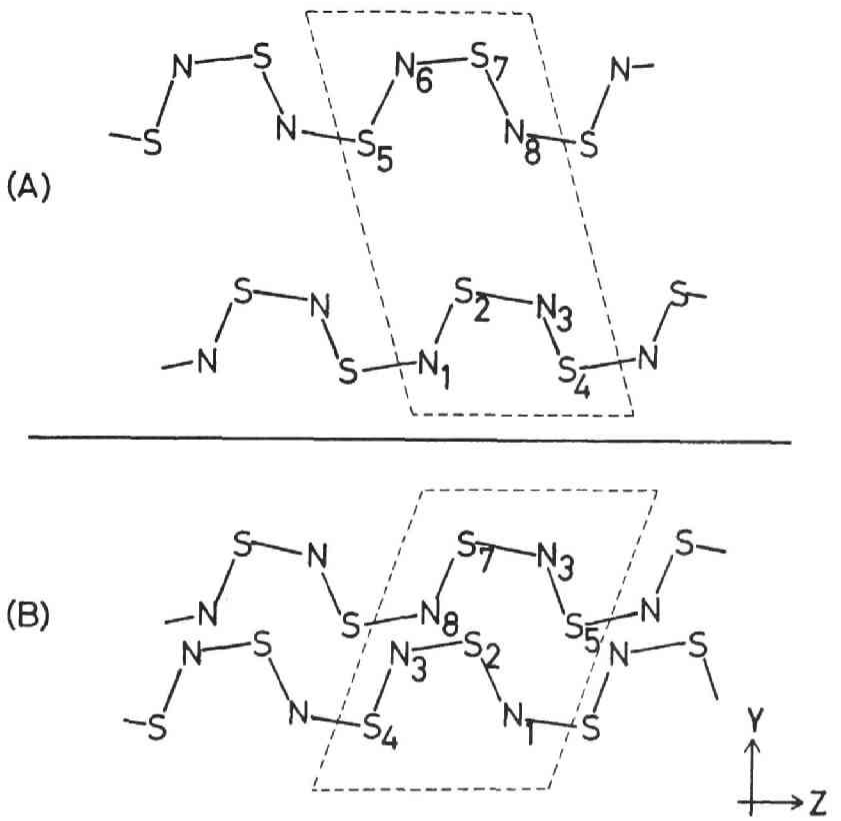

Figure 1. The geometries of two chains of $(SN)_x$. (A) In the $(\bar{1}02)$ plane; (B) In the (100) plane. Note that mean planes of the two chains are separated by 3.25Å in (B). The unit cell employed in the calculation is indicated by the broken line in each case.

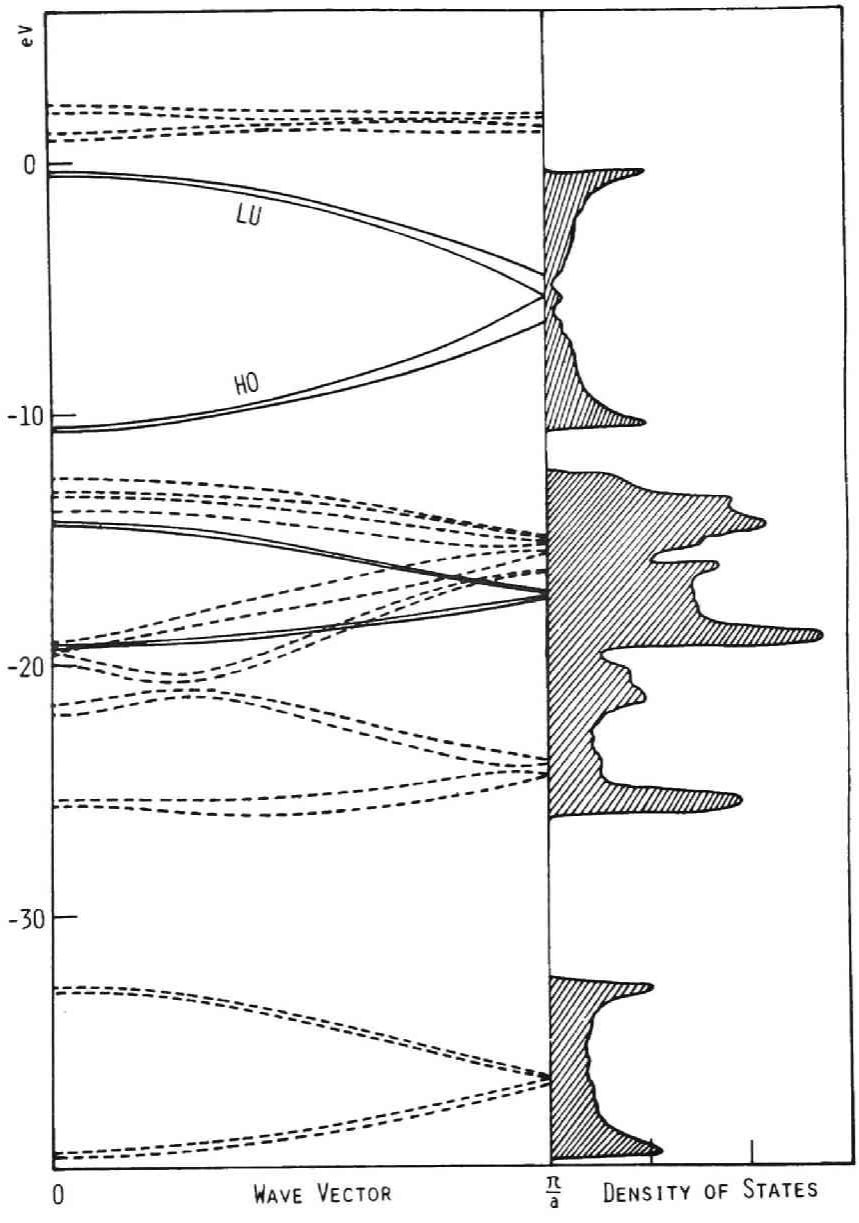

(A) In the ($\bar{1}02$) plane

Figure 2. The band structures and the densities of states of two chains of $(SN)_x$. Dotted lines and solid ones indicate σ bands and π bands, respectively, in (A) and (C), and a is the unit vector of the translation. The upper several unoccupied bands and the densities of states of those which are upper than the (LU+1), or LU in (C), are not essential and omitted here.

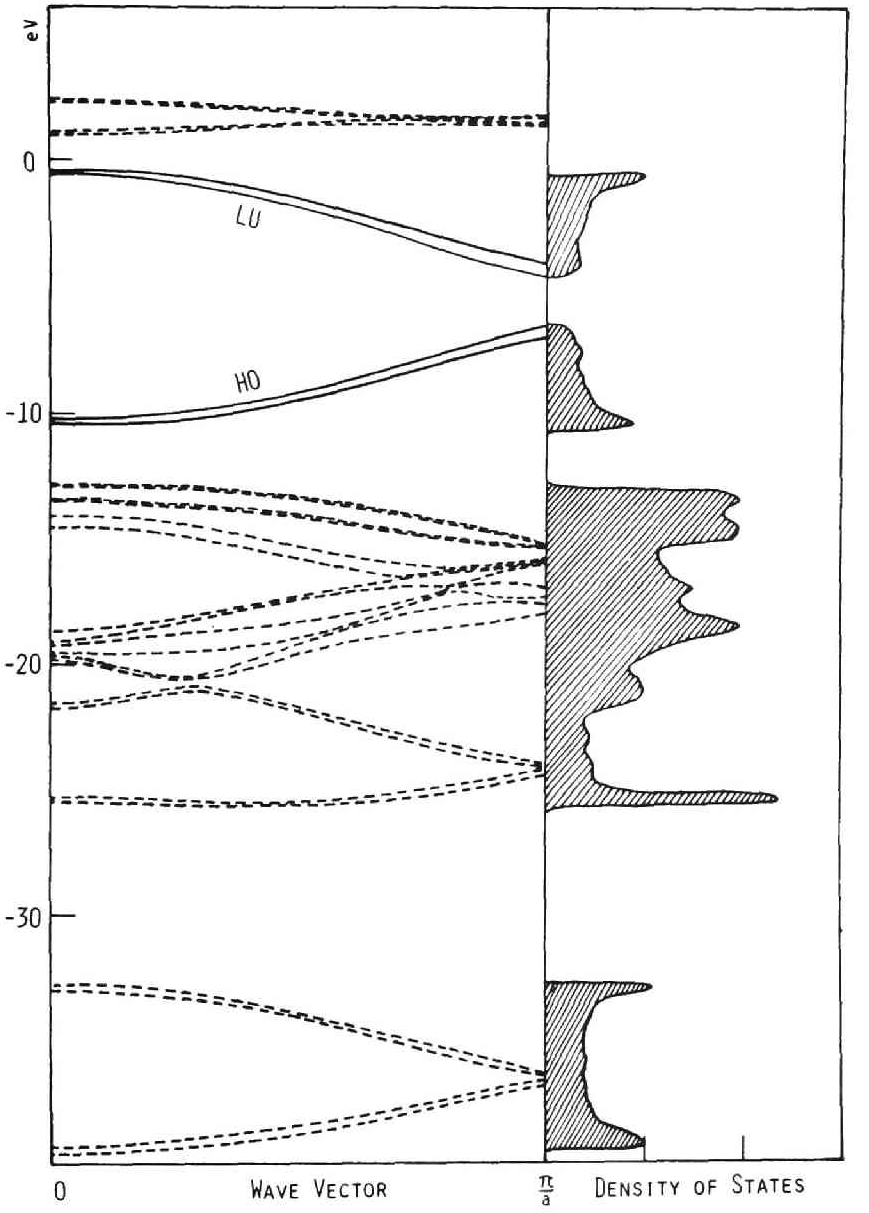

(B) In the (100) plane

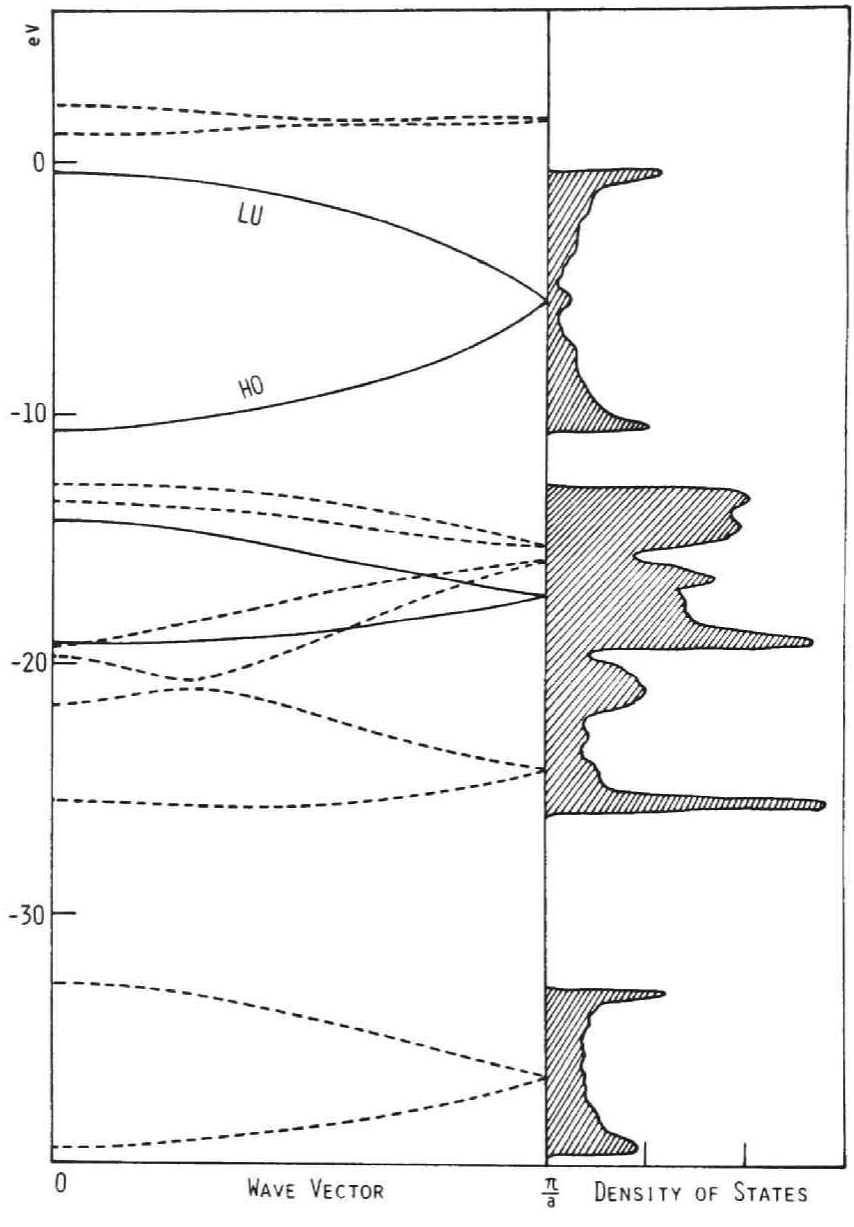

(C) In the infinitely separated case

of states of the ($\bar{1}02$) case is not a little similar to that of the infinitely separated case. These results suggest the larger influence of the interchain interaction in the (100) plane than that in the ($\bar{1}02$) plane on the HO and LU bands which serve as the conduction band in the $(SN)_x$ polymer in accordance with the result of Messmer and Salahub.[19,20] Both in the ($\bar{1}02$) and the (100) cases, the (HO-1), HO, LU, (LU+1) bands mainly consist of almost equal weight of $3p_x$ AO's of S_2, S_4, S_5, and S_7 in the neighbourhood of K=0 (K is the wave vector), but as approaching the Brillouin zone boundary, $3p_x$ AO's of S_2 and S_5 become main components of (HO-1) and (LU+1) bands, whereas those of S_4 and S_7 of HO and LU bands. Therefore, the stabilizations of (HO-1) and HO bands in the (100) case are due to S_2-S_5 and S_4-S_7 interchain ($p\sigma+p\pi$) bonds. Thus there will be different types of interactions between HO-LU, (HO-1)-LU, HO-(LU+1), or (HO-1)-(LU+1) bands at the Brillouin zone boudary, which suggests that some large interaction among them would have an effect on the temperature-sensitive properties of this polymer.

The AO densities, π electron densities, and the atomic net charges of the above three cases are shown in Table 1 along with the total energies per unit cell. The atomic net charges on sulfur atoms in both the planes are $+0.173 \sim +0.180$ being rather smaller than the experimental values from the X-

Table 1.

AO densities, π electron densities, atomic net charges, and the total energies per unit cell

	atom	AO densities									π electron density [a]	atomic net charge	total energy (eV)
		s	p_x	p_y	p_z	d_{xz}	d_{xy}	d_{yz}	$d_{x^2-y^2}$	d_{z^2}			
in the ($\bar{1}02$) plane	N_1, N_6	1.539	1.187	1.233	1.214						1.187	-0.173	-2457.028
	N_3, N_8	1.537	1.198	1.229	1.211						1.198	-0.175	
	S_2, S_5	1.809	1.432	0.837	0.746	0.246	0.128	0.287	0.091	0.249	1.806	+0.175	
	S_4, S_7	1.810	1.438	0.842	0.745	0.242	0.129	0.285	0.087	0.249	1.809	+0.173	
in the (100) plane	N_1, N_6	1.540	1.202	1.231	1.211						1.202	-0.184	-2457.010
	N_3, N_8	1.538	1.192	1.229	1.211						1.192	-0.170	
	S_2, S_5	1.809	1.426	0.841	0.745	0.246	0.131	0.285	0.088	0.249	1.803	+0.180	
	S_4, S_7	1.810	1.427	0.844	0.748	0.244	0.130	0.286	0.088	0.249	1.801	+0.174	
infinitely separated case	N	1.546	1.192	1.239	1.218						1.192	-0.195	-2456.812
	S	1.807	1.441	0.839	0.741	0.242	0.126	0.280	0.085	0.244	1.809	+0.195	(-2455.462) [b]

[a] In the (100) case, $2p_x$ AO of N and $3p_x$, $3d_{xz}$, and $3d_{xy}$ AO's of S are considered for the sake of comparison.

[b] The total energy of two infinitely separated monomers (the most stable square form) of S_2N_2.

ray photoemission (XPS) measurements, that is +0.30∿+0.42 by Mengel *et al.*[10] and +0.5 by Salaneck *et al.*[26,27] The present underestimation of these quantities may be due to the CNDO/2 version as previously mentioned.

The contributions from 3d AO's uniformly increase in the ($\bar{1}02$) and the (100) cases more than in the infinitely separated case. It is also seen that the polarities of S-N bonds in the former cases decrease comparing with those in the latter case as a whole, showing a delocalization tendency of the electrons in two interacting chains, and that $3p_x$ AO densities of sulfur atoms in the (100) case changes more than in the ($\bar{1}02$) case under the influence of interchain ($p\sigma+p\pi$) bonds in the (100) plane. The discrepancies of the atomic net charges between N_1, N_6 and N_3, N_8 or between S_2, S_5 and S_4, S_7 in the (100) case are due to the two-chain model employed here and will be improved by considering more numbers of parallel chains in this plane. On the other hand, in the ($\bar{1}02$) case, the atomic net charges turn out to be of almost the same values among nitrogen atoms and sulfur atoms. The values of the total energies indicate that there are stabilizations in both the ($\bar{1}02$) and the (100) cases, but a little more in the former. This is probably because of the difference in the distance between two chains. For instance, some remarkable interatomic distances of S_2-S_5 (3.721Å), S_2-N_8 (3.459Å), and N_3-N_8 (3.363Å) in

the (100) case are a little larger than those of S_2-S_5 (3.476Å), S_2-N_8 (3.257Å), and N_3-N_8 (3.356Å) in the ($\bar{1}02$) case as a whole. Since the approximate van der Waals radii are 3.70Å and 3.35Å for S-S and S-N contact, respectively, the above interatomic interactions are of much interest. These interaction energies were analyzed by decomposing them into the core-resonance terms, the exchange terms, and the electrostatic terms after Imamura and Fujita[21] as shown in Table 2. It is indicated that, in both of the cases, N-N interactions are repulsive and that S-S and S-N are attractive, among which S-S interactions are dominant. According to the values of the partitioned terms, the core-resonance terms and the electrostatic terms are important to S-S and N-N interactions, respectively. It should be noticed that these S-S core-resonance terms are mainly due to the interactions between $3p_x$ AO's of S_2 and S_5, and that the interchain interactions among lone-pairs of S and N formed by sp^2 hybridizations on the plane of a single chain of $(SN)_x$ are rather small. That is, the $p\pi$-type interaction in the ($\bar{1}02$) case and the $(p\sigma+p\pi)$-type interaction in the (100) case by the interchain S-S coupling are of importance.

In Table 3 are listed the intracell- and intercell (between the central and the N-th nearest neighbouring cells)-interchain interaction energies as illustrated in Figure 3.

Table 2.

The contributions of decomposed terms of the interatomic interaction energies (in eV)

	in the $(\bar{1}02)$ plane			in the (100) plane		
	S_2-S_5	S_2-N_8	N_3-N_8	S_2-S_5	S_2-N_8	N_3-N_8
Core-resonance term						
	-0.392	-0.136	0.010	-0.303	-0.053	0.026
Exchange term						
	-0.062	-0.017	-0.002	-0.087	-0.012	-0.010
Electrostatic term						
	0.144	-0.129	0.132	0.131	-0.125	0.125
Total						
	-0.310	-0.282	0.140	-0.259	-0.190	0.141

Table 3.

Intracell- and intercell-interchain interaction energies (in eV)

	intracell	intercell				total[a]
		1st	2nd	3rd	4th	
in the ($\bar{1}02$) plane	-0.595	-0.247	0.003	0.005	0.004	-0.825
in the (100) plane	-0.651	-0.333	-0.013	0.003	0.005	-0.979

[a] Summation of the intracell- and the intercell-interchain interaction energies as far as the 7th nearest neighbouring cell.

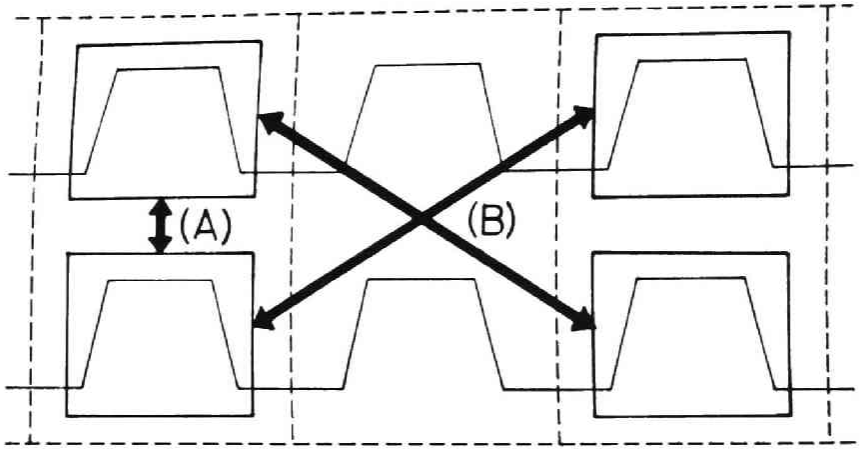

Figure 3. Schematic representation of interchain interactions. (A) Intracell case; (B) intercell case (between the central and the 2nd nearest neighbouring cells, for example). The block surrounded with the broken line is the unit cell employed in the calculation.

The interaction energies turn to be repulsive with the increase of N/ because of the dominance of the electrostatic terms. In the case of N>4, the interaction energies in both of the cases are all repulsive and very small decaying with Coulomb tails. The total interchain interaction energies indicate also that the interchain interaction in the (100) case is the larger in spite of the reverse situation for the total energies. These interchain interactions, especially those in the (100) plane, may be sufficient to relax the metal-insulator transition in the actual $(SN)_x$ crystal as has been observed.[6)]

References and Notes

1) M. Boudeulle and P. Michel, Acta Crystallogr., A28, S199 (1972).

2) V. V. Walatka, Jr., M. M. Labes, and J. H. Perlstein, Phys. Rev. Lett., 31, 1139(1973).

3) C. Hsu and M. M. Labes, J. Chem. Phys., 61, 4640(1974).

4) C. M. Mikulski, P. J. Russo, M. S. Saran, A. G. MacDiarmid, A. F. Garito, and A. J. Heeger, J. Am. Chem. Soc., 97, 6358(1975).

5) R. L. Greene, P. M. Grant, and G. B. Street, Phys. Rev. Lett., 34, 89(1975).

6) R. L. Greene, G. B. Street, and L. J. Suter, Phys. Rev. Lett., 34, 577(1975).

7) M. Schlüter, J. R. Chelikowsky, and M. L. Cohen, Phys. Rev. Lett., 35, 869(1975).

8) L. Ley, Phys. Rev. Lett., 35, 1796(1975).

9) W. E. Rudge and P. M. Grant, Phys. Rev. Lett., 35, 1799 (1975).

10) P. Mengel, P. M. Grant, W. E. Rudge, B. H. Schechtman, and D. W. Rice, Phys. Rev. Lett., 35, 1803(1975).

11) H. Kamimura, A. J. Grant, F. Levy, A. D. Yoffe, and G. D. Pitt, Solid St. Commun., 17, 49(1975).

12) W. I. Friesen, A. J. Berlinsky, B. Bergersen, L. Weiler,

and T. M. Rice, J. Phys., C8, 3549(1975).

13) M. J. Cohen, A. F. Garito, A. J. Heeger, A. G. MacDiarmid, C. M. Mikulski, M. S. Saran, and J. Kleppinger, J. Am. Chem. Soc., 98, 3844(1976).

14) A. Zunger, J. Chem. Phys., 63, 4854(1976).

15) H. Kamimura, A. M. Glazer, A. J. Grant, Y. Natsume, M. Schreiber, and A. D. Yoffe, J. Phys., C9, 291(1976).

16) C. H. Chen, J. Silcox, A. F. Garito, A. J. Heeger, and A. G. MacDiarmid, Phys. Rev. Lett., 36, 525(1976).

17) A. A. Bright and P. Soven, Solid St. Commun., 18, 317 (1976).

18) T. Yamabe, K. Tanaka, A. Imamura, H. Kato, and K. Fukui, Bull. Chem. Soc. Jpn., 50, 798(1977).

19) R. P. Messmer and D. R. Salahub, Chem. Phys. Lett., 41, 73(1976).

20) D. R. Salahub and R. P. Messmer, Phys. Rev., B14, 2592 (1976).

21) A. Imamura and H. Fujita, J. Chem. Phys., 61, 115(1974).

22) D. P. Santry and G. A. Segal, J. Chem. Phys., 47, 158 (1967).

23) J. A. Pople and D. L. Beveridge, "Approximate Molecular Orbital Theory," McGraw Hill Book Co., Inc., New York (1970).

24) H. Fujita and A. Imamura, J. Chem. Phys., 53, 4555(1970).

25) The present author recalculated here the electronic structure of a single chain of $(SN)_x$ for the infinitely separated case with more appropriate extrapolation for the density matrix at the Brillouin zone boundary than that in the previous Chapter.

26) W. R. Salaneck, J. W-p Lin, and A. J. Epstein, Phys. Rev., B13, 5574(1976).

27) The Siegbahn's relationships used for the evaluations of the atomic net charges in Refs. 10 and 26 give usually rather rough estimations. Therefore it seems that the above two experimental values require further examination, because, for example, the atomic net charges on sulfur atoms in S_4N_4 crystal have been shown to be +0.6 by Salaneck *et al.* from XPS method,[28] while , recently more accurate values through the direct evaluation from X-ray diffraction data have been shown to be +0.3 by Coppens.[29]

28) W. R. Salaneck, J. W-p Lin, A. Paton, C. B. Duke, and G. P. Ceasar, Phys. Rev., B13, 4517(1976).

29) P. Coppens, Conference on Synthesis and Properties of Low-dimensional Materials, New York Academy of Sciences, New York (1977).

Conclusion

Theory of intra- and intermolecular interactions has been re-examined and extended in some directions. An extension is a theory of intramolecular interactions in the excited state concerning biradical and photoisomerization in a conjugated polyene. Another is a theory of local perturbation in molecular aggregates. Application of MO theory for molecular aggregates is also made to the electronic structure of $(SN)_x$ polymer on which current interest in the field of solid state physics and chemistry is focused.

In Chapter 1, a method of calculation for the upper and lower bounds of the second-order perturbation energy is investigated as a theoretical ground for the study of long-range interactions. The expression for the upper bound is based on Hylleraas's variation perturbation condition and is an improved version of that obtained by Goodisman. The lower bound is based on the Temple-type inequality and is an improved version of that by Prager and Hirschfelder. The result is numerically tested for examples of the polarizability of a hydrogen atom and the coefficients of R^{-6} and R^{-8} terms (C_6 and C_8, respectively) in the multipole expansion of the dispersion force between two separate hydrogen atoms, yielding fairly good results. Particularly, the result of the upper bound for C_8 is the best so far calculated in a non-empirical way.

In Chapter 2, the long-range force between a hydrogen atom and a hydride ion has been studied by means of the second-order perturbation theory. This $H\text{-}H^-$ system has been chosen as the simplest example of a system composed of a neutral atom and an anion. The results seem to suggest that the analytical closed form of the second-order energy under the framework of the Unsöld approximation is desirable for any discussion of the long-range interaction between H and H^- in place of the usual multipole expansion. According to the multipole expansion until R^{-12} term, the nature of the long-range force operating in this system seems to be dispersive, and it seems to become inductive at a much larger R because of the existence of the leading R^{-4} term.

In Chapter 3, intramolecular interactions and optimum configurations of several ion-non polar molecule complexes ($NH_4^+\text{-}CH_4$, $H_3O^+\text{-}CH_4$, and $NH_4^+\text{-}H_2$) have been discussed with the use of the semi-empirical MO (CNDO/2) method. The configurations of $NH_4^+\text{-}CH_4$ and $H_3O^+\text{-}CH_4$ turned out to be quite different from those previously proposed by the calculations based on the classical electrostatic model. It has been shown that these systems are stabilized by a kind of hydrogen bond where charge transfer effect from a neutral molecule to a cation plays an important role, according to the configuration analysis.

In Chapter 4, a concept of the cross-bicyclization complementary to that of the cycloaddition was defined concerning simultaneous bicyclization in a linear conjugated polyene, and the stereoselective modes in thermal and photo-induced reactions were discussed. It was shown that the prediction of the stereoselection in cross-bicyclization recalls the "symmetry-disfavoured" reactions from the usual cycloadditions into the category of the concerted ones.

In Chapter 5, an interpretation was given on the characteristics of biradicaloids, such as the bonding, polar, and biradical characters of singlet biradicals. Systematization of the reactivity of singlet and triplet biradicals was shown on the basis of the principle that (i) deformation takes place in the direction of bonding in singlet biradicals, and (ii) deformation or bond formation occurs to separate unpaired-electrons from each other in triplet biradicals. Combination of the two principles was applied to the theory of orientation and stereoselection in excited-state reactions.

In Chapter 6, a perturbation theory method was developed in the tight-binding LCAO MO treatment of a one-dimensional polymer under local perturbation with the aid of the Wannier function. As the first step, electronic structures of an infinite polyene under a few of significant cases of perturbation were formulated in the scheme of Hückel MO approach,

giving the changes in total energies, electron densities, and bond orders of the perturbed systems.

In Chapter 7, the process of the dimerization of S_2N_2 into S_4N_4 was studied with regard to two essentially different types of stacking interaction models of S_2N_2. It was shown from the viewpoint of orbital interaction consideration that the stacking model of S_2N_2 in such a way that S and N approach to stack together and the geometry of S_4N_4 with coplanar N atoms are favoured. The latter geometry is in agreement with experimental result.

In Chapter 8, concerning the initial stage of solid state polymerization of $(SN)_x$, the semi-empirical MO (INDO-type ASMO-SCF) calculations were performed for the precursor S_2N_2, and several "deformed" structures of $(SN)_2$, the dimeric unit $(SN)_4$, and the trimeric unit $(SN)_6$. According to the results of calculations, the triplet biradical nature emerges in appropriately "deformed" structures of $(SN)_2$. This agrees well with the experimental results wherein paramagnetism was observed at the initial stage of polymerization. $(SN)_4$ and $(SN)_6$, however, show no triplet nature probably corresponding to the fact that the system gradually becomes diamagnetic as the polymerization proceeds. The mechanism of polymerization at the initial stage was discussed based on the calculated results.

In Chapter 9, one-dimensional $(SN)_x$ and its isoelectronic system $(SCH)_x$ polymers were treated on the basis of the SCF-tight-binding MO theory. The Pennsylvania structure of $(SN)_x$ was shown energetically favourable comparing the Lyon structure. Judging from the density of states at the Fermi level of $(SCH)_x$, it may be expected to be a metallic conductor under some favourable condition.

In Chapter 10, the interchain interactions in $(SN)_x$ polymer were discussed. It has been concluded that the interchain interaction in the (100) crystallographic plane is more significant than that in the $(\bar{1}02)$ plane and that these interactions are mainly caused by the shortest interchain S-S coupling in both the planes.